Chapter 4

Egg Production

Ganias K., Murua H, Claramunt G., Dominguez-Petit R., Gonçalves P., Juanes F., Keneddy J., Klibansky N., Korta M., Kurita Y., Lowerre-Barbieri S., Macchi G., Matsuyama M., Medina A., Nunes C., Plaza G., Rideout R., Somarakis S., Thorsen A., Uriarte A., Yoneda M.

Table of contens

4.1 Introduction 5

4.2 Gravimetric estimation of fish fecundity 10

4.2.1 Basic Principles 10

4.2.2 Ovarian fixation and preservation 12

4.2.3 Effect of preservation on oocyte size 16

4.2.4 Preparation of ovarian whole mounts 17

4.2.5 Oocyte counting and size measurement using particle analysis 18

4.2.6 Whole mount staining 25

4.2.7 Low cost alternatives to microscopy 26

4.3 Stereological estimation of fish fecundity 30

4.3.1 Basic principles 30

4.3.2 Model-based methods 31

4.3.2.1 The Weibel method 31

4.3.2.2 Ovarian packing density 31

4.3.3 Assumption-free methods 35

4.3.3.1 The physical disector 35

4.3.3.2 The fractionator 37

4.3.4 Final remarks 42

4.4 Batch fecundity 39

4.4.1 Hydrated oocytes method 39

4.4.2 Use of other stages 40

4.4.3 Use of intermediate batches 41

4.5 Daily fecundity and spawning frequency 44

4.5.1 Estimation of daily fecundity 44

4.5.2 Estimation of Spawning Frequency 46

4.5.3 The postovulatory follicle (POF) method 47

4.5.3.1 POF staging: an interspecific approach 47

4.5.3.2 POF 3-D reconstruction: a quantitative validation of POF staging 50

4.5.3.3 POF ageing: basic principles 53

4.5.3.4 Spawning induction and POF ageing in tank experiments 55
4.5.3.5 Using POF size in POF ageing 57
4.5.4 Methods based on imminent spawners 59
4.5.4.1 The hydrated females method 60
4.5.4.2 The gonadosomatic index method 60
4.5.4.3 The oocyte growth method 62
4.5.5 Methods for species with high spawning frequency 65
4.5.5.1 Negative relationship between Day 0 and Day1 spawners 66
4.5.5.2 Co-occurrence of pre- and post-spawning stages 68
4.5.6 Spatio-temporal effects on fecundity estimates 69

4.6 Annual fecundity 72
4.6.1 Determinate fecundity species 72
4.6.1.1 The autodiametric method 72
4.6.1.2 Atresia and fecundity down-regulation 74
4.6.1.3 Skipped spawning 77
4.6.2 Indeterminate fecundity species 84
4.6.2.1 Annual fecundity 84
4.6.2.2 Total egg production 85

4.7 References 88

4.8 Table of contributions 106

4.9 Authors Index 108

Chapter 4

Egg Production

Chapter formated by:
Mª Dolores Domínguez Vázquez

4.1 Introduction

For all animal organisms fecundity is a measure of gamete production. In other words, fecundity is a quantitative variable, and not an abstract indicator of individual reproductive success, expressing the number of eggs or sperm produced by females and males respectively. In fish and fisheries biology fecundity measurements are of particular importance to explore the reproductive dynamics and the spawning energetics of a fish stock, and to estimate its annual reproductive output and consequently how this is linked to recruitment. In addition, estimates of fecundity are used in the appraisal of spawning biomass through egg production methods. There are several measures of fish fecundity, such as batch fecundity, daily fecundity, potential annual fecundity, and relative fecundity, which should be considered depending on the oocyte recruitment strategy (indeterminate vs. determinate fecundity; BOX 4.1) of the species investigated. All these terms are explicitly described in Hunter *et al.* (1992).

The development in the understanding of fecundity of fish stocks in relation to egg production methods has been reviewed recently by Stratoudakis *et al.* (2006) and by Armstrong & Witthames (2012). Moreover, during the last decade there have been a number of review papers that provide a detailed overview on various aspects of applied fish reproductive biology (Hunter & Macewicz, 2003; Murua & Saborido-Rey, 2003; Murua et al., 2003; Kjesbu, 2009; Lowerre-Barbieri , 2011a; Brown-Peterson *et al.,* 2011; Ganias, 2013).

The present chapter deals with the estimation of fecundity in female fishes. Most fishes are highly fecund and thus fecundity measurements may only be carried out by counting the number of oocytes in ovarian subsamples of known weight/volume and multiplying resulting oocyte densities to the total weight/volume of the ovary (gravimetric or volumetric method respectively). Apart from their number, the size of the oocytes is also very important since it might be used either as a threshold for designating the standing stock of oocytes in estimations of potential annual fecundity or for constructing oocyte size frequency distributions to assess the fecundity pattern of a fish population, i.e. determinate or indeterminate. Finally, there is an increasing interest in fish reproductive biology for other types of follicles, apart from the developing oocytes, such as atretic and postovulatory follicles (POFs). For example, the quantification of atretic follicles is used in the correction of potential annual fecundity in determinate spawners, whilst the ageing of POFs is used in the estimation of spawning frequency in indeterminate spawners.

There are several issues that should be taken into account when measuring fecundity in female fish. A very detailed description of the methodology for the gravimetric estimation of fish fecundity is given in Hunter *et al.* (1985) covering most of the basic issues of fecundity measurements, among them:

- the location of tissue samples within the ovary ,
- the optimum number of tissue samples,
- the optimum number of individuals for fecundity estimation,
- the procedure and the required infrastructure for oocyte measurements.

These criteria were developed for the measurement of batch fecundity of indeterminate spawners, using northern anchovy, as a case study. In Hunter *et al.* (1992), the same group of authors re-evaluated these methodological issues for the measurement of total fecundity in determinate fecundity species, using the Dover sole, as a case study. Since there are no

BOX 4.1. *Oocyte recruitment patterns in fish populations*

The knowledge of the oocyte recruitment process or the fecundity strategy; which determine the strategy of how the oocytes are recruited and developed from the previtellogenic to vitellogenic stock; is necessary to appropriately estimate the fecundity (Murua & SaboridoRey, 2003). Two reproductive strategies have been identified in this regard, indeterminate and determinate oocyte recruitment or fecundity (Hunter *et al.*, 1992; Murua & SaboridoRey, 2003). In indeterminate fecundity fish species, potential annual fecundity (defined as the total number of advanced vitellogenic oocytes matured per year uncorrected for atretic losses (Hunter et al, 1992) is not fixed before the onset of spawning, because previtellogenic oocytes are recruited into the vitellogenic oocytes pool during the spawning season. In this species the potential annual fecundity cannot be considered as the realized annual fecundity and, thus, the combination of batch fecundity (the number of oocytes spawned in each spawning event or batch), spawning fraction (the fraction of mature females spawning per day) and the duration of the individual spawning season is needed to estimate annual fecundity (Hunter *et al.*, 1992). In contrast, the number of vitellogenic oocytes (total fecundity) measured prior to the commencement of spawning is considered equivalent to the potential annual fecundity in determinate fecundity fish species because the recruitment of oocytes to the vitellogenic pool ended before the spawning season (for further definitions, see Hunter *et al.*, 1992; Murua *et al.*, 2003). In these species annual realized fecundity is estimated as after discounting oocyte atresia (the process of oocyte and follicle resorption altering the oocyte structure indicating that the oocyte will not complete the maturation process to be spawned) from total fecundity.

Several criteria have been published to distinguish between indeterminate and determinate type fecundity. The most common criteria used to distinguish between both types of fecundity are the following lines of evidence (Hunter *et al.*, 1989; Greer Walker *et al.*, 1994 & Murua & SaboridoRey, 2003): (i) stage-specific and monthly-specific variation of oocyte size-frequency distribution; (ii) seasonal variation in the percentage of different oocyte classes during spawning season (i.e previtellogenic and early vitellogenic vs. advanced vitellogenic oocytes); (iii) seasonal variation in the mean diameter of the advanced vitellogenic oocytes; and (v) incidence of atresia through the spawning season.

The first criterion is to study the stage-specific variation of oocyte size-frequency distribution during the reproductive cycle. A gap in the oocyte size frequency between the vitellogenic oocyte stock from the previtellogenic oocyte population (synchronous and group-synchronous) will indicate that annual fecundity is determinate, whereas the lack of a hiatus may indicate that annual fecundity is indeterminate. The fecundity indeterminacy based on the lack of the hiatus needs to be corroborated with other line of evidences as species with a continuous size frequency distribution of oocytes has been classified as species with determinate fecundity by captive experiments (Hislop & Hall, 1974). Secondly, the percentage throughout the spawning season of developing oocytes (previtellogenic

BOX 4.1. (cont.)

and early vitellogenic oocytes) is similar when oocyte recruitment of new oocytes into the standing stock of developing oocytes occurs; which is a characteristic of indeterminate fish species. In contrast, in the case of determinate fish species the percentage of the developing oocytes decrease as the spawning season is reached and during spawning season, because the standing stock of oocytes diminishes as they are not replaced during the spawning season.

Similarly, the evolution of the number of advanced vitellogenic oocytes in the ovary may present more evidences in favor or against of each type of fecundity. In this sense, a decrease in the stock of advanced vitellogenic oocytes during the spawning season supports evidence for determinate oocytes as total fecundity decreases with each spawning event because the standing stock of yolked oocytes is not replaced during spawning season.

Thirdly, the decrease in mean diameter of advanced yolked oocytes, through the spawning season, can be considered also as evidence for indeterminate fecundity due to the recruitment of newly formed small yolked oocytes into the stock of advanced vitellogenic oocytes. In fishes with determinate fecundity it may be expected a seasonal increase in the mean diameter of the advanced vitellogenic oocytes, over the spawning season, because no new yolked oocytes are recruited to replace those that have been spawned during the season. Nevertheless, this line of evidence should be taken with caution because the diameter of the advanced stock of oocytes (which are in vitellogenesis) of some species with determinate fecundity decrease after the spawning has started, i.e. cod, where the egg mean diameter decrease as the spawning evolves (Kjesbu *et al.*, 1990).

Finally, the seasonal development of atresia throughout reproductive cycle differs between species with indeterminate and determinate fecundity (Murua & Saborido-Rey, 2003). In this sense, fishes with indeterminate fecundity show an increase in intensity and prevalence of atresia at the end of the spawning season (Korta, 2010b; Murua & Motos, 2006). The continuous recruitment of newly formed oocytes into the standing stock of vitellogenic oocytes, become atretic when fishes approach the end of their spawning season (Murua & Motos, 2006) as the surplus production of oocytes needs to be resorbed. On the other hand, determinate fecundity fishes in normal condition show a lower level of atresia during spawning season and at the end of the spawning season as less surplus production of oocytes is observed.

The fecundity strategy of the fish species determines the fecundity variable to be measured to estimate the annual realized fecundity (or the actual number of eggs spawned); which in a large extend fix the methodological approach to be used. The methodological approach can be different from gravimetric to volumetric estimation of fish fecundity which can be accomplished through manual counting and/or modern image analysis; and modern stereological approaches. The different methods should consider various issues to assure precision in the fecundity estimation.

significant improvements in these issues, apart from some species specific tests on the homogeneity of the ovary, these two publications still provide most of the methodological background for the applications of the gravimetric method. In that respect the present chapter only provides a brief description of the basic principles of the gravimetric and the volumetric methods [Section 4.2.1], giving emphasis to issues that were not fully explored in the aforementioned set of criteria such as the appropriate methods for ovarian fixation and preservation [Section 4.2.2], the effect of preservatives on oocyte size [Section 4.2.3] and the treatment of ovarian subsamples [Section 4.2.4] .

Even if these two early publications by John Hunter and his colleagues still constitute the frame of reference in fish fecundity studies they suffered from several technological and methodological restrictions. For example, up to that period fecundity measurements were traditionally performed through direct counting of oocytes under ocular microscopes, which made fecundity estimations labour-intensive and often inaccurate. Moreover, oocyte size frequency distributions were constructed by averaging the maximum and minimum axes in a number of oocytes again through direct observations under binocular microscopes which could be painstaking and highly inaccurate (e.g. biased selection of oocytes, repeated measurements, etc.). The present chapter gathers several improvements in the measurement and the quantification of various follicular types including developing oocytes, postovulatory and atretic follicles. We will show how digital image processing and routines of particle analysis might be used in the measurement and estimation of oocyte size and number [Section 4.2.5]. These procedures might be improved though staining specific follicular types in ovarian whole mounts [Section 4.2.6]. It is quite impressive that even with inexpensive equipment including a medium resolution flatbed scanner, few consumables and a license-free image analysis software someone may quickly produce precise measurements of fish fecundity [Section 4.2.7].

Another important advance deals with the reliable quantification of follicular types that may only be identified through ovarian histology (e.g. previtellogenic oocytes, atretic and postovulatory follicles). Even if there are some promising results on the identification of postovulatory and atretic follicles in ovarian whole mounts by means of specific staining protocols [Section 4.2.6] the aforementioned routines optimally work for the identification and quantification of healthy follicles. On the other hand, histology still constitutes the most unbiased method for identifying these structures but has many limitations in accurately quantifying their intensity and abundance (Murua *et al.*, 2003). To avoid bias of simple profile counting many fish fecundity studies now use the principles of stereology which lead to either assumption-based [Section 4.3.2] or to assumption-free [Section 4.3.3] estimations of follicular intensity. The first group of estimations is advisable only for counting objects of regular shape as they rely on assumptions about particle shape and size distribution [Section 4.3.2.1]. Another model-based method that has been used in estimations of fish fecundity involves the prediction of oocyte density hierarchically from the size, fractional volume, shape and specific gravity of the oocytes [Section 4.3.2.2]. The biggest problem with assumption-based methods is that they provide density estimates of 3-D objects (follicles of various types) using 2-D images (photomicrographs, histological sections). On the other hand, design-based stereological methods such as the physical disector [Section 4.3.3.1] or the fractionator principle [Section 4.3.3.2] convert measurements on 2-D images into 3-D structural quantities, leading to assumption-free estimates of particle density.

As already mentioned, there are several measures of fecundity. The simplest measure is batch fecundity which provides estimates of the number of eggs released per spawning event [Section 4.4]. The most popular method for estimating batch fecundity is the hydrated oocytes method [Section 4.4.1] even if previous developmental stages [Section 4.4.2] or even the intermediate batches [Section 4.4.3] could also be used in its estimations. Another measure of fecundity is daily fecundity [Section 4.5] which is the number of eggs spawned per female (or per unit of female weight) per day. For fish that spawn daily, fecundity equals batch fecundity. However, most fish display larger spawning intervals and in this case daily fecundity equals batch fecundity multiplied by spawning frequency. Due to its importance in assessing reproductive biology and spawning dynamics especially in indeterminate spawners Section 4.5.2 deals with the estimation of S, mainly covering the POF method [Section 4.5.3] and its most common bias issues related to POF staging [Sections 4.5.3.1 & 4.5.3.2] and POF ageing [Sections 4.5.3.3]. Apart from the postovulatory follicle method a set of other methods for estimating S is also provided such as methods that are based on imminent spawners [Section 4.5.4], methods for stocks with high S values [Section 4.5.5], and methods based on the assessment of spawning sites [Section 4.5.6].

For determinate spawners estimates of annual fecundity could be theoretically based on the total fecundity of females just prior to spawning. In this case the autodiametric method [Section 4.6.1.1], provides an easy and valid tool for estimating potential annual fecundity in determinate spawners. However, due to follicular atresia the potential annual fecundity is down-regulated and thus accurate estimates of annual fecundity may only be achieved by correcting for this effect [Section 4.6.1.2]. Another important issue when estimating the potential annual fecundity for a fish stock is to take into account the number of fish that skip spawning in the current season, a phenomenon which is quite frequent in populations of determinate spawners [Section 4.6.1.3]. On the other hand for indeterminate spawners, annual fecundity could be estimated by combining values of daily fecundity with the duration of the spawning season [Section 4.6.2.1]. These measures of fecundity provide estimates of egg production at an individual level. The population equivalent of annual egg production is Total Egg Production (TEP) which serves together with SSB as an index of stock reproductive potential and could, thus, be used in stock-recruitment models. Furthermore, there is increasing evidence that TEP is a better index of stock reproductive potential because it includes the size-dependent capacity of females to produce eggs and the demographic structure of the spawning stock [Section 4.6.2.2].

In summary, the present chapter is organized in three main blocks: (i) the first block included in Section 4.2 and 4.3 is devoted to review the technical issues in fish fecundity from fixation to automatic oocyte counts; (ii) the second block is focused on methods that are available for the estimation of some important variables of fish fecundity such as batch fecundity (4.4), and daily fecundity and spawning fraction (4.5); (iii) the third block incorporates knowledge acquired in the two other blocks to review what is needed to estimate the annual realized fecundity (the ultimate goal of fecundity studies) in determinate and indeterminate fish species. In short, this chapter will offer the reader an overview of all methodological aspects that needs to be considered in fish fecundity investigations.

4.2 Gravimetric estimation of fish fecundity

4.2.1 Basic Principles

As already mentioned, fish are usually highly fecund and, thus, ovarian subsamples are almost always required for estimating fecundity. These are related to either ovarian weight (gravimetric method) or to the total volume of an aqueous suspension of all oocytes in the ovary (volumetric method). These methods can be used to estimate batch fecundity, total fecundity and potential annual fecundity.

In the volumetric method the fixation of the ovaries is normally done with Gilson's fluid (100 ml 60% alcohol, 880 ml water, 15 ml 80% nitric acid, 18 ml glacial acetic acid, 20g mercuric chloride) which frees the oocytes from the ovarian tissue by breaking down the connective tissue. However, the process also destroys the ovarian structure making histological analysis impossible. Also, while allowing the oocytes to separate this fluid destroys the hydrated oocytes. Thus, Gilson's fixative could be used for the volumetric method, only when the examined females are mature and non-hydrated for the estimation of potential fecundity or of batch fecundity when the oocytes constituting the batch are identified using the oocyte size-frequency method. Also, oocytes shrink more when preserved in Gilson's fluid, than in formaldehyde preserved ovaries. Another factor that should be evaluated is whether shrinkage is differential among oocyte size classes. In top of that, Gilson's fluid is highly toxic and, thus, should not be used for routine fecundity estimations. Because of all these reasons the volumetric technique is not recommended for fecundity measurements and the gravimetric method should be used instead.

A gravimetric analysis relies on some final determination of weight as a means of quantifying fecundity. Since weight can be measured with greater accuracy than almost any other fundamental physical property, gravimetric analysis is potentially one of the most accurate methods available. The gravimetric method is currently the most common method used to estimate fecundity; and is based on the product of ovary weight and oocyte density in the ovaries. Thus, counting oocytes in weighed subsamples and multiplying it to the total ovary weight gives an estimate of the number of oocytes in the ovary.

To apply the gravimetric method, ovaries are removed from each female and weighed. Hunter *et al.* (1985) provide an explicit logistical approach on the optimum number of ovarian tissue samples required for batch fecundity measurements while Table 4.1 summarizes the ovarian sampling characteristics for several fish fecundity studies. The selection of the optimum ovarian subsample weight is rather complicated because it depends not only on the desired number of oocytes required for fecundity measurements but also on the size of oocytes and dimensions of the visual field during the microscopic processing of the ovarian tissue (BOX 4.2).

Ovarian subsamples are taken and stored in separate sample tubes. The number and the weight of ovarian subsamples are decided based on criteria described in Hunter *et al.* (1985). The number of oocytes in the desired group (e.g. the most advanced group for batch fecundity, or the standing stock of vitellogenic oocytes for total fecundity) in the

Table 4.1.

Characteristics of ovarian subsamples used for the gravimetric measurement of fecundity of various fish stocks. A: anterior; M: middle; P: posterior.

Species	Subsample No. (mass)	Location	Reference
Arcto-Norwegian cod ***Gadus morhua***	4 (0.15–0.25g)	Middle of right ovary	Kjesbu *et al*., 1998
Argentine hake ***Merluccius hubbsi***	3 (0.1–0.2g)	Anterior, middle, and posterior of a random ovary	Macchi *et al*., 2004
Atka mackerel ***Pleurogrammus monopterygius***	1 (0.3-2.5g)	Central location of either ovary	McDermott *et al*., 2007
Atlantic cod ***Gadus morhua***	3 (0.05-0.1g)	Random ovary	Alonso-Fernández *et al*., 2009
Northern Atlantic cod ***Gadus morhua***	3 (0.1-0.2g)	Middle of right ovary	Wroblewski *et al*., 1999
Black drum ***Pogonias cromis***	3 (0.1g)	Anterior, middle and posterior of one ovary	Macchi *et al*., 2002
Haddock ***Melanogrammus aeglefinus***	3 (0.05–0.1g)	Anterior, middle, and posterior of a random ovary	Alonso-Fernández *et al*., 2009
Horse mackerel (Portugal) ***Trachurus trachurus***	3 (0.1-0.2g)	Anterior, middle, and posterior of a random ovary	Gonçalves *et al*., 2009
Iberian Sardine ***Sardina pilchardus***	1-3 (0.05-0.15g)	Center of a random ovary	ICES, 2010
Grey mullet ***Liza parsia***	6 (0.1g)	Anterior, middle, and posterior of each ovary	Rheman *et al*., 2002
Gulf of Maine cod ***Gadus morhua***	2-3 (0.1-0.2g)	Center of right ovary	Klibansky and Juanes, 2008
Mediterranean sardine ***Sardina pilchardus sardina***	3 (0.04–0.06g)	Anterior, middle and posterior of a random ovary	Ganias *et al*., 2004
Norwegian spring-spawning herring ***Clupea harengus***	3 (0.15-0.2g)	Middle of right ovary	Óskarsson *et al*., 2002
Snapper ***Pagrus auratus***	1 (0.2g)	Middle of a random ovary	Zeldis and Francis, 1998
Yellow Sea bream ***Dentex hypselosomus***	1 (0.2-0.5g)	Center of the left ovary	Yoda and Yoneda, 2009

subsamples is counted and the total number of oocytes in the original sample (whole ovary) is subsequently calculated. The total number of oocytes in the target group is calculated by multiplying the sum of the number of oocytes in the subsamples divided by the sum of the subsample weights (i.e. density of oocytes) by the weight of the ovaries (4.1).

Fecundity is estimated, according to Equation 4.1, as:

$$N = \frac{W_n}{W'} \qquad 4.1$$

where, N is the total number of the selected type of oocytes in the ovary (e.g. yolked or hydrated), W is the total weight of the ovary; n is the number of oocytes counted in the subsamples and W^1 is the weight of the subsamples. Variations of this method are related to whether total fecundity for potential annual fecundity or batch fecundity is estimated; which determines the development stage of the oocytes to be counted. To estimate batch fecundity the hydrated oocytes within the subsamples are counted; whereas to estimate total fecundity or potential annual fecundity the advanced yolked oocytes, or oocytes larger than a diameter threshold, are counted.

Another factor to take into account is that the number of subsamples per ovary, as well as the place where they were cut, should be representative of the whole ovary. Thus, the accuracy and precision of fecundity estimation should be evaluated for each species, especially regarding the number and location of samples used based on the oocyte distribution along the ovary. As a way of evaluating if the oocyte distribution is homogeneous within the

ovary, subsamples should be taken from the anterior, middle and posterior part of the left and right lobes. Then, the density of oocytes per subsample should be determined and compare statistically between samples to assure that the density between lobes, or between subsample locations within the lobes, are not statistically different. A similar exercise should be carried out to check the minimum subsample weight to be used for the estimation of fecundity. In that case, subsamples of different weights should be selected to estimate the optimum subsample size for the species when the estimation of the subsample density is stabilized around an asymptotic value.

4.2.2 Ovarian fixation and preservation

Preservation and fixation of biological tissue are two connected procedures: fixation is arresting all the chemical and physical changes that follow cell death, like enzyme autolysis and microbial activity, while preservation is maintaining the results of fixation for a certain period of time. Most common fixatives and preservatives for microanatomical work in fish reproduction studies are formalin-based fluids like 10% neutral buffered formalin (NBF) and the Bouin's fluid since both are suitable for gonadal histology and fecundity measurements. Alcohol solutions such as ethanol (EtOH), which is one of the most common preservatives of animal tissue or isopropanol (e.g., Heins & Baker, 1999) may also serve as alternative preservation protocols to formalin.

Formaldehyde and ethanol seem to react with cellular structures in different ways, targeting different substrates: formaldehyde dissolves glucose, glycogen, phospholipids and inorganic salts whilst ethanol can coagulate proteins and extract much of the lipids that are present in the specimen. This is why the two preservatives might exhibit quite diverse effects in the size and weight of tissues, organs and species of different chemical composition. Moreover, both formaldehyde and ethanol should alter the water content of cells and tissues based on differences in osmolarity and passive diffusion. This explains the varying level of oocyte shrinkage in EtOH treatments of varying concentration shown in Figure 4.1.

NBF is the most common fixative and preservative of ovarian tissue in fish fecundity studies (Hunter, 1985) providing optimum results both for histological preparations and for whole mounts having a limited effect on oocyte size (see Section 4.2.3). However, formalin is known to cause a number of health issues

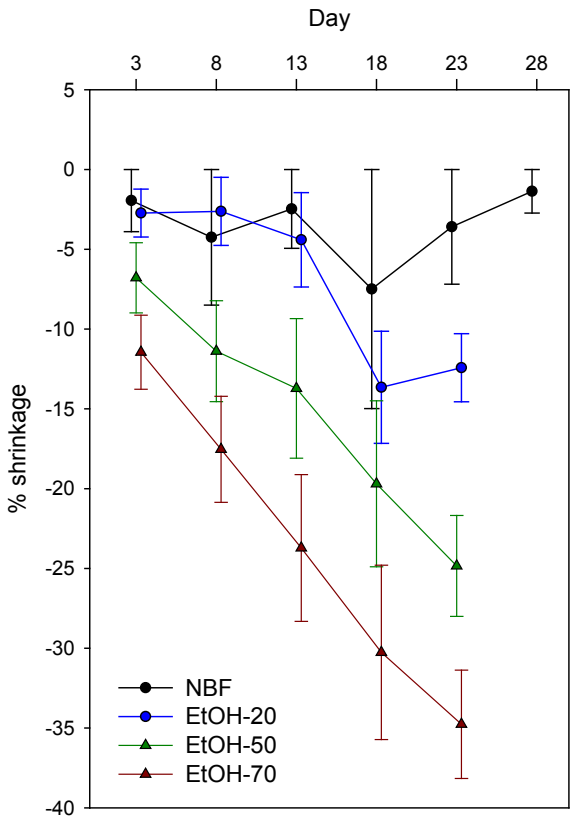

Figure 4.1.

Effect of four different preservation protocols (neutral buffered formalin 10%: NBF; ethanol 20%: EtOH-20; ethanol 50%: EtOH-50; ethanol. 70%: EtOH-70;) on the size of the oocytes (OS) of sardine, Sardina pilchardus. Each point represents the %ΔOS values (and 95% CIs) for each 5days -species-preservation protocol group.

to laboratory workers. The immediate effects are nausea, headache, and ocular irritation that causes tear overflow and a burning sensation in the throat. Long-term exposure to formaldehyde can cause contact dermatitis, congenital defects, and cancer (Raja & Sultana, 2012). To protect the user from formaldehyde vapor few fish fecundity labs have microscope working places equipped with a suction hood (see Section 4.2.5). However, this is not standard equipment for most labs, suggesting that alternative, less toxic preservation protocols should be explored. Pure EtOH solutions may offer this possibility since apart from being almost non-toxic (they may even have less alcohol content than distilled beverages) they also have several logistic advantages over NBF since they are quite cheaper and easier both to find and to prepare. However, EtOH solutions cause significant oocyte shrinkage proportionally to their concentration (Fig. 4.1). The same goes for other ethanol-based, formalin-free protocols such as the toxic Gilson's fluid or its modified non-toxic alternative proposed by Friedland *et al.* (2005), which serve in separating oocytes from ovarian tissue for fecundity measurements.

Here are some important steps in ovarian fixation and preservation process:

1. Ovaries should ideally be fixed immediately after capture. However, when this is not possible, as for example when samples are collected at landing or from fish markets then storage at low temperatures for some hours does not seem to create big problems in ovarian condition. Figure 4.2 presents the variation in oocyte and postovulatory follicles' (POFs) size from sardines fixed at 0h, 4h, 8, and 12h after capture. Oocyte size was not significantly different between the four fixation times whilst the size of POFs only significantly increased for the earliest age class. This happened because POFs were shown to become looser with time at fixation.

2. Ovaries should ideally be dissected and placed in jars of appropriate size with the fixation fluid directly when samples are processed. However, when this is not possible, e.g. when samples are processed on board and

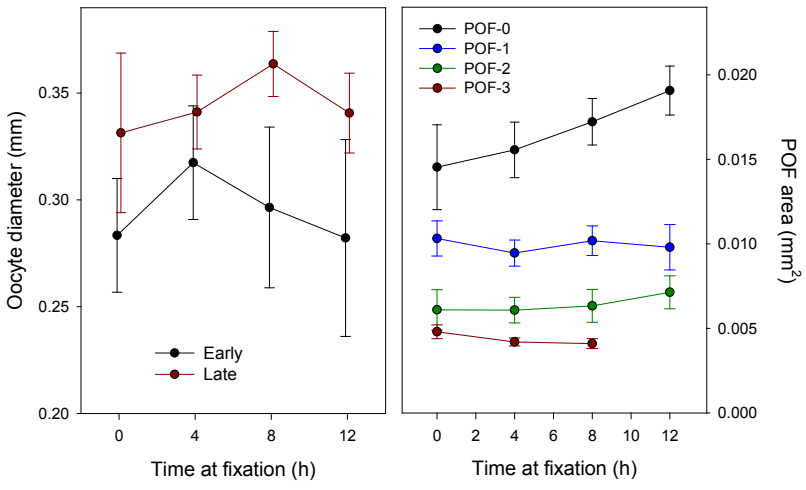

Figure 4.2.

Variation in oocyte size (left panel: early and late vitellogenic stages) and postovulatory follicles (POF) size (right panel: POF-0 to POF-3) with time at fixation after capture for sardine, Sardina pilchardus, ovaries. Vertical bars correspond to 95% confidence limits.

BOX 4.2. Choosing the right ovarian sub-sample weight in fecundity measurements.

Figure shows the relationship between ovarian sub-sample weight (SSW) and gonadosomatic index (GSI) for various classes of oocyte counts (only the advanced batch) for sardine, *Sardina pilchardus*, batch-fecundity measurements. The relationship between SSW and GSI changes a lot among the different classes of oocyte counts. In the lowest class (<300 oocytes) SSW increases steeply at lower GSI values while it tends to stabilize at a value of ca. 0.11g for GSI values >10%. Changes in GSI mostly reflect changes in oocyte size/mass and thus for a given value of oocyte counts higher GSI values would result in higher SSW values. In the next two classes (300-600 and 600-900 oocytes) the relationship between GSI and SSW is still positive, though less steep suggesting that for the same values of GSI, higher oocyte counts lead to higher SSWs. These two curves again tend to stabilize at ca. SSW=0.11g with increasing GSI. However, in the >900 class of oocyte counts the relationship changes and SSW slightly decreases with increasing GSI, again tending asymptotically to a value of SSW=0.11g.

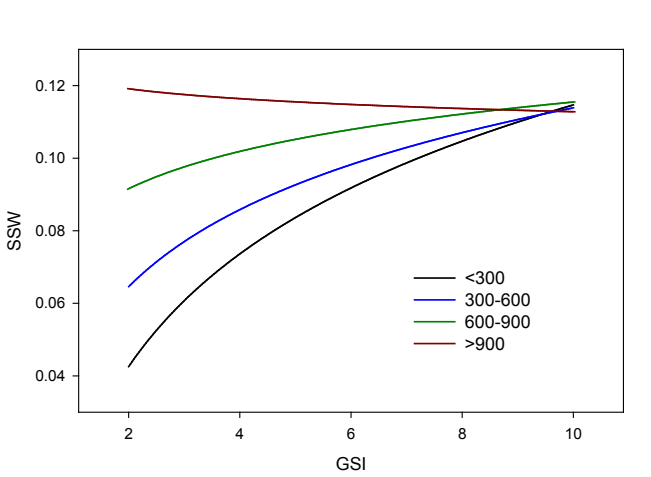

Relationship between ovarian sub-sample weight (SSW) and gonadosomatic index (GSI) for various classes of oocyte counts (only the advanced batch) for sardine, Sardina pilchardus, batch-fecundity measurements.

These results are explained by the finite visual field in microscopic observations. As already shown, all SSW vs. GSI relationships have a common asymptotic value of SSW which equals to ca. 0.11g. It will be explained that this asymptotic value corresponds to the ovarian tissue capacity of the microscopic field. The aforementioned SSW vs. GSI relationships were constructed after analyzing pictures of ovarian whole mounts taken at 4x magnification; thus, total area in each photo-micrograph was 12.6cm^2. Given that oocytes in each of the sub-samples formed a single layer and that their diameter may reach about 0.1cm at oocyte hydration (i.e. when GSI reaches a value of 10% and above) the tissue volume capacity of the visual field should be 0.1x12.6=0.126ml which corresponds to

BOX 4.2. (cont.)

0.119g of ovarian tissue (given that specific gravity of sardine ovaries at hydration is 1.051) which is quite close to the asymptotic value of SSW. The small difference between the asymptotic SSW value and the carrying capacity of the visual field is attributed to the fact that oocytes are usually removed from the borders of the visual fields.

The slightly negative relationship between SSW and GSI in the class of >900 oocyte counts could be explained by differences in the specific gravity between vitellogenic and hydrated oocytes. In this class, there is a significant trade-off between oocyte size and number. Therefore, the subsample volume in the whole range of GSI values should equal to the volume capacity of the visual field. Given that the specific gravity of sardine ovaries at vitellogenesis (1.051g/ml) is slightly higher than hydration, SSW should drop from 0.126x1.051=0.134g to 0.119g

fish are fixed as a whole, proper exposure of ovaries to fixative should be insured by slitting the abdomen of fish before fixing.

3. The depth (d) reached by a fixative is directly proportional to the square root of duration of fixation (t):

$$d = k\sqrt{t} \qquad 4.2$$

The constant (k) is the coefficient of diffusability which is specific for each fixative (0.79 for NBF). In that respect, NBF will penetrate ovarian tissue to the depth of approximately 1mm in one hour, e.g. for a 1cm sphere NBF will not penetrate to the center of the sphere until $(5)^2/0.79=32$h of fixation.

4. Gross specimens, e.g. whole fish, should not rest on the bottom of the container; they should be separated from the bottom by wadded fixative soaked paper or cloth allowing penetration of fixative fluids.

4.2.3 Effect of preservation on oocyte size

With regard to data quality, preservatives used in fecundity studies should retain the natural shape of oocytes and have minimal or at least predictable effects on oocyte size and sample weight. To be conservative, one should expect that preservation will affect variables of interest and should develop methods such that results are not biased by these effects, or account for them. An example of the former approach would be to collect fresh weights of both ovaries and ovary subsamples when using the gravimetric method so that these weights can be used together in calculations. If however one weighed whole ovaries fresh but only obtained a preserved subsample weight, then the effect of preservation on subsample weight must be determined. Though relatively little research has been conducted on the effects of preservation on ovarian tissue weight and oocyte size, there are a few publications that show that preservation usually affects these variables, sometimes in complex ways.

Preservation can affect oocyte size differently among species. Formalin preservation has been shown to increase the mean diameter of fresh catfish eggs by 4–11% (Tan-Fermin, 1991), and cod oocytes by 3.5% (Svåsand *et al.,* 1996), but had no effect on the weight of salmon eggs (Fleming & Ng, 1987). In a study on cod, haddock and American plaice, the effect of preservation of vitellogenic oocytes in four experimental treatments (modified Gilson's solution, ethanol, freezing, and «formalin») was evaluated. Percent change in mean oocyte diameter did not differ between cod and haddock in any of the experimental treatments, but when comparing cod and American plaice, differences were found in all four (Klibansky & Juanes, 2007). Results of this study suggest that differences between species are more likely when species are more distantly related. Unfortunately, different studies sometimes produce conflicting results. Schaefer & Orange (1956) & Joseph (1963), both studying yellowfin and skipjack tuna, compared diameters of oocytes preserved in Gilson's solution to oocytes in formalin. While the former study found no difference, the latter found oocytes in Gilson's solution to be 24% smaller than formalin preserved oocytes. Preservation can also affect ovarian material weight. In Ramon & Bartoo's (1997) work on albacore tuna, formalin preserved ovaries weighed 1% less than fresh ovaries on average, but the change in individual ovaries ranged from a 33% loss to an 11% gain. Frozen ovaries weighed 6% less on average than fresh ovaries, but ranged from a 26% loss to a 6% gain. Klibansky

& Juanes (2007) found that when large portions (mean=120g) of fresh cod and haddock ovaries were preserved in formalin, there was little or no change in weight. However, when small subsamples (mean=1.5g) of ovarian tissue were preserved in formalin there was a significant increase in weight of ~20% for both cod and American plaice. In small subsamples preserved in a modified Gilson's solution there were 14% and 20% average losses in weight, frozen subsamples gained 51% and 8%, and in ethanol subsamples lost 4% and gained 25% in cod and American plaice respectively, all representing significant differences between species. The ranges in weight change were also high, being highest for frozen subsamples of cod tissue (25-90%).

Formulation and concentration of chemical preservative solutions and duration of preservation should also be considered. It is cumbersome to write out the entire formula for a preservative solution throughout a manuscript, so shorthand is commonly used. In this section, the term formalin has been used to refer to formaldehyde solutions, following custom. But the term formalin may be used to describe solutions of various concentrations (e.g. 4% formaldehyde), mixed by a chemical manufacturer or diluted from a stronger concentration by the investigators, often with seawater. For most species, the effects of one formulation versus another on oocyte size are not known, so whenever possible researchers should either conform to a standard formulation or determine these effects. Time in preservation can also affect oocyte and egg size. Tan-Fermin (1991) showed that most of the swelling in catfish eggs preserved in formalin occurred within the first 24 hours, and was relatively stable through 120 hours (i.e. the end of the experiment). Friedland *et al.* (2005) showed that mean size of American shad oocytes preserved in modified Gilson's solution did not change between 30 and 60 days in preservation, but then decreased gradually, resulting in an 8% decrease by the end of the experiment (170 days).

If one intends to use preserved ovary tissue for analyses like histology, in addition to fecundity estimation, these may have stricter preservative requirements. There is a clear logistical advantage to preserving a single piece of tissue rather than multiple pieces, so if the preservative required for other analyses is also suitable for fecundity analysis, it may be wise to use this preservative. Though certain methods may be more desirable than others, a range of preservatives may be effective in fecundity analysis of some species (Klibansky & Juanes, 2007), thus preservative requirements of fecundity analysis are relatively flexible compared to other procedures. For instance, histology analysis requires initial fixation in formalin or a similar fixative, while most genetic and lipid analyses cannot be done on formalin fixed tissue. Perhaps because it can be used for both fecundity and histology analyses, formalin is now widely used in fecundity studies, though it clearly restricts the use of that tissue for other purposes.

4.2.4 Preparation of ovarian whole mounts

To estimate oocyte size distribution or fecundity, it is necessary to separate and preserve oocytes, avoiding, as much as possible, oocyte diameter/form changes, damages or destruction of oocytes and ovary structures. As mentioned in Section 4.2.1, although oocytes can be separated with strong acid solutions such as Gilson's fluid or a less toxic nitric acid formulation (Friendland *et al.* 2005), these can cause unacceptable levels of shrinkage (Witthames & Greer-Walker, 1987, and potential loss of atretic follicles and POFs (Hunter & Macewicz, 2003). Most importantly, if the tissue is to be used to estimate batch fecundity based on the hydrated oocyte method (Hunter & Macewicz, 1985b), these solutions can cause

disintegration of hydrated oocytes (Hunter, 1985; Lowerre-Barbieri & Barbieri, 1993). Formalin, as a preservative, has several key advantages over these solutions, including preservation of all cytological components and relatively low shrinkage from 0 to 7% (Hiemstra, 1962; Fleming & Ng, 1987; Hislop & Bell ,1987; Klibansky & Juanes, 2007). The disadvantage of formalin is that if ovarian tissue is preserved whole, it may become fixed into a hard mass and be extremely tedious or impossible to separate individual oocytes without damaging them (Caillet *et al.,* 1986). This problem can be overcome by using simple method of separating the oocytes from ovarian tissue with hydraulic pressure prior to preservation in formalin (Lowerre-Barbieri & Barbieri, 1993). The equipment used with this method is very basic and accessible, i.e. standard faucets with a minimum flow rate of 133 mL/s (or simple jet water sprays) and any sieve that has mesh small enough to retain less-developed oocytes and deep enough to not allow tissue and water to flush out.

With this method, once ovaries have been removed from the fish, oocytes are separated from each other and connective tissue by flushing them with tap water into a sieve. If homogeneous distribution of oocytes is assumed, independently of their developmental stage, the sub-sampled area effect is not a concern and, thus, a single cross section of tissue will be enough. However, if there is potential non-homogeneous distribution of oocytes of different development stage along the anterior/posterior axis, then it is important to flush the subsamples taken in different locations of the ovary (or in extreme cases the entire ovary). If it is necessary to flush the entire ovary, because the ovary is too small or in other cases, the ovarian wall is incised from the posterior to anterior end and turned inside out to expose the follicles to high-pressure tap water. The separated oocytes are washed into a 100 micron mesh sieve. Oocytes are then rinsed again to help separate them from one another. The water is then drained and the oocytes transferred to containers with formalin. Although (Lowerre-Barbieri & Barbieri, 1993) suggested preserving oocytes in 2% formalin to minimize shrinkage and changes in appearance, if these are not of primary concern, higher concentrations can be used.

Samples should be processed within 6 to 7 months to ensure that shrinkage rates remain within those reported by (Lowerre-Barbieri & Barbieri, 1993). To start processing these whole mounts (e.g. counting oocytes or measuring their size under ocular miscroscopes), the following steps should be taken: (1) stir the oocyte sample to reduce bias due to settling; (2) under a fume hood, decant the sample into a sieve, draining the formalin; (3) tare a gridded petri dish on the balance (preferably a glass petri dish as plastic is not as effective due to water tension); (4) remove approximately 0.3 g of the oocyte sample with any blunt utensil (i.e., a plastic spoon) and spread on a paper towel to remove excess water; (5) allow sample to sit for 30 s and then put a subsample of the oocytes weighing approximately 0.1g (see also Table 4.1 , and Box 4.2) on the petri dish; (6) add a small amount of tapwater or isotonic solution to the dish to keep oocytes moist; (7) repeat steps 4-6 for a second (replicate) sub-sample; (8) count and record the number of oocytes in each sub-sample under a dissecting microscope, either manually or with image analysis software (see Section 4.2.5).

4.2.5 Oocyte counting and size measurement using particle analysis

Image based particle analysis can be a very effective tool for oocyte counting and size measurements (Thorsen & Kjesbu, 2001). Typically oocyte counting is performed on ovary subsamples

taken gravimetrically or volumetrically with the purpose finding the oocyte density (n/g), which is multiplied by ovary weight to calculate total or batch fecundity. Oocyte frequently used as a measure of maturity, stage of spawning, or to estimate potential fecundity using the auto-diametric fecundity method (Thorsen & Kjesbu, 2001; see Section 4.6.1.1).

Microscope

A stereomicroscope (Fig. 4.3) or microscope with a high resolution digital camera is usually the best tool for making high quality images of whole mount oocyte samples. However, it is also possible to use a high resolution digital SLR with a macro lens or simply a flatbed scanner (see Section 4.2.7). Most stereomicroscopes found on biological labs have sufficient optical resolution and quality for this purpose since these pictures are usually taken using low magnification (6-10x) and colour is not important. The sample illumination is however a critical factor that determines the quality of the image. It is usually best to use transmitted light (light from underneath) and the light source should ideally be able to illuminate the whole sample area evenly. Unfortunately, most light sources are stronger in the centre compared to the periphery (Fig. 4.4). To a certain degree this can be compensated for using a subtract background function in the image analysis software (see below), but for optimum quality the light source should be as even as possible. It is also very important that the light source results in high contrast between the oocytes and the bright background. Using some light sources transparent previtellogenic or early vitellogenic oocytes are almost invisible because of poor contrast (Fig. 4.5). If the light source is covered by protective glass this should be clear glass and not the matte type which

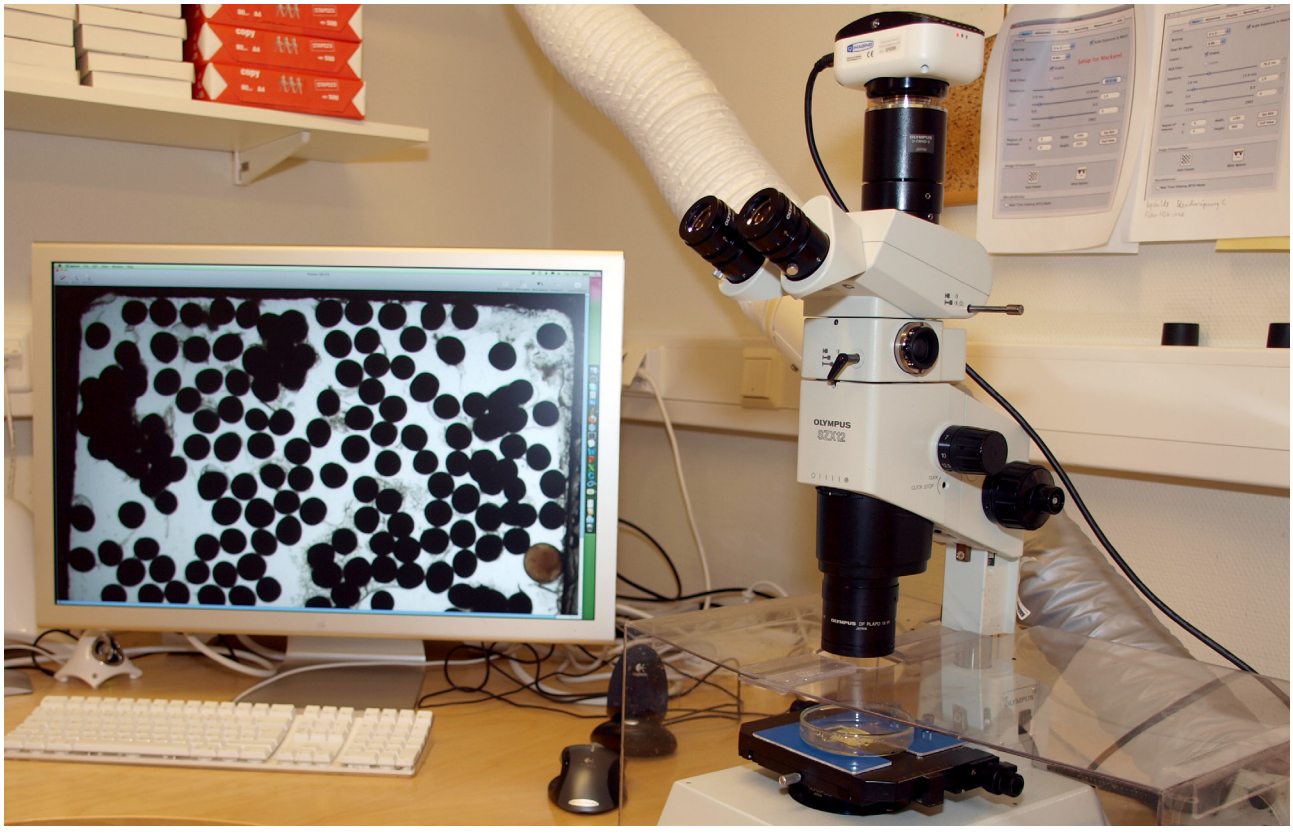

Figure 4.3.

Equipment for fecundity work consisting of stereo microscope with transmitted light and 5MP camera. The microscope is used in a fume hood to protect the user from formaldehyde gas.

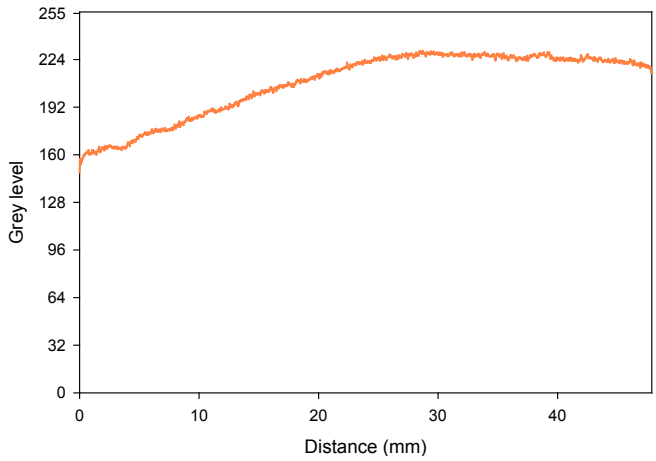

Figure 4.4.

The grey value measured along the diagonal between upper left corner and lower right corner in a background image taken from a stereo microscope. The gradient found here can be considered typical for a stereo microscope and acceptable if using software background correction. A grey value of 0 corresponds to black while 255 corresponds to white.

may reduce contrast considerable. Before buying a microscope for fecundity work it is recommended that these matters are tested on real samples.

Microscope camera

For efficient sample workup it is usually best to combine a high-resolution camera (≥ 5 MP) with a large field of view obtained by low microscope magnification (6-10 x). Specialized microscope cameras seldom have higher resolution than 5 MP since higher resolution usually do not result in improved image quality due to optical limitations in microscopes. Digital SLR cameras can also be used for this type of work, either coupled to the microscope with an adapter (http://www.lmscope.com), or by using a macro lens. In general SLR cameras are capable of capturing excellent images and because of mass production they are usually less costly than specialized microscopy cameras.

Many SLR's can be set up with a computer for teth

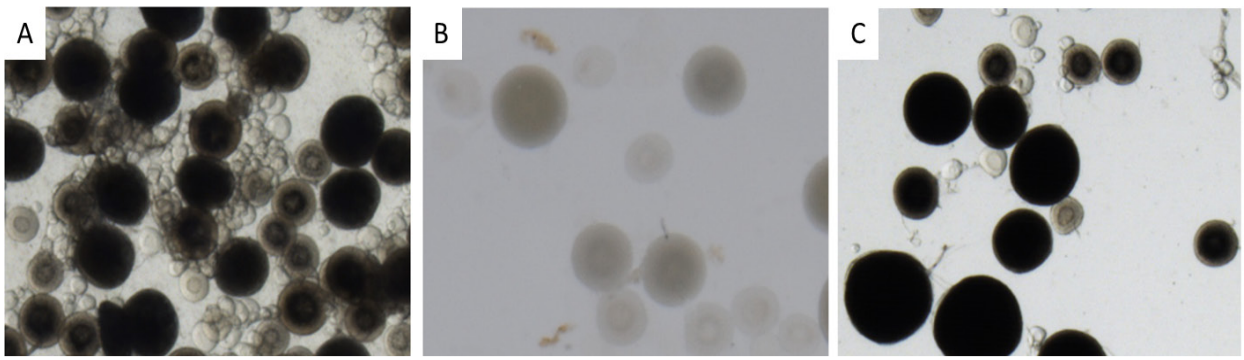

Figure 4.5.

Image quality and sample preparation for fecundity analysis. A: Oocytes have not been sufficiently separated and oocytes are aggregated in dense clumps. Accurate sample work up will not be possible neither in automatic mode nor in manual mode. B: The image has low contrast and transparent and semitransparent oocytes cannot be properly detected. C: Image suitable for fecundity analysis; good contrast and oocytes are sufficiently separated.

ered shooting with live preview on the computer screen and direct computer storage of images. However, for use with a microscope they are in general more complicated to handle than specialized microscope cameras. A typical SLR camera has 10-20 knobs and a large number of menu items which are meant to deal with a wide variety of situations. In contrast a specialized microscope camera seldom has any knobs at all and the menu items on the computer screen are limited and streamlined for microscopy use.

Photographic chamber

The sample can be placed on a Petri dish or something similar for photography. If it is mandatory to count all the oocytes in the subsample it can be useful to restrict the sample area on the Petri dish to an area that exactly fits the area of view in the picture. The sample is then spread in the photographic chamber (Fig. 4.6) and a picture is taken. If it is not possible to fit the entire sample into one chamber the sample is divided into two or more parts and images taken subsequently. The photographic chamber is filled to the rim. The construction prevents the liquid from forming a curved surface above the sample material that would have resulted in optical aberration. The curved part of the surface will be close to the rim and outside the more restricted sample area.

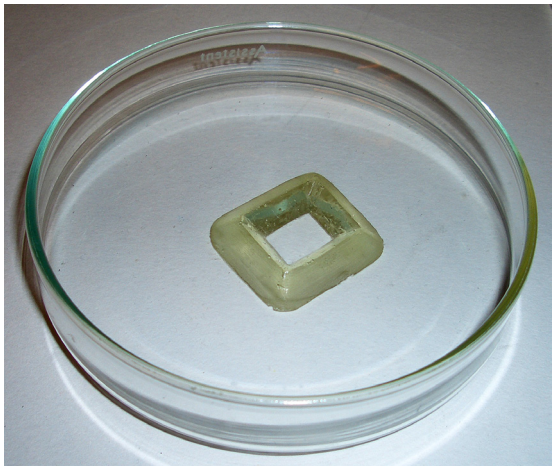

Figure 4.6.

Photographic frame glued to the bottom of a petri-dish. The bottom of the photographic chamber is slightly smaller than the photographic area. The walls of the chamber is 0.5 cm high and have an inside angle of 45 ° so that they will not cast shadow on the sample.

Sample preparation

For precise and efficient particle analysis the sample should be treated so that as many oocytes as possible are free from other oocytes and connective tissue. For some species, like cod and herring, oocytes separate well simply by inhalation into a pipette with a narrow opening and subsequent expulsion into the photographic chamber. For other species, e. g. mackerel, the process is more laborious demanding in addition work with needles and forceps or other means (see Section 4.2.4). However, the amount of work needed for separation of oocytes is not only dependent on qualities of the ovary material, but also the purpose of sample analysis. If the purpose is simply to measure the size of vitellogenic (maturing) oocytes it is usually not necessary to measure all oocytes in the sample since the measured oocytes can be considered randomly selected (Thorsen & Kjesbu, 2001). Thus for size measurements, crude sample preparation may be sufficient. If the purpose is to measure and count all oocytes in the sample, as in gravimetric fecundity counting, separation should be better. All oocytes that are not detected automatically will have to be measured or counted manually, which can be a time consuming and tedious process. In addition to the techniques described above there are also examples from the literature of using special chemical treatment to help separating oocytes (see Section 4.2.4). The most known is probably Gilsons Fluid (Simpson, 1951; Witthames & Greer Walker, 1987). However this treatment usually demands 6-8 months, cause considerable shrinkage and degradation of the oocytes, and results in considerable amounts of toxic waste.

In some cases it can be advantageous to use stain (see Section 4.2.6), particularly if semitransparent objects such as follicles in the previtellogenic, cortical alveoli, hydrated stages are to be measured or counted.

Image quality

The first step in a particle analysis procedure is to make images of the samples. Most commonly such images are made with transmitted light (from underneath), and the oocytes will be seen as dark objects on a bright background (Fig. 4.5). Since this type of particle analysis is based on grey-scale thresholding it is very important to standardize the light settings. Practically this can be achieved by setting the background light to the same value every time (Fig. 4.7). An image resolution of approximately 0.2 px/µm is usually a good choice for this kind of work. At this resolution it is possible to properly see and measure oocytes in the transition phase between pre-vitellogenesis and vitellogenesis (typically 150-250 µm) and at the same time be able to have a large field of view so that many oocytes (>100) can be counted and measured in the same picture. As discussed in the microscopy section it is important that the image has enough contrast for proper thresholding and detection of the oocytes. This is mainly a light source issue; however, some image post-processing adjustments ("Level" or "Gamma" tool) can also be made for better visibility

Image analysis software

There are several image analysis programs that can successfully be used for fecundity work. However, for this text we will limit the description to the open source Image analysis program ImageJ (http://rsb.info.nih.gov/ij) added the plugin ObjectJ (http://simon.bio.uva.nl/objectj). ImageJ is programmed in Java, which means that it will run both on Linux, Macintosh and Windows computers.

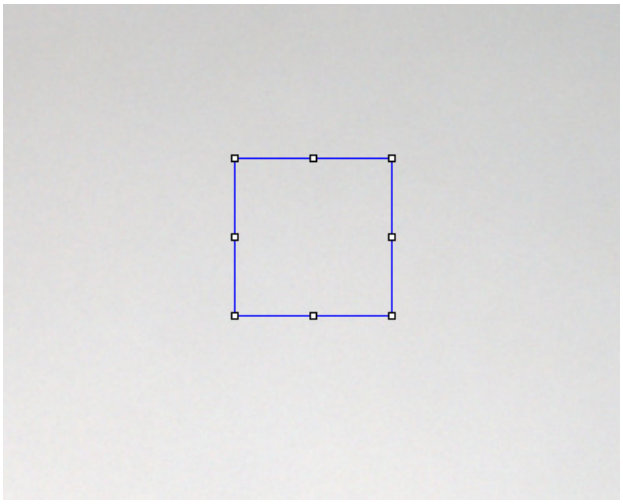

Figure 4.7.

Bacground light is standardized by measuring the light in the middle of the picture. The measuring area must be clean and free of particles. It is important that grey tone in all parts of the image is below maximum (white = grey level 255). In the paper by Thorsen et al. (2001) a grey value corresponding to 206 ± 2 was used as the set point for the measured area. The set point can be achieved by iteration; adjust the light on the microscope, or preferable the exposure time of the camera and then subsequently measure the grey value in the image analysis software until the set point has been found. This procedure is repeated every time equipment is started for a new batch of images to be captured.

The program can be downloaded for free and a vast amount of plugins and macros are available for specialized analysis, including fecundity work. Probably the most advanced software for fish fecundity work is the ImageJ/ObjectJ project Oocytes (http://simon.bio.uva.nl/objectj/examples/oocytes). This software enables the user to measure and count round and oval oocytes both automatically and manually. In addition the user has the possibility to manually stage the oocytes based on visual interpretation.

Using automatic particle analysis to count and measure oocytes

This section describes step by step the automatic particle analysis procedures of the Oocytes project. For routine work the user may not have to know and understand all these matters, but in case something

does not work as expected, or special adaptions have to made for new species, it is an advantage to understand the procedure so that proper adjustments can be made.

The most common adjustments can be set in the Mark oocytes dialog (Fig. 4.8) while the skilled user may do even more changes in the oocyte macro text.

1. Grey-scale conversion

In most cases the camera that is used is a colour camera. Since the particle analysis procedure only can use an 8 bit (256 levels) grey-scale image, the first step in the procedure is therefore to convert the colour image to a 8 bit grey-scale version.

2. Substract background

During this step the Substract background function is applied. This means that an uneven background illumination will be evened out. In many cases this is an important step since most microscopes do not produce a flat illumination. Be aware though that this procedure use a "rolling ball" procedure where the radius of the ball (in pixels) should be at least as large as the radius of the largest object in the image that is not part of the background. In the oocytes project this value is set to 100, which works for most samples. However if your oocytes are very large this value might be too small and should be increased. In such case this has to be done in the macro text.

3. Thresholding

When the background illumination has been flattened out, the image is ready for thresholding. During this process, pixels in the image that have a grey value low er than a certain threshold value are selected (default value is 180). The selected dark pixels become black while the brighter unselected pixels become white, converting the grey scale image to a binary image (Fig 4.9B). The threshold value can interactively be changed in the Mark Oocytes dialog. The value should ideally be set so that only the maturing (vitellogenic) oocytes are selected. This is usually somewhat possible since vitellogenic oocytes are usually darker than previtellogenic oocytes and connective tissue.

4. Erode and dilate

In the binary image the vitellogenic oocytes will appear as black objects on a white background. However, visual inspection (Fig. 4.9B) reveals that a few small pre-vitellogenic oocytes and some small fragments of connective tissue have also been selected. To remove as many of these small objects as possible, an erosion-dilation procedure is applied. The first step in this procedure is the application of an erosion filter in which the black objects are eroded from the edge. By default this filter is applied four times. Each time the filter is applied the objects shrink in size and rough edges caused by fragments of connective tissue or previtellogenic oocytes are evened out. In addition smaller objects may disappear completely. In the next step the dilation filter is applied the same number of times such that remaining objects regain their original size but have smoother

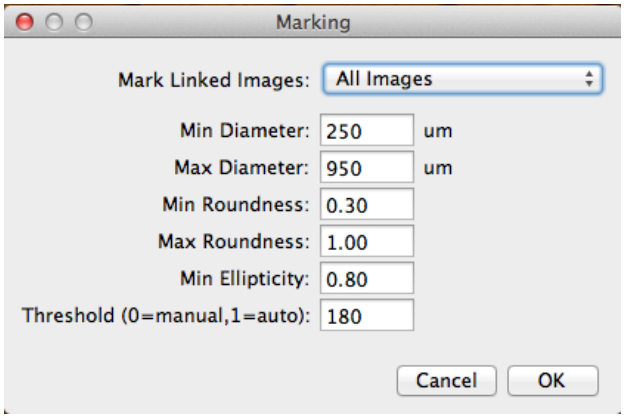

Figure 4.8.

Particle analysis control panel in the ImageJ/ObjectJ oocytes project. The user can decide to analyze only the open front image, all linked images, or all unmarked (not analysed) linked images. In addition the user can set threshold values for particle size, roundness and ellipticity. Grey level threshold can be set to a fixed value or adjusted interactively.

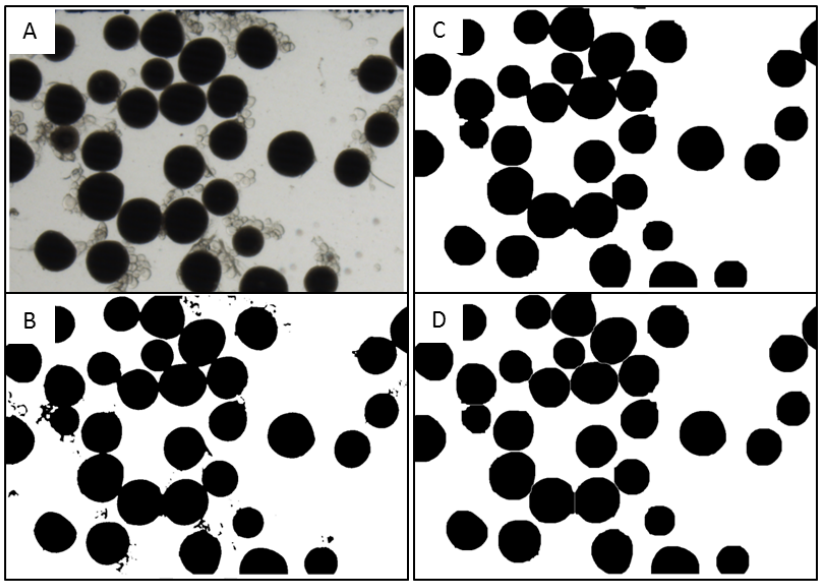

Figure 4.9.

Major steps during particle analysis. A: Original picture of oocytes. B: Binary image resulting from grey-scale thresholding. C: Binary image after application of erode and dilate filters. D: Binary image after the watershed procedure. Note the narrow (1 px) openings between the oocytes.

edges. Smaller objects may have disappeared completely (Fig. 4.9C). The number of erosion and dilations can be changed in the macro text.

5. Watershed

After the previous step the binary image contains objects mainly consisting of vitellogenic oocytes. However, these oocytes will often be attached to each other such that two or more oocytes appear as one large object. A watershed filter is applied to the image to separate these attached oocytes, before particle analysis. This filter is a special variant of an erosion-dilation procedure and after use most connected oocytes will be separated (Fig. 4.9D).

6. Particle analysis

The binary image is now ready for particle analysis. During the particle analysis procedure all the black objects are selected and size measured. However, to further improve our selection of objects of interest we will set up a selection filter based on some key threshold values on size and shape-factors (Fig. 4.8). Typically we chose minimum and maximum particle size according to our previous knowledge about the oocytes size range. Also we apply threshold values on roundness (minor axis/major axis) and ellipticity In this case ellipticity can be understood as a shape factor that describes how well the object conforms to a perfect elliptic shape (note that a round object also is included in this definition of an ellipse). Round or elliptic particles with a completely smooth edge will have a value of 1, less smooth objects will have smaller values. These threshold values can be changed in the oocyte particle analysis dialog.

Manual counting and measuring

Automatic particle analysis is seldom perfect and usually some oocytes are left out or are measured incorrectly. If the purpose of the analysis is to count or measure all the oocytes in the sample the remaining oocytes have to be measured or counted manually. In the Oocytes project a special tool (Variable ellipse

tool) has been developed for manual measurements of oocytes (Fig. 4.10). The tool can efficiently help the user to measure both round and elliptic oocytes as well as categorize (stage) them. For fish species with a clearly determinate spawning strategy the maturing oocytes can be clearly distinguished from the much smaller and more transparent pool of previtellogenic oocytes. However, when working with indeterminate species (e. g. horse mackerel or hake) this can be difficult since there is no clear size gap between the previtellogenic and the vitellogenic pool. In such cases the procedure is often to measure or count the oocytes above a certain size threshold. In the Oocytes project the circular size measuring tool (the moving circle) also function as a size reference tool (Fig. 4.10) that follows the mouse pointer. The user can manually adjust the size of the moving circle so that it exactly fits with the size threshold. Then the user can easily see which oocytes are above or below the size threshold by holding the circle above the oocyte in question.

4.2.6 Whole mount staining

For whole mounts image analysis, it is necessary to separate the particles (i.e. oocytes) and sometimes, depending on the image analysis tools, to stain the ovary subsample to improve the contrast of the particles in the image. Several stains are used to improve the identification and measurement of developing oocytes. For example, eosin and PAS are used to stain plaice, cod, and mackerel oocytes respectively with relative success (Greer Walker *et al.*, 1994; Kennedy *et al.*, 2007; Whittames *et al.*, 2009) whereas Rose of Bengal is

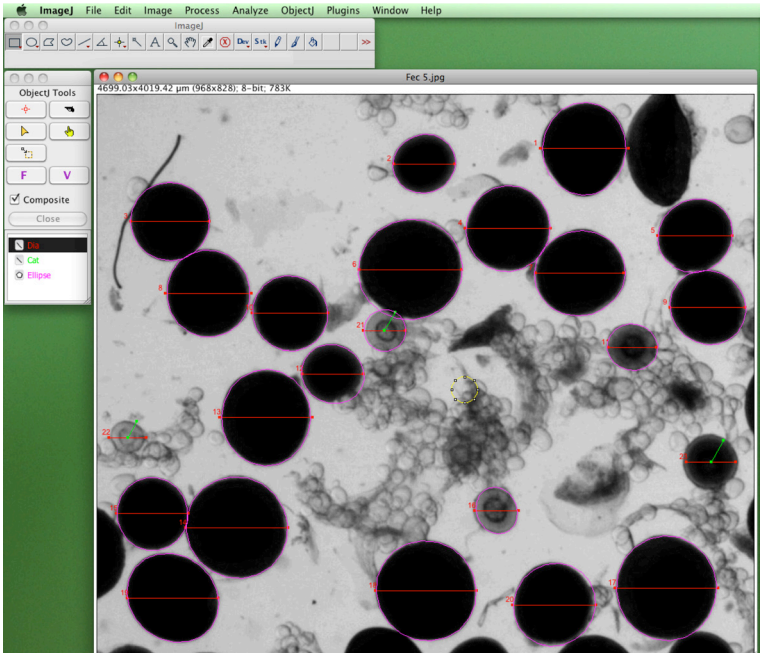

Figure 4.10.

Particle analysis using the Oocytes project in ImageJ/ObjectJ. Using automatic particle analysis each detected oocyte is surrounded by the best-fitting ellipse. Each detected oocyte also get a horizontal line that represents the diameter of a perfect circle with the same area as the surrounding ellipse. Manually measured oocytes (number 21 and 22) will get the same markings although oocytes measured as perfectly round will only have the horizontal red line. The manually measured oocytes also get a green line that by the analogy of a clock show the category (1-9) that the user have assigned to the oocyte. The automatic measured oocytes can manually be assigned to categories by pointing at them and using keyboard shortcuts (1-9). The yellow circle in the lower left part of the image is the moving circle that follows the mouse pointer and functions as a manual measuring tool and size reference.

used to stain European hake oocytes on whole mounts. Rose of Bengal stain is originally used for detecting micro-organisms in the soil or in benthic macrofauna sampling (Rumohr, 1999) allowing the distinction of organic matter from inorganic at the time of collection. The different stains are produced combining water soluble with 1% eosin and 0.02% rose of Bengal weight to volume dissolved in buffered formaldehyde solution, respectively. The concentration of PAS varies from 1% to 15% weight to volume (Whitthames *et al.*, 2009).

Staining allows to improve further segmentation in the image processing of developing oocytes, especially of translucent oocytes such as those at cortical alveoli, early vitellogenesis, hydration or POFs. The main disadvantage of these stains is that they tend to leach out and require washing the sub-sample. Standard procedure is to immerse the oocyte sub-sample in stain solution for 1 day. Nonbound stain is removed from the sub-sample by smoothly spraying through a mesh sieve that retained oocytes larger than a certain size (for example for European hake a mesh size of 125 µm is used in potential fecundity studies as the cortical alveoli oocyte diameter range 150-250 µm (Murua & Motos, 2006); however, similar results might be achieved simply by flushing them with tap water into a sieve (Section 4.2.4)

4.2.7 Low cost alternatives to microscopy

As mentioned above (section 4.2.5), high quality digital images may be captured with a flatbed scanner (FS) taking the place of a microscope and camera. Using an FS coupled with free image analysis software can result in a very low cost setup. FSs have been used to capture detailed images of American shad (Friedland *et al.,* 2005), haddock, American plaice (Klibansky & Juanes, 2007), Atlantic cod (Klibansky & Juanes, 2008, 2007), and European anchovy (Orfanidis & Ganias, 2011) oocytes, which were then measured and counted using image analysis software and procedures similar to those described in section 4.2.5.

FSs are primarily designed to capture images of flat objects like photographs or pages of text, so they have a very limited depth of field compared to most cameras. But for the purposes of scanning fish oocytes which are usually less than 1mm in diameter, the depth of field available in certain types of FSs should be quite adequate. Depth of field in FSs is largely dependent on the type of light sensor it uses and for this reason scanners that use contact image sensors (CIS) are likely to produce disappointing results when scanning three-dimensional objects like oocytes. FSs that use CIS chips tend to be thin, lightweight, and very portable, but capture images in such a way that portions of an object not in direct contact with the scanner glass become blurred (Fig. 4.11A). In contrast, FSs that employ charge coupled device (CCD) sensors capture images in much the same way that digital cameras do and the depth of field is much greater (Fig. 4.11B, C and D) and d. A light inside the scanner illuminates the object causing an image of that object to be reflected by a series of mirrors onto a lens, which focuses the image onto the light-sensitive CCD sensor array. The CCD sensor array essentially serves the role of the film used in film cameras. FSs also vary in terms of the quality of optics and the size of the CCD sensor arrays. Larger arrays contain more sensors resulting in higher optical resolution. FS manufacturers often advertise interpolated resolution or maximum resolution values higher than the optical resolution, but the most relevant value is the optical resolution.

Though it might be fruitful to scan images of oocyte samples on several FSs side by side to find which produced the best results, it seems not to be a necessary exercise. Friedland *et al.* (2005) produced clear images

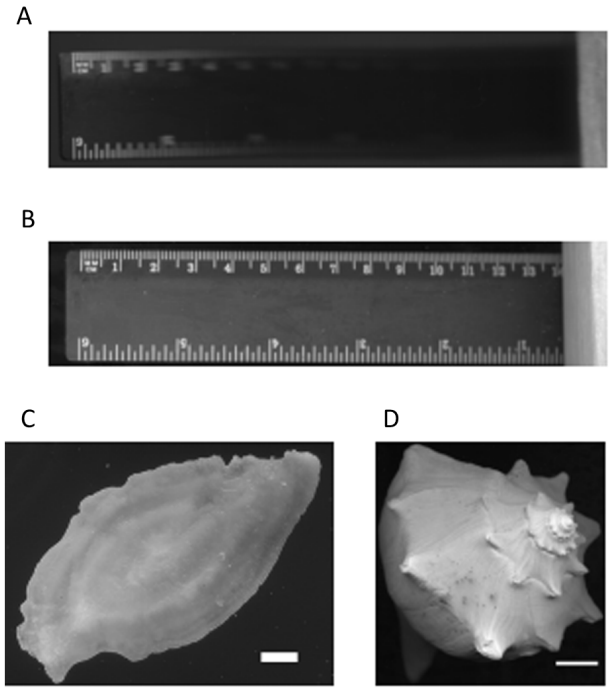

Figure 4.11.

Image of a ruler where the right end was raised up on a 3.8cm block of wood and scanned on two different flatbed scanners. Note the minimal depth of field in image (A) captured with a CanoScan LiDE 200 which uses contact image sensors (CIS). Only the edge of the ruler touching the glass can be seen clearly. The depth of field is much higher in image (B) captured with an Epson Perfection V500, which uses charge coupled device (CCD) sensors. CCD scanners can be used to capture detailed images of small three dimensional objects like an (C) otolith (2400dpi; scale bar = 1mm) or large ones like a (D) whelk shell (2400dpi; scale bar = 10mm).

FS with CCD sensors (Hewlett Packard Scanjet 4400C; 1200dpi optical resolution) which had good optical resolution for the time, but which is low compared to FSs available today. When devising their setup, Klibansky & Juanes (2008) first tested one of the less expensive models with CCD sensors available at the time (Epson Perfection 1670; 1600dpi optical resolution), found it to produce very clear images of vitellogenic oocytes (Fig. 4.12), and used it for the remainder of their research.

In an ongoing fecundity study on black sea bass (*Centropristis striata*) at the University of North Carolina Wilmington, Klibansky & Scharf tested a similar FS model with CCD sensors (Epson Perfection V500 US; 6400dpi optical resolution) and found that it also produced very clear images of vitellogenic and hydrated standard FS models with CCD sensors would be capable of capturing oocyte images sufficient for image analysis.

There are advantages to using a flatbed scanner

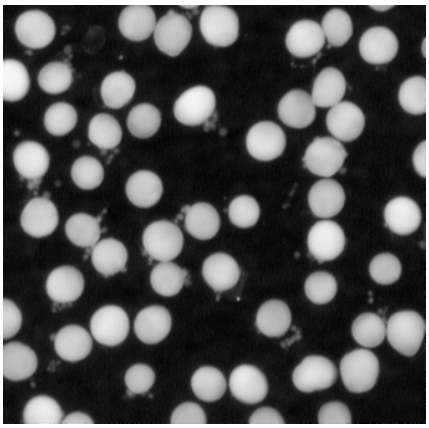

Figure 4.12.

Cod oocytes preserved in 10% formalin scanned on an Epson Perfection 1670 flatbed scanner at 1600dpi.

over a camera and a microscope in addition to the much lower cost. The large field of view allows many oocytes to be captured in a single image compared to images captured with a microscope camera (Fig. 4.13). One could potentially capture an image as large as the scanner glass, which is usually at least 22 X 28cm. The image capturing procedure is also very easy to standardize since the scanned object is lit from within a contained space. However, this also means that lighting cannot be varied in as many ways as with a microscope setup. The quality and detail of FS images is generally not as high as when using a microscope setup, though current FSs have high enough optical resolution that even some details of individual oocytes like oil droplets are visible (Fig. 4.13B).

Capturing an image of oocytes with an FS has many of the same requirements as capturing an image with a microscope setup. Most importantly, the oocyte cohort one is interested in counting should be well separated from other oocytes, and debris in the sample should be minimized. Oocytes should be spread out so that they are not touching, in a single layer against a contrasting background. The FS lights the sample and senses reflected light from beneath, making oocytes appear pale, and thus a black background should provide the highest contrast. A Petri dish makes a good container for spreading out oocytes for scanning because it is wide, shallow, and has a flat bottom. However, reusing Petri dishes tends to lead to scratches and water spots that add noise to the image, so it may be preferable to use them once for imaging, then wash and retire them to another use. Trying different dark backgrounds will help researchers find one that provides the best contrast for their particular setup. The lid of a Petri dish blackened with paint or black paper works well. A cylinder, open on one end, about twice the depth and 1.5 times the diameter of a Petri dish, made of stiff black paper provided the best background in the setup used to capture the images in Figure 4.13A and B. The reflectivity of the background (e.g. matte versus glossy paper) and even the shade of black can affect contrast with oocytes and light scatter around the sample which adds to image noise. Time spent preparing the sample for scanning in ways that improve image quality usually decreases time spent processing images so it can be valuable to work out these details beforehand. Most FS software allows one to change many scan settings and save them to be used later. By doing this, one can easily assure that all images are scanned the

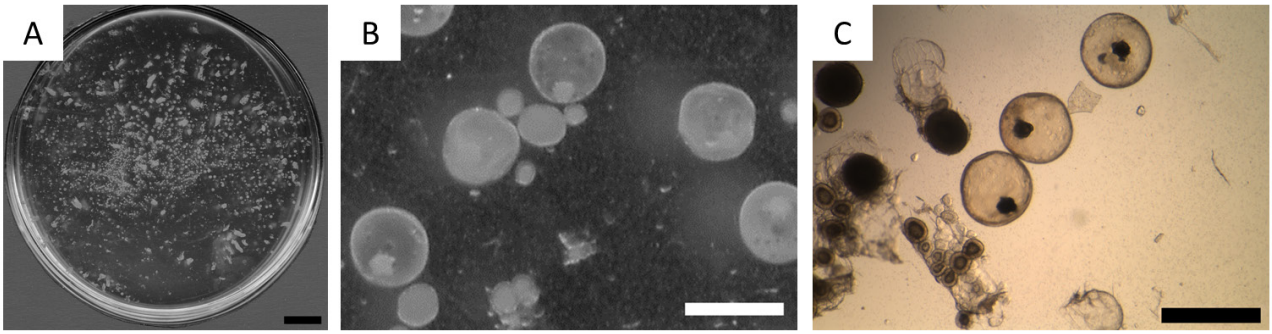

Figure 4.13.

A flatbed scanner (Epson Perfection V500) was used to capture (A) an image of an entire Petri dish of black sea bass oocytes at the 2400dpi (image size = 67.2MB; scale bar =10mm). (B) Zooming in on oocytes from the scanned image shows that even the oil droplet in many hydrated oocytes can clearly be seen (scale bar = 1mm). (C) Oocytes from the same sample photographed with a camera mounted on a dissecting scope (Zeiss Stemi SV6; scale bar = 1mm) show better detail, but permit a much smaller field of view to be photographed at a time. This image shows the entire field of view that could be captured by the camera.

same way. The main image settings to set are the image resolution, image type (e.g. greyscale, color), the marquis size and placement, and image format (e.g. bitmap, tiff). Image resolution is important because it determines how detailed the image will be, though it also greatly influences file size. Very large files can quickly fill up storage space on a hard drive, but more importantly may greatly slow down certain image processing procedures. Thus it is sometimes preferable to scan images at a resolution that is lower than the FS's optical resolution. Image type also influences file size and can be somewhat dependent upon image processing software since some procedures must be run on certain types of images. The marquis setting allows the user to tell the FS the location and size of the area of the glass to scan. By physically marking the portion of the glass corresponding to the marquis with a template, one can be sure to place the sample dish in the exact location of the marquis to streamline processing. Also the marquis setting allows one to assure that all images are exactly the same size, which is very helpful when devising image processing routines. Various image formats are available, but tagged image file format (TIFF; file extension ".tif") is typically preferable because it preserves greyscale or color data for each pixel in the image without compressing or averaging data over portions of the image.

4.3 Stereological estimation of fish fecundity

4.3.1 Basic principles

Estimates of fecundity in fishes can also be obtained by applying stereological methods to histological sections of the ovaries. Stereology is the science of the three-dimensional interpretation of bidimensional images. Stereological applications provide quantitative information about 3-D structures from measurements made on 2-D sections. The first practical stereological method was based on the Delesse Principle, which states that the fractional volume of a component in a material is proportional to its fractional cross-sectional area. So far, the most widely used stereological procedure to estimate fish oocyte numbers (Christiansen *et al.*, 1973; Christiansen & Weiss, 1974; Emerson *et al.*, 1990; Macchi Wöhler, 1994; Greer Walker *et al.,* 1994, Bromley *et al.,* 2000, Coward and Bromage, 2002; Medina *et al.*, 2002, 2007; Murua *et al.*, 2003; Cooper *et al.*, 2005) is based on the equation developed by Weibel & Gomez (1962). As this method relies on assumptions about particle shape and size distribution (i.e. a model-based method), it should not be used to count objects of irregular shape and/or highly variable size, such as atretic or postovulatory follicles. Unlike model-based methods, the Disector Principle (Sterio, 1984) provides unbiased estimates of the number of objects in a given volume of tissue (numerical density, N_V) with no need for assumptions, models, or correction factors. The disector is actually a three-dimensional technique, as it performs counts of particles in volumes delimited by pairs of parallel planes separated by a known distance, with a frame of known area superimposed on the sections. Hence, the method allows unbiased estimates of numbers irrespective of the particle's physical features (Howard & Reed, 2005). Both of the above methods provide estimates of the number of particles (N) from numerical density estimations extrapolating N_V to the whole volume (V) of the reference space ($N = V \cdot N_V$). Therefore, the volume of the organ should be known. The ovarian volume can be measured either directly by the fluid displacement method or obtained using Cavalieri's principle (Michel & Cruz-Orive, 1988). Measurements of the ovarian volume on-board sampling vessels are frequently difficult or impractical. In such circumstances, it may be useful to define a priori the function that best fits the relationship between the gonad volume and its mass, such that ovary volumes can be reliably estimated from weight data.

Another disadvantage of these stereological procedures is that they are significantly affected by volume changes following tissue processing for microscopic examination. This problem may be overcome with frozen section procedures, as the frozen ovarian piece keeps the original shape and volume (Christiansen & Weiss, 1974; Macchi & Wöhler, 1994). Paraffin embedding of formaldehyde-fixed tissues enables the production of thinner sections and high-quality microscopic images, but has the major drawback of tissue shrinkage by about 30% (Medina *et al.*, 2007) to 50% (Dorph-Petersen *et al.*, 2001) in volume reduction. Other fixatives (e. g., Bouin's solution) and embedding media (e. g., resins) appear to result in lesser tissue retraction, but the proportion of volume losses should be calculated in all cases in order to correct for N_V and N overestimations caused

by shrinkage of the histological specimens. This section is intended to provide some rudiments of stereology and its application in the context of fish reproduction assessment and fisheries research. It does not comprise a full description of stereological methods, but is rather conceived as a practical introductory reference that might serve as a basic guideline and should be widened with the relevant specialized literature.

4.3.2 Model-based methods

4.3.2.1 The Weibel method

A stereological procedure that has been often adopted for counting the fish ovarian follicles is the one based on the formula (Weibel & Gomez, 1962; Weibel *et al.*, 1966):

$$N_V = \left(\frac{K}{\beta}\right) \cdot \left(\frac{N_A^{3/2}}{V_V^{1/2}}\right) \qquad 4.3$$

where N_V is the numerical density (number per unit volume) of the considered follicle type, K is a size distribution coefficient, β is a shape coefficient, N_A is the number of profiles per unit area, and V_V is the partial area or volume fraction (also known as volume density). N_V is usually calculated on about 10 randomly chosen fields from separate histological sections of the ovary.

For each follicle category, β is determined as a function of the axial ratio λ (long axis/short axis), according to the graph provided by Weibel (1969), assuming that all ovarian follicles conform to an ellipsoidal shape. K is defined as: $K = (D_3/D_1)^{3/2}$, where D_1 and D_3 are the first and third moment of the size distribution. To determine the minimum number of measurements needed to calculate λ and K, measures from multiple sections of the relevant follicle category are taken until the data become stable about an asymptotic value. In a study on bluefin tuna ovaries, for example, the values of both λ and K became stable from 40 measurements in all follicle types (Aragón, 2010). Depending on the follicle type, K varied between 1.01 and 1.19, and the estimated value of β ranged from 1.4 to 1.52 (Medina *et al.*, 2002).

N_A is the number of transverse sections of oocytes per unit section area, and is obtained from the number of oocyte profiles lying within the stereological test system divided by the test surface area; transections that are cut by the right and upper margins are counted, whereas those cut by the left and lower margins are rejected (Fig. 4.14). In the original methodology, V_V is calculated by the superimposition of a stereological test grid system on to the micrographs, then counting the number of points of the grid that overlay the transections of the considered particle and dividing it by the total number of points in the test system area. V_V can also be determined by image analysis of digital micrographs using suitable computer software (Fig. 4.14).

4.3.2.2 Ovarian packing density

Another model-based method that has been used in estimations of fish fecundity involves the prediction of oocyte density from its relationship with oocyte size. The first trial is to estimate the fecundity on the assumption that oocytes are perfect sphere and the specific gravity equals to unity (Kucera & Kennedy, 1977; Hunter et al. 1989) and that the fractional volume of the standing stock of oocytes equals to unity. The second trial is just fitting a curve on the relationship between oocyte packing density (number of oocytes per a gram of ovary) and the mean diameter of the advanced oocytes (Thorsen & Kjesbu, 2001;Witthames et al. 2009). The most recent trial is oocyte packing density theory which considers the fractional volume, the shape, and the specific gravity of the advanced oocytes (Kurita & kjesbu, 2009; Korta et al., 2010b).

Packing density of a specific follicle in the ovary

Packing density of a specific follicle in the ovary

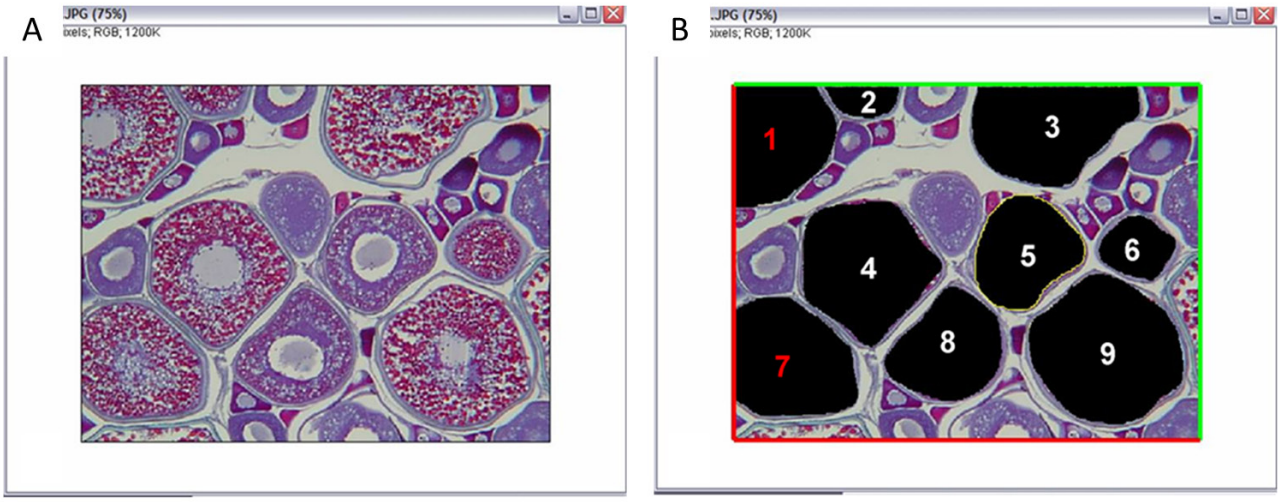

Figure 4.14.

Quantification of large yolked (late vitellogenic) oocytes by a modification of the model-based stereological method of Weibel and Gomez (1962) using image analysis on 6-µm ovarian paraffin sections. The numerical density of oocytes (N_V) is estimated from the equation $N_V = (K/\beta)\cdot(N_A^{3/2}/V_V^{1/2})$. Usually, about ten images are analyzed per sample. First, all the oocytes belonging to the stage to be quantified are selected manually and their fractional area (V_V) is obtained by image analysis as the total area of the oocyte transections related to the total test area, which is equivalent to 1.072 mm^2. N_A is calculated dividing the number of oocyte sectional profiles lying within the test area by the test surface area; transections (1 and 7) that are cut by the forbidden margins (red lines) are rejected, whereas those (2 and 3) cut by the admittance margins (green lines) are counted (in this example, N_A = 7/1.072 mm^{-2}). The parameters K (1.025) and β (1.418) for this specific oocyte type were previously calculated as described in the text.

(follicle packing density: FPD) indicates the number of the follicles per gram ovary. Thus, the total number of the follicles in the ovary can be estimated as FPD times the ovary weight (see also the Section 4.6.1.1 on the auto-diametric method).

The fundamental concept of a specific follicle (or oocyte) packing density in the ovary bases on the volume relation ship between the follicles and the ovary:

$$FPD = \frac{(V_{1g\ ov})\cdot(VF_{foll})}{(MV_{foll})} \qquad 4.4$$

where:

$V_{1g\ OV,}$ volume of 1g of ovary, VF_{foll}: volume fraction of a specific follicle in the ovary, MV_{foll}: mean volume of a specific follicles in the ovary

When these three terms on the right side of the Eq.(4.4) are acquired, the packing density of any follicles; i.e. vitellogenic oocytes and atretic oocytes (Kurita & Kjesbu 2009), pre-vitellogenic oocytes (Korta *et al.,* 2010b), and POF in the ovary can be calculated. Volume of 1g ovary is estimated with the specific gravity of the ovary (ρ_o: g cm-3) as ($1/\rho_o$). Specific gravity of the ovary is usually estimated from the relationship between ovary weight and ovary volume; however, it can also be estimated using %water, %lipid and %solids data (Kurita & Kjesbu, 2009). The volume of the ovary can be measured by the displacement of 0.9% saline water (Witthames, 2001). Volume fraction of the follicles is estimated with standard grid count (Delesse principle: Howard & Reed, 1998). Mean volume of the follicles can be estimated by, for example, Cavalieri method (Howard & Reed, 1998) or 3D-reconstruction (Korta *et al.* ,2010c). In the case of oocytes, size measurement

(long and short axis) also gives the approximate volume. This method is useful to estimate the number of very small follicles (e.g. pre-vitellogenic oocytes and POF) which are difficult to count with binocular microscope. The understanding of FPD equation (4.4) is also useful to select the most appropriate fitting curve(s) on the observed FPD (especially vitellogenic oocyte packing density)–oocyte diameter (OD) relationship, which have been empirically established for determinate and indeterminate spawners (Witthames *et al.,* 2009) and are the key formula of the auto-diametric method (Thorsen & Kjesbu, 2001; Section 4.6.1.1).

Oocyte packing density (OPD)

The concept is the same as Eq. (4.4). More specifically, OPD (g^{-1}) is expressed as,

$$OPD = \left(\frac{1}{\rho_0}\right) \cdot \left(\frac{V_{vto}}{V_{ova}}\right) \cdot \left(\frac{1}{OV_{vto}}\right) \quad 4.5$$

Where,

ρ_o is specific gravity of the ovary (g cm^{-3}), V_{vto}: total volume of vitellogenic oocytes in the ovary (cm^3), V_{ova}: ovary volume (cm^3), OV_{vto}: mean volume of vitellogenic oocyte (cm^3). Note that V_{ova} includes ovarian wall, stroma, and all other tissues. Here,

$$OV_{vto} = \sum_i \frac{\left[\left(\frac{4\pi}{3}\right)\cdot\left(\frac{L_i}{2}\right)\cdot\left(\frac{S_i}{2}\right)^2\right]\cdot 10^{-12}}{n} =$$

$$= \left(\frac{\pi}{6}\right) \cdot \sum_i \left\{\left[\frac{8k_i}{(1+k_i)^3}\right] \cdot OD_i^3\right\} \cdot \frac{10^{-12}}{n} \quad 4.6$$

where :

L_i is long axis of the i-th oocyte (μm=10^{-4}cm), S_i is short axis of the i-th oocyte (μm), OD_i is the individual oocyte diameter [(μm); =$(L_i+S_i)/2$], n is number of vitellogenic oocytes which are measured, k_i is ratio of the long and short axis (=L_i/S_i), and Σ_i is summation of the calculated values from the 1st to the n-th oocyte. As the term $[8k_i/(1+k_i)^3]$ in Eq. (3) is almost constant among oocytes in the same ovary, this term approximates to $[8k/(1+k)^3]$, where k is the mean of k_i. In that respect, Eq. (4.6) is expressed as:

$$OV_{vto} = \left(\frac{\pi}{6}\right) \cdot \left[\frac{8k}{(1+k)^3}\right] \cdot 10^{-12} \cdot \frac{\sum_i OD_i^3}{n} =$$

$$= \left(\frac{\pi}{6}\right) \cdot \left[\frac{8k}{(1+k)^3}\right] \cdot 10^{-12} \cdot OD_v^3 \quad 4.7$$

Where OD_V (volume-based mean oocyte diameter; transformed from mean oocyte volume) is defined as

$$OD_v^3 = \frac{\sum_i OD_i^3}{n} \quad 4.8$$

This formula is introduced from

$$\frac{\sum_i\left[\left(\frac{4\pi}{3}\right)\cdot\left(\frac{OD_i}{2}\right)^3\right]}{n} = \left(\frac{4\pi}{3}\right) \cdot \left(\frac{OD_v}{2}\right)^3 \quad 4.9$$

Insertion of Eq. (4.7) in Eq. (4.5) results in

$$OPD = \left(\frac{1}{\rho_0}\right) \cdot \left(\frac{V_{vto}}{V_{ova}}\right) \cdot \left[\frac{(1+k)^3}{8k}\right] \cdot$$

$$\cdot 10^{12} \cdot \left(\frac{6}{\pi}\right) \cdot OD_v^{-3} \quad 4.10$$

or

$$log(OPD) = \log\left\{\left(\frac{1}{\rho_0}\right) \cdot \left(\frac{V_{vto}}{V_{ova}}\right) \cdot \left[\frac{(1+k)^3}{8k}\right]\right\} +$$

$$+12.28 - 3 \cdot log(OD_v) \quad 4.11$$

which are the oocyte packing density formulae published in Kurita & Kjesbu (2009).

Where OD_V is defined differently from Eq. (4.8) as

$$OD_v^3 = \frac{\sum_i (L_i \cdot S_i^2)}{n} \quad 4.12$$

then, the term "$(1+k)^3/(8k)$" in Eqs. (4.10) and (4.11) is cancelled.

Note that OD_V is different from OD_N, which is arithmetic mean oocyte diameter (Table 4.2). Although OD_V is almost equal to OD_N for determinate fecundity species (e.g. Atlantic herring), OD_V is apparently different from OD_N for indeterminate fecundity species (e.g. Japanese flounder) because the size range of vitellogenic oocytes is wide for this type of species. This is especially the case when the ovary contains hydrated oocytes (Kurita & Kjesbu, 2009). Therefore, OD_N can be practically used for OPD-OD relationship only of determinate species (Thorsen & Kjesbu, 2001; Witthames *et al.,* 2009).

The three terms on the right side of the Eq. (4.5) of vitellogenic oocytes have been examined through oocyte growth for a determinate fecundity and single batch spawning species Atlantic herring and an indeterminate fecundity and multiple batch spawning species Japanese flounder. Then, theoretically estimated oocyte packing density (OPD) by Eq. (4.5) and observed OPD by gravimetric method (Section 4.2) have been compared to understand OPD-OD relationships (Kurita & Kjesbu 2009).

Table 4.2.

Simple example showing the difference between volume-based mean oocyte diameter (OD_V) and arithmetic mean oocyte diameter (OD_N). Oocyte is assumed to be sphere. ODi indicates diameter of individual oocyte.

	ODi	ODi3
Oocyte 1	1	1
Oocyte 2	2	8
Oocyte 3	3	27
Mean	2[a]	12[b]

a: $OD_N = \frac{\sum_i OD_i}{3} = 2$

b: $OD_V^3 = \frac{\sum_i OD_i^3}{3} = 12$ Thus, $OD_v = \sqrt[3]{12} \approx 2.29$

Specific gravity of the ovary (ρ_o) and ratio of long and short axis of oocyte (k) do not change largely as oocyte diameter grows. In contrast the volume fraction of vitellogenic oocytes in the ovary (V_{vto}/V_{ova}) changes largely as oocyte grows (Fig. 4.14). This means that Eq. (4.10) mainly consists of two terms which are functions of OD_v, i.e. (V_{vto}/V_{ova}) and OD_V^{-3}:

$$OPD \approx (constant) \cdot \left(\frac{V_{vto}}{V_{ova}}\right) \cdot OD_v^{-3} \quad 4.13$$

The volume fraction varies from 0 at the start of vitellogenesis and is approaching its maximum value as OD_V grows. In the ideal situation that vitellogenic oocytes are perfect sphere (k=1), that ovarian specific gravity equals to unity (ρ_o=1), and that any other stages of oocytes (pre-vitelogenic oocytes) and structures (ovarian wall, blood capillaries, connective tissue, etc.) are negligible [(V_{vto}/V_{ova})=1], OPD-OD relationship [Eqs. (4.10) and (4.11)] can be expressed:

$$OPD = 10^{12} \cdot \frac{6}{\pi} \cdot OD_v^{-3} = (constant) \cdot OD_v^{-3} \quad 4.14$$

or

$$log(OPD) = 12.28 - 3 \cdot log(OD_v) \quad 4.15$$

The latter formula is shown by grey line in (Fig. 4.15D). This is the formula of so-called sphere volume method (Kucera & Kennedy, 1977; Hunter *et al.* 1989). The difference of the actual OPD (solid lines in Fig. 4.15) from the ideal situation (grey line) is mainly due to the volume fraction of vitellogenic oocytes which varies with OD and is approaching to

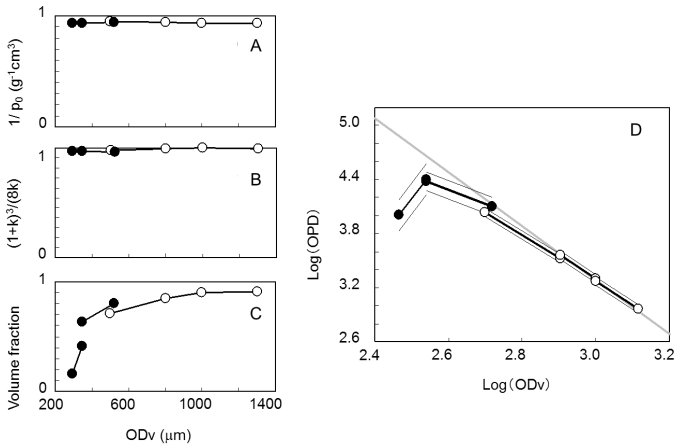

Figure 4.15.

Changes in (A) specific gravity ($1/\rho_o$; $g^{-1}cm^3$) of the ovary, (B) shape factor $[(1+k)^3/(8k)]$ of vitellogenic oocyte, (C) volume fraction of vitellogenic oocytes in the ovary, and (D) oocyte packing density (OPD; log-transformed) with ODv (µm) [log-transformed). Solid circles are for Japanese flounder, indeterminate fecundity species, and open circles for Atlantic herring, determinate fecundity species. Grey line in (D) indicates the line: log(OPD)=12.28–3×log(ODv), when the ovary is hypothesized to consist of only fully spherical vitellogenic oocytes and the ovarian specific gravity is 1 [Eq. (4.15)]. The differences between the log(OPD)-log(ODv) lines and the grey line are due to the term, log $\{(1/\rho_o)\times(V_{vto}/V_{ova})\times[(1+k)^3/(8k)]\}$, in Eq. (4.11). Thin lines indicate 95% confidential intervals period.

the maximum value < 1. This explains why the OPD-OD relationship works so well for determinate species, where there is no de-novo production of vitellogenic oocytes during the current spawning season and thus the fraction of pre-vitellogenic follicles and ovarian structure are getting lower and less variable (Fig. 4.15 (Kurita & Kjesbu, 2009) as oocytes grow (e.g. 360-1390 µm for Atlantic herring). On the other hand, in indeterminate fecundity species continuous production of new vitellogenic oocyte batches and smaller size of vitellogenic oocytes (e.g. 280-630 µm for Japanese flounder) keep the fractional volume of the standing stock relatively low and variable and consequently affects the predictive power of the OPD-OD relationship (Fig. 4.15 (Kurita & Kjesbu, 2009).

Thus, theoretically, a formula wich includes the volume fraction of the oocytes as a variable or several formulae covering different parts of maturation cycle are needed to be established. On the other hand, practically, the formula of OPD-OD relationship could be established as a single formula which is a function fitting on the actual OD_V (or OD_N) with the power >–3.0 for determinate spawners (Eqs. (4.10) and (4.11), and Fig. 4.15 (Thorsen & Kjesbu, 2001; Kurita & Kjesbu, 2009; Witthames *et al.,* 2009).

4.3.3 Assumption-free methods

4.3.3.1 The physical disector

In the physical disector procedure, the two consecutive sections of the disector pairs (referred to as "reference" section and "look-up" section, respectively) should be separated by a distance (h) short enough to ensure that no particle in between can be missed (Fig. 4.16). Afterwards, a counting frame of known area is overlaid on to the reference section and then on to the look-up section making sure that both frames are precisely aligned with respect to each other. The reference volume would thus be the space defined by the counting frame area (a/f) and the separation between sections (h). The disector counting rules state

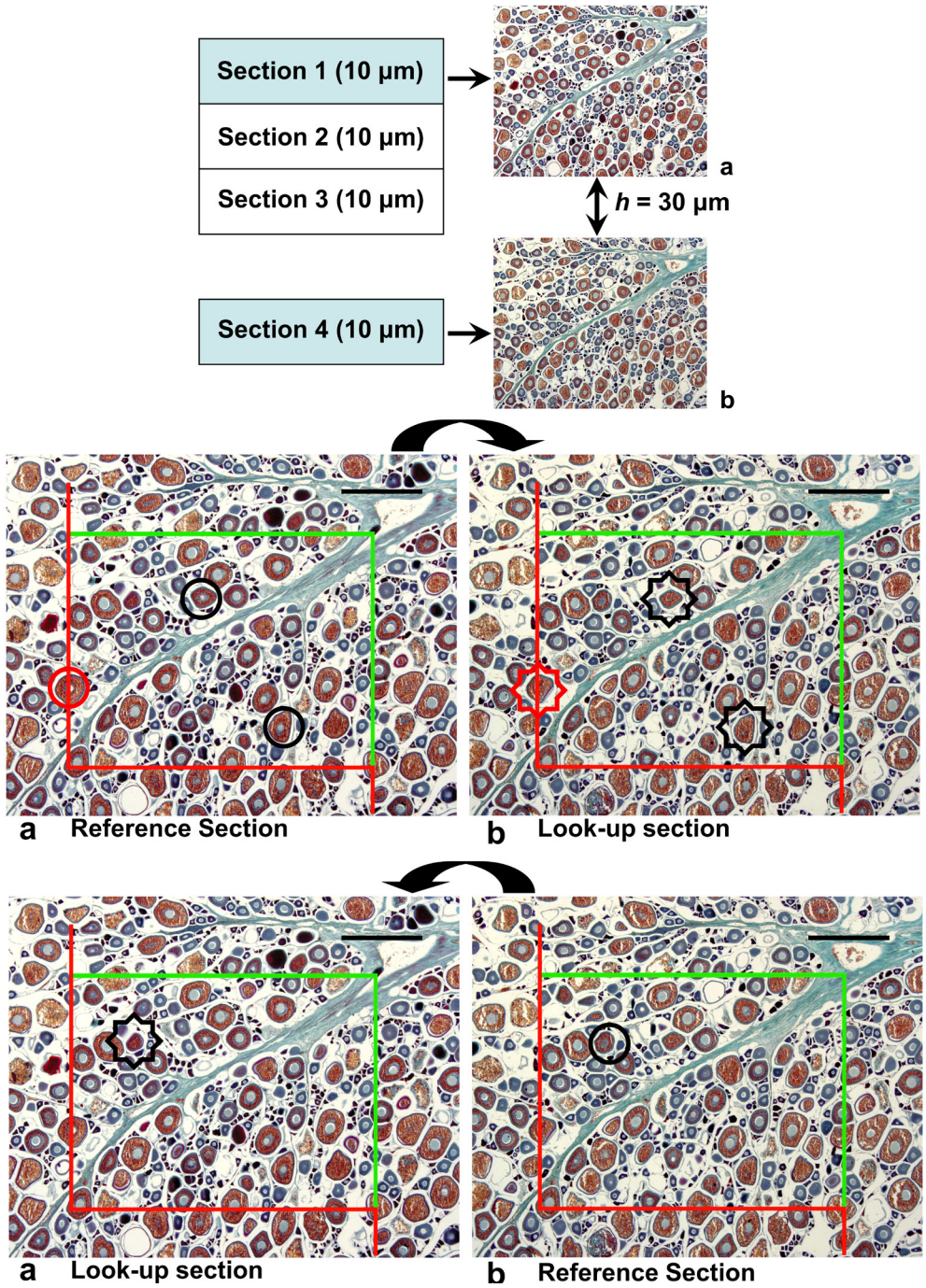

Figure 4.16.

Application of the physical disector procedure for counting large yolked (late vitellogenic) follicles (10-µm paraffin sections of bluefin tuna ovary; only one counting frame is shown). The number of follicles is estimated from counts of their nuclei. As two consecutive sections are inserted between the sections making up the dissector pair (a and b), the height of the reference volume (h) is 30 µm. The counting area (a/f) is equivalent to 12.15 mm². According to the disector practical rules, all nuclei that appear in the reference section (enclosed in black circles) but are not present in the look up section (black stars) should be counted, unless they touch the exclusion edges (red circle and star), which are represented as red lines. The disector pair is first operated from left to right, taking section a as the "reference" section and b as the "look-up" section; then the disector pair is worked in the opposite direction, exchanging the relative roles of sections a and b (bottom). Thus, in this particular case $Q^- = 3$, and the formula to be applied for the final calculation of the numerical density of large yolked follicles (N_v) once the counts of all the used disectors (ΣP) have been summed (ΣQ^-) would be: $N_v = \Sigma Q^- \cdot (2 \cdot \Sigma P \cdot a/f \cdot h)^{-1}$, the factor 2 being due to counting in the two opposite directions.

that i) only the particles that appear in the counting frame on the reference section, but not on the look-up section, are counted, and ii) when the particles touch the forbidden edges of the counting frames (usually, left and bottom margins; red lines in Fig. 4.16),, they are not counted. The numerical density of the quantified particles is then estimated according to the formula:

$$N_v = \frac{\sum Q^-}{\sum P \frac{a}{f} \cdot h} \qquad 4.16$$

where ΣQ^- is the total number of particles counted, ΣP is the total number of disectors used, h is the disector thickness, and a/f is the area of the working frame. In order to increase the efficiency of the method, the counting pairs can be worked in the opposite direction too, such that the total reference volume used is doubled, whereby the chance of detecting particles becomes double, and the numerical density is hence calculated as:

$$N_v = \frac{\sum Q^-}{2 \cdot \sum P \frac{a}{f} \cdot h} \qquad 4.17$$

The requirement of a short distance between planes to avoid missing particles and reduce problems of matching between sections causes a relatively low number of objects to be detected, so that a large section area or several microscopic fields are often needed to obtain enough counts for statistical reliability (ideally, 100-200 object intersections).

An alternative to the physical disector technique is the optical disector, which uses single, relatively thick (~25 µm), paraffin or (preferably) plastic sections (Howard & Reed, 2005), and then makes up disector pairs with thin optical sections that are obtained by focusing the histological sample at different planes, whether using conventional transmitted light microscopy or confocal microscopy systems. This approach avoids the cumbersome process of alignment of sections, but is not well suited to counting large particles like entire follicles or postovulatory follicles.

Figure 4.16 exemplifies a case which attempts to estimate the numerical density of large yolked follicles in a tuna ovary from 10-µm thick paraffin sections applying the physical disector principle. As these follicles are fairly large (~400-500 µm in diameter), an easier way to proceed is counting the oocyte nuclei instead of the whole follicles (we know that fish oocytes are mononucleated cells). This allows us to use a smaller spacing between planes (that is, parallel sections that are closer to each other), thus facilitating the orientation of the microscope fields and enabling a faster and more precise alignment of the disector frames. In this particular case, a suitable h for counts of nuclei was estimated to be 30 µm, which lays between ¼ and ⅓ of the smaller nuclear diameter of late vitellogenic oocytes (Aragón *et al.*, 2010). Therefore, the disector pairs are defined by using the third consecutive section starting from the predetermined reference section as the look up section (Fig. 4.16).

4.3.3.2 The fractionator

Ideally, stereology should be based upon unbiased sampling designs, ensuring that all parts of the studied organ have the same chance of being sampled. This is efficiently achieved by using systematic uniform random sampling (SURS) designs. SURS procedures often give a better spatial coverage and reduce the variance when compared to simple random sampling. The fractionator (Gundersen, 1986), for instance, is based on a SURS scheme that allows estimations of the total N in an organ, eliminating the potential effects of tissue shrinkage (Gundersen, 1986; Gundersen *et al.,* 1988). The method is based on a direct count of particles in a known predetermined fraction of the organ. The organ is first divided arbitrarily into slices

where the cutting planes do not intersect (e. g., parallel slices are perfectly acceptable) and a predetermined fraction of the slices ($1/f_1$) is randomly sampled. In a second step, the slices are cut into smaller pieces and a fixed fraction of them ($1/f_2$) is selected. This operation may be repeated as many times (k) as needed. Eventually, the total number of particles in the whole organ (N) is calculated by multiplying the number of counts by the reciprocal of the sampling fractions: $N = n \cdot f_1 \cdot f_2 \cdot f_k$,, where n represents the number of particles counted in the final sample.

A design-based scheme using the fractionator sampling method in combination with the disector counting technique (e. g., Myers *et al.*, 2004) allows reliable estimates of ovarian follicles with no need for assumptions, models, correction factors or even volume measurements. Korta (2010b) first performed a design-based stereological method for counting oocytes in fishes applying SURS and disector techniques in ovaries of European hake. More recently (Bucholtz *et al.*, 2013), the oocyte dynamics and fecundity of Baltic herring were assessed using a SURS protocol based on the fractionator principle followed by the application of the disector method using specific software.

When SURS becomes impossible to perform, unbiased estimations of numbers must rely on the certainty that the distribution of the counted particles is homogeneous throughout the entire organ (Murua *et al.*, 2003), such that any sub-sample should be representative of the overall organ structure. A homogeneous configuration has been reported for ovaries of a variety of teleostean species (e. g., Sánchez *et al.*, 1986; Stéquert & Ramcharrun, 1995; Cooper *et al.*, 2005; Murua *et al.*, 2006; Witthames *et al.*, 2009; Korta, 2010b; Alonso-Fernández, 2011), but where an even distribution of follicles has not been demonstrated, studies of ovaries at different developmental stages should be performed to confirm homogeneity between the pair of ovaries and within the ovaries.

4.3.4 Final remarks

Until the advent of design-based stereology, model-based stereology was the only form of stereology. Model-based methods are biased unless the objects exactly match the model, which is usually unlikely and difficult to determine in practice. For this reason, modern stereologists see no reason to keep on using protocols that are not design-based (Mayhew & Gundersen, 1996) and claim that any forthcoming stereological approaches be based on unbiased methodologies. Multiple data on fish fecundity and reproductive assessment in fishes have, however, been drawn from assumption-based stereological procedures, so they are, by definition, biased. Now, the question arises as to whether those data are potentially valuable and worth of consideration in future research. A comparative study on bluefin tuna ovaries (Aragón *et al.*, 2010) concluded that the assumption-based method provided significantly lower counts of vitellogenic follicles and higher estimates of β-atretic follicles than the disector method, but the degree of discrepancy between methods was not determined. Kjesbu *et al.* (2010) assessed the bias of the model-based profile counting method comparing it with the disector technique, and have developed a calibrated approach, called stereo-profile method, to quickly estimate the abundance of atretic follicles. It is, thus, of interest to check whether model-based methods traditionally used in fish reproduction studies provide results equivalent to those obtained with design-based procedures in order to validate pre-existing data. Otherwise, if significant differences are detected, calibration analyses might be made to define relevant corrections for previous model-based data.

4.4 Batch fecundity

4.4.1 Hydrated oocytes method

Batch fecundity is the number of eggs released per fish during a single spawning event and can be estimated by identifying and quantifying the cohort of hydrated oocytes in the gonad. It can also be estimated from the most advanced vitellogenic oocyte stage (just before hydration), when it is possible to correctly identify and isolate the oocytes from a single batch (see Section 4.4.2). However, batch fecundity measurements are traditionally performed with the hydrated oocyte method, because hydrated oocytes can be easily distinguished from other oocytes by their large size and translucence (nonhydrated oocytes are relatively opaque and smaller), see Figure 4.17. The outline of the method is as follows: all hydrated or running females are macroscopically detected, measured and weighed. The gonads are removed, weighed (0.01 g) and preserved (e.g. in 4% buffered formaldehyde solution). When the gonad is not weighed on sampling site (i.e. the fixed gonad is weighed in the lab), a correction factor should be applied to correct the weight difference due to the fixative. Ovaries should be previously processed histologically to guarantee that batch spawning did not start before sampling. This is done through checking for the presence of brand new POFs, and the ovaries containing POFs are excluded from batch fecundity estimation because it means that some eggs have already be spawned. However, samples with hydrated oocytes and old POFs are not excluded, because these old POFs do not belong to the same batch of the hydrated oocytes. The gravimetric method is subsequently applied either through direct counting of hydrated oocytes un

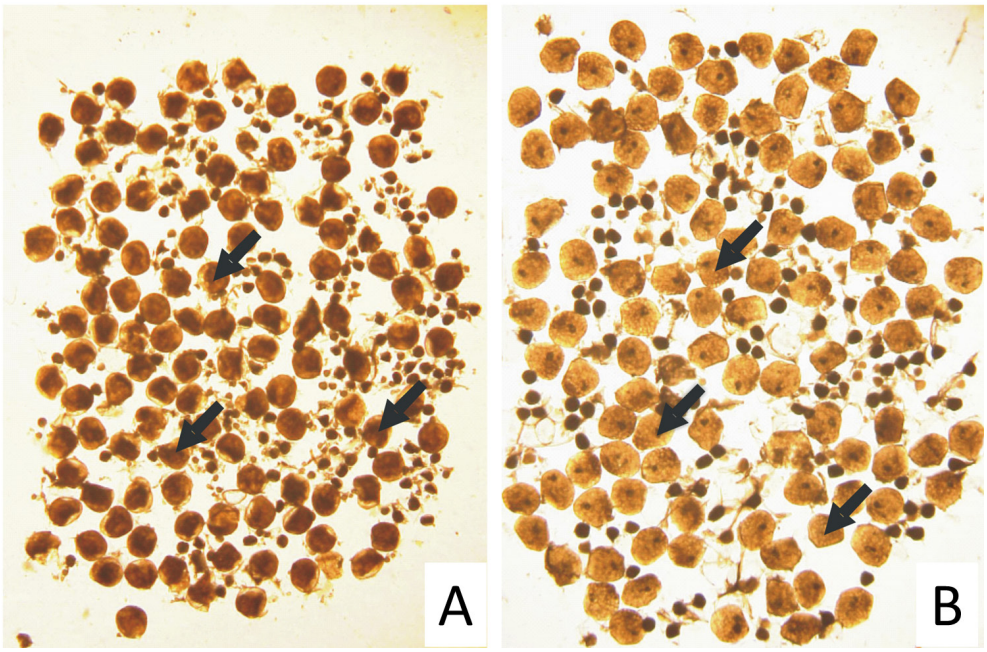

Figure 4.17.

Hydrated oocytes (arrows) in an ovarian sub-sample taken from sardine, Sardina pilchardus, preserved in 70% ethanol solution (A) and in 10% neutral-buffered formalin (B).

der an ocular microscope or by means of digital particle analysis (see Section 4.2.4). For counting them manually under the microscope it is recommended to add 2-3 drops of glycerine which will facilitate the counting of the hydrated oocytes of the sub-sample.

4.4.2 Use of other stages

The main problem with the 'hydrated oocytes' method is the scarceness of hydrated females in samples of adult fish which is can be due to the limited time course of oocyte hydration, to the aggregating behavior of imminent spawners (Ganias, 2008), and to different selectivity of hydrated females. These factors make hydrated females almost unavailable to certain sampling gears and as a consequence other developmental stages should be employed for batch measurements (e.g. Macewicz et al., 1996, Ganias et al., 2004). The present section presents a procedure which uses micrographs of ovarian whole mounts to recognize, separate and count oocytes belonging to the spawning batch both in hydrated and non-hydrated sardines, *Sardina* pil*chardus* (see also Ganias et al. 2010). The procedure is based on the ability of most image-analysis software to count and measure objects in binary or thresholded images (see Section 4.2.5). Apart from increasing the number of analyzed specimens the automated procedure could contribute to saving time and work-load and in improving accuracy in batch fecundity measurements.

The first step of the analysis is the calibration of the automated measurements of oocytes using the hydrated oocytes. This could be performed through producing a first set of batch fecundity measurements in hydrated ovaries because, as already mentioned, at this stage the spawning batch is clearly distinguished both in size and shape and fecundity measurements are considered unbiased. The Petri dish with the ovarian subsample should be placed under an ocular microscope with an attached microscopy-camera and photographed so that all the oocytes fit into the micrograph (Fig. 4.18A). In order to have micrographs of the best possible quality for subsequent oocyte counting, prior to photography, each subsample should be cleaned from membranes and other non-oocyte material.

Digital micrographs are first processed 'manually' through distinguishing and counting the hydrated oocytes on-screen. This could easily be done by using the 'cell counter' plugin of ImageJ software (http://rsb.info.nih.gov/ij/). This procedure is far more efficient compared to direct oocyte counting under the ocular microscope both because of the enhanced representation of the analysed visual field on the computer screen compared to the ocular lens of the stereoscope, and because of the facilities of the image analysis software, e.g. colour marking and automatic enumeration of counted oocytes (reference method). As a next step, an automated procedure is developed for recognizing, separating and counting only the oocytes of the spawning batch, i.e. hydrated oocytes from the smaller oocytes. The routine (which is explicitly described in Section 4.2.5) includes consecutively the adjustment of brightness and contrast, the conversion of the image type to 8-bit, the restriction of colour spectrum to a region that includes all the oocytes (thresholding), the separation of individual particles (segmentation) and counting of all particles above the size order of previtellogenic oocytes (Fig. 4.18B, D). Parameter values in each of these individual processes (e.g. brightness, thresholding, etc.) are selected so as to give a number of hydrated oocytes as close as possible to the reference method. When this goal is achieved (using a subset of ca. 15 specimens) ImageJ offers the possibility for the development of a macro which may automate the entire process, from the opening of the image file to the counting of the hydrated oocytes ('automated method'). This macro is

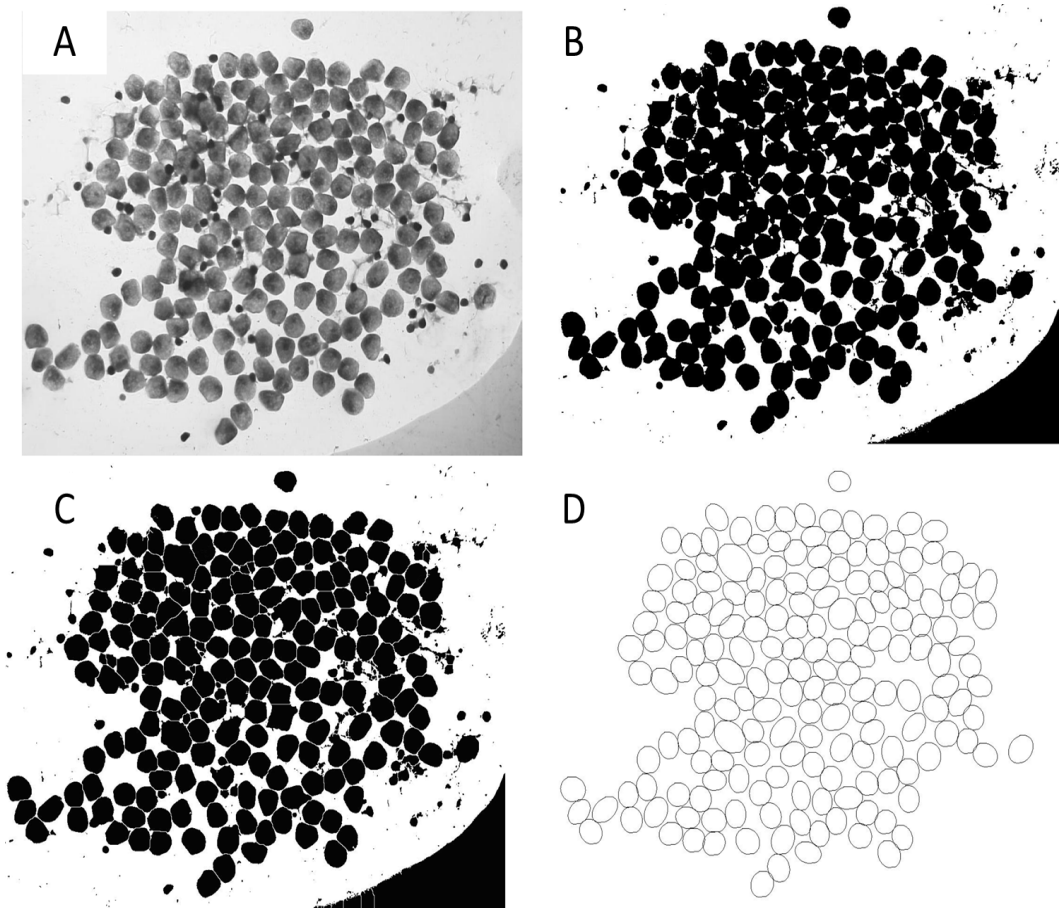

Figure 4.18.

Consecutive phases of the processing of ovarian whole mounts of sardine, Sardina pilchardus, for the counting of hydrated oocytes through the macro of ImageJ: (A) converting image to the 8bit format, (B) thresholding, (C) particle segmentation and (D) counting of oocytes through selecting particles corresponding to the size and the circularity of hydrated oocytes

then applied to the entire set of micrographs of hydrated females. The results obtained by the automated method are then validated through comparison with the reference method, e.g. through comparing the regression line of the relationship between two sets of hydrated oocyte counts to the diagonal line (intercept and slope to 0 and 1, respectively) (Fig. 4.19).

The automatic procedure can then be applied to non-hydrated females in order to assess the size/stage at which the spawning batch separates in size from the smaller oocytes. This can be done through examining oocyte size frequency distributions in a number of females with vitellogenic, non-hydrated ovaries at sequential developmental stages. Processing and photography of ovarian whole mounts and the analysis of digital micrographs are the same as the one described previously for hydrated ovaries. After measuring the size of individual oocytes and producing size frequency distributions for each ovary separately, all frequency histograms are plotted together in ascending order of mean oocyte size (Fig. 4.20). The resulting graph should then be examined in order to identify the stage/size at which the spawning batch separates from the remaining batches and the critical size at which the gap is established.

The automated method is then applied to all females from this stage onwards either by counting all size particles above the estimated gap (oocyte-size threshold

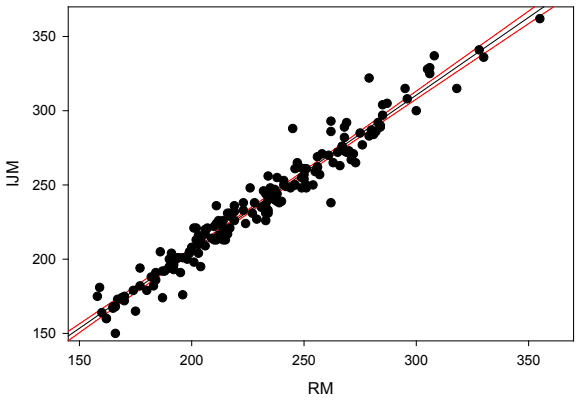

Figure 4.19.

Relationship between the number of oocytes resulted from the estimation made by the automated method applied to hydrated females with ImageJ (IJM) and the hydrated oocytes counted by the reference (RM) method.

method) or through decomposing composite oocyte size distributions and estimating the number of particles in the distribution that corresponds to the spawning batch (e.g. through the Bhattacharya's method).

4.4.3 Use of intermediate batches

In indeterminate spawners there is a continuous recruitment process in all developmental stages of intra-ovarian oocytes, resulting in a size frequency distribution with several modes of oocyte groups but with a notorious overlap (Wallace & Selman, 1981; Murua & Saborido-Rey, 2003 Kurita & Kjesbu, 2009; Korta *et al.*, 2010b; Fig. 4.21). However, as oocyte development progresses the overlap between the most advanced mode of oocytes (encompassing an imminent spawning event) and the less developed mode (i.e., intermediate mode composed of unyolked oocytes) decreases although without reaching a complete hiatus between both modes, such as in the case of determinate spawners (Wallace & Selman, 1981; Witthames *et al.*, 2009; Korta *et al.*, 2010b). To date, the most advanced modes have been extensively used to determine batch fecundity on a regular basis in most commercial batch spawning fishes as part of assessment protocols to either characterize reproductive traits or reproductive potential through egg production methods. However, the intermediate mode has been largely ignored, perhaps because this mode might not accurately represent the numbers of eggs that will be spawned in the next batch, if additional oocytes are recruited from earlier stages of development and/or some oocytes from this mode are lost due to atresia. Still, the information contained in the intermediate mode is very valuable because overlapping frequency distributions can be decomposed into their normal components to estimate means and variances, and consequently get an estimate of intermediate fecundity. When this information is analyzed along with estimates of batch fecundity in an annual cycle it may be possible to evaluate seasonal changes in batch size (number of oocytes) and mean oocyte size of each batch. Methodological issues associated with the determination of intermediate fecundity are similar

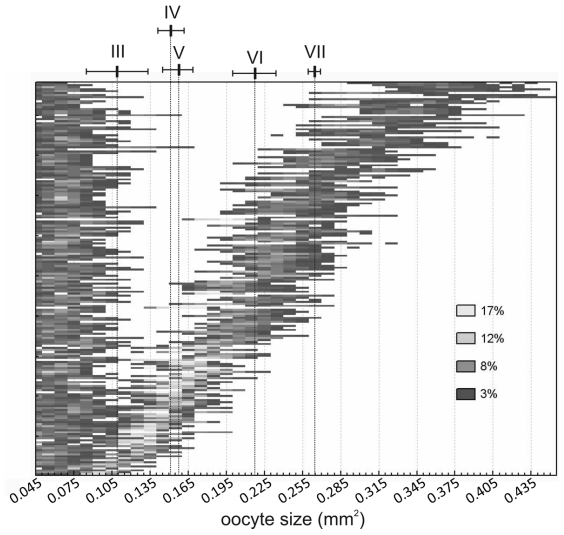

Figure 4.20.

Oocyte size frequency distributions in 184 sardine ovaries between the primary yolk stage and late migratory nucleus stage in ascending order of average oocyte size. Mean oocyte size and 95% CI per developmental stage is superimposed. III: primary yolk stage; IV: secondary yolk stage; V: tertiary yolk stage; VI: early migratory nucleus stage; VII: late migratory nucleus stage.

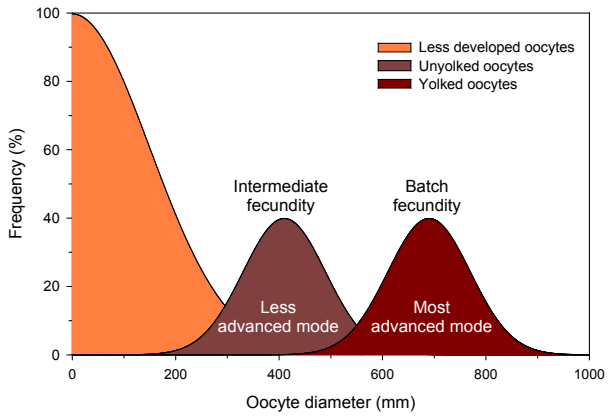

Figure 4.21.

Theoretical scheme of frequency distribution of oocyte diameter in an indeterminate fecundity species to illustrate normal components associated to intermediate and batch fecundities.

to those reported in the previous sections for batch fecundity. Some suggestions, however, can be taken from Plaza *et al.* (2002) who reported estimations of intermediate fecundity in the Pacific Sardine (*Sardinops sagax*) by using a gravimetric method (Fig. 4.22). In brief, Plaza *et al.* (2002) followed a similar approach of that described in section 4.2.4 to separate the oocytes and then oocytes were separated by size class using a sieve system ranging from 1000 to 200 µm mesh decreasing by 50 µm between consecutive sieves. The system of sieves was set over a variable speed shaker connected to a small suction pump to remove the cleaning water to facilitate the passing of the oocytes. The retained oocytes were manually counted under a stereomicroscope (but can be done by image analysis) to obtain oocyte diameter frequency distributions and, then, normal components were determined by using the Bhattacharya's based MPA (Modal Progression Analysis) detailed (Gayanillo *et al.*, 1988).

To reduce as much as possible the degree of overlap between the least and most advanced modes, mature ovaries close to hydration should be used, preferably identified using histological analysis. Strictly speaking hydrated ovaries provide the best resolution to study intermediate fecundity, although the low probability of collecting hydrated ovaries on a regular basis makes its use very unlikely.

Modal Progression Analysis: Once frequency distributions are obtained, modes can be separated into their normal components using the classic Bhattacharya method either available in specific modules of fisheries computer-based packages (e.g., ELEFAN and /or FISAT; Gayanillo *et al.*, 1996) or in modules of frequency tables available in modern statistical packages. It is important to note that determination of intermediate fecundity is not only restricted to the use of a sieve system. Some modern image-based methods (e.g., those described in Section 4.2 of the present handbook) can also be used to obtain frequency distribution to then be analyzed using MPA.

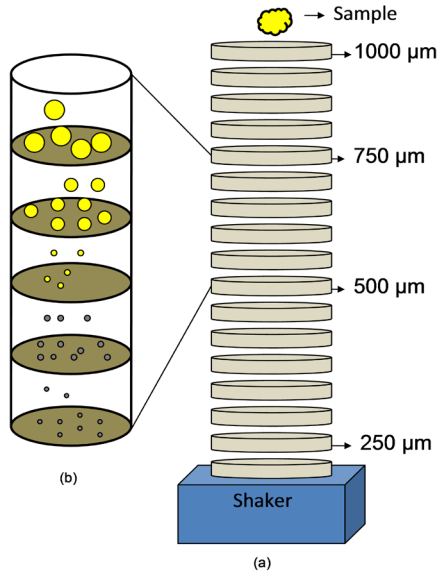

Figure 4.22.

(A) Illustration of a sieve system, firstly described by Fischer & Balbontín (1970), used to obtain frequency distribution of oocytes by size class (diameter) using different mesh size (1000-200 µm). (B) A magnification to illustrate how oocytes are being retained according to their size. Yellow and grey spheres denotes yolked and unyolked oocytes, respectively.

4.5 Daily fecundity and spawning frequency

4.5.1 Estimation of daily fecundity

Daily specific fecundity (DSF) is the number of eggs produced daily per unit weight of the population. It is a very useful parameter since when combined with the daily egg production at sea it can provide estimates of the spawning biomass through the Daily Egg Production Method (DEPM, for more details see Fisheries Research 2012 Special Issue on Egg Production Methods in Marine Fisheries). DSF can be estimated by the formula:

$$DSF = \frac{R \cdot F \cdot S}{W} \qquad 4.18$$

where BF: is the average batch fecundity (number of eggs released per female per spawning); S: is the daily spawning frequency (i.e. fraction of mature females spawning each day); W: in the average weight of mature females (g); and, R: is the weight-specific sex ratio of mature population (total weight of females/total weight of males and females).

The adult parameters are usually estimated from different components of the same set of fish samples. Fixed subsamples are attempted for each parameter. Methods of calculating BF and S and aspects related to their accuracy and precision are described in other sections of this manual. With regard to R and W, macroscopic sex identification and weighing of fish are required, correction factors for W are applied when using preserved fish (Hunter, 1985), whereas the weight of hydrated females is typically corrected for the increase in weight of hydrated oocytes (Hunter *et al.,* 1985). Regression equations of total weight on ovary-free weight calculated from non-hydrated females in the same samples are used for this purpose (Picquelle & Stauffer 1985). The daily specific fecundity is calculated for the mature part of the population, i.e., fish that have reached sexual maturation. When immature and mature fish co-exist in the samples, the two must be separated using macroscopic, histological or other criteria (see Chapter 3 on maturity). Daily specific fecundity is highest during the peak of the spawning period, i.e. when batch fecundity, spawning frequency and the fraction of females that are reproductively active reach their highest values.

For the unbiased estimation of adult parameters, representative samples from the mature population are required. Judgment sampling is the most common method for selecting the location of fishing stations. It uses independent information to place stations where fish abundances are high (Picquelle & Stauffer, 1985). This information may consist of results from a recent survey or in situ evidence of local fish concentrations, such as acoustic detections and/or occurrence of spawning products in plankton samples. The resulting distribution of sampling stations will be patchy with more stations located in areas with high densities of fish. With judgment sampling, sampling effort allocation strategy is considered to approximate the sampling technique of probability proportional to a measure of size. The ratio estimator (Picquelle & Stauffer, 1985) is then used for estimating parameters W, R, BF, and S:

$$\bar{y} = \frac{\sum_{i=1}^{n} m_i \cdot \bar{y_i}}{\sum_{i=1}^{n} m_i} \quad 4.19$$

with sample variance

$$V\hat{a}r(\bar{\bar{y}}) = \frac{\sum_{i=1}^{n} m_i^2 \cdot (\bar{y_i} - \bar{\bar{y}})^2}{\left[\sum_{i=1}^{n} \frac{m_i}{n}\right]^2 \cdot n \cdot (n-1)} \quad 4.20$$

where,

$\bar{\bar{y}}$: the estimate of the population mean ,

n: the number of stations,

$\bar{y}_i = \sum_{j=1}^{m_i} \frac{y_{ij}}{m_i}$:the mean of the i^{th} station 4.21

and,

m : the number of fish sampled from the i^{th} catch.

Data on the number of eggs per batch (B_j) and the ovary free weight (W_{ij}^*) recorded for the females in which fecundity was actually measured are used to fit a linear regression:

$$F_{ij} = a + b \cdot W_{ij}^* + \epsilon_{ij} \quad 4.22$$

Using Equation (4.22), batch fecundity is estimated for each mature female sub-sampled, and Equation (4.19) is subsequently used to estimate average batch fecundity. However, in this case, the variance is derived using the equation:

$$V\hat{a}r\left(\bar{\bar{F}}\right) = \frac{\sum_{i=1}^{n} m_i^2 \cdot \left[\frac{(\bar{F}_i - \bar{\bar{F}})^2}{n-1} + \frac{s_h^2}{n_h} + (\overline{W_i^*} - \overline{W_h^*}) \cdot V\hat{a}r(\hat{b})\right]}{\left[\sum_{i=1}^{n} \frac{m_i}{n}\right]^2 \cdot n} \quad 4.23$$

where,

$\bar{\bar{F}}$: the estimate of batch fecundity for the whole population of mature females,

$\bar{F}$: the average batch fecundity of the ith sample,

$$\bar{F}_i = \sum_{j=1}^{m} \frac{\widetilde{F_{ij}}}{m_i} \quad 4.24$$

where,

$\widetilde{F}$:is the estimated batch fecundity for the *j*th female in the ith sample,

s_h^2 : the variance about the regression (Equation (4.22)),

n_h : the number of hydrated females used to fit the regression (Equation (4.22)),

$\overline{W}_i^*$: the average ovary-free weight of the ith sample,

$\overline{W}_h^*$: the average ovary-free weight of the n_h hydrated females, and

$\hat{Var}(\hat{b})$: the variance of the slope of the regression (Equation (4.22)).

The daily specific fecundity is a population parameter and its calculation assumes that parameters involved are constant over the geographical range or duration of the sampling survey.

The variance of the DSF estimates according to the variances of the individual parameters (BF, S, W and R) are estimated by the delta method (Seber 1973) as (Sanz *et al.*, 1992):

$$V\hat{a}r(DSF) = DSF^2 \cdot [CV(R)^2 + CV(F)^2 + CV(S)^2 + CV(W)^2 + 2 \cdot COVS] \quad 4.25$$

Where CV means coefficient of variation and COVS means the sum of the relative covariances of the parameters (with positive signs for the covariances between the parameters in the numerator and negative for the covariances involving W).

4.5.2 Estimation of Spawning Frequency

Spawning frequency in iteroparous fishes expresses the number of spawning events per unit time, usually per day. Spawning frequency can be estimated either as an individual parameter through interspawning interval, ISI, i.e. the time lag between subsequent spawning events, or as a population parameter through the spawning fraction, S, i.e. the proportion of females spawning per day. Spawning fraction is usually estimated by the proportion per sample of mature females with post-ovulatory follicles (POFs) pertaining to an identifiable daily spawning cohort. Alternatively, S can also be obtained from the proportion of imminent pre-spawning females, as detected by the presence of ovaries undergoing oocyte maturation (OM). The requisite to estimate S is to be able to identify daily spawning classes (or cohorts) from gonadal histological indicators of imminent or recent spawning activity. For it to be possible the process of oocyte maturation (OM) and/or of POF degeneration in time is to be understood, so that females can be assigned to pre- or post- daily spawning classes.

As already mentioned, S is estimated as the fraction of Day_i, (i=0, 1, 2, etc.) spawners to the number of females analyzed, usually the mature fish. The first daily class, i.e. Day_0 spawners are usually fish that had, were or would spawn the night of sampling with hydrated oocytes and/or new POFs; Day_1 spawners are fish that had spawned the previous night, Day_2 spawners are fish that had spawned two nights before, etc. Then S is estimated using the ratio estimator described in Section 4.5.1.

As mentioned before, a Day_i class could comprise exclusively of imminent spawners. For species with a restricted peak spawning time in the day, the knowledge about the dynamics of late oocyte maturation (OM), from nuclear (germinal vesicle) migration to hydration and ovulation is usually achieved from the analysis of a collection of samples obtained throughout a daily cycle. Usually the OM process is subdivided in about 3 to 4 stages (initial nuclear migration, advanced migration and hydration –initial and advance-) which allows visualization of their successive occurrence in the 24-hour cycle. This allows establishing the duration and the occurrence of these stages of OM relative to peak spawning time. Once that knowledge is achieved, the occurrence of these stages in the gonad of a female will give indication of the time pending to next spawning and, hence, the female can be assigned to a predefined spawning class directly. Examples of such studies can be found in Clarke (1987), Funamoto & Aoki (2002), Lowerre-Barbieri *et al.* (2009), Motos (1996), Uriarte *et al.* (2012). These works show that nuclear migration starts earlier than 24 hours before spawning and hydration starts usually around 10-12 hour before spawning.

For several fish stocks, especially for batch spawning clupeids it has been observed that Day_0 females are oversampled during the hours of spawning (Picquelle & Stauffer, 1985; Alheit, 1993; Ganias *et al.,* 2003b; Ganias, 2008). In the case of such bias, Day_0 females should be excluded from the analysis and m_i in Equation (4.19) corrected. This correction can be made by either considering the number of Day_0 equal to the number of Day_1 spawners (when only Day_1 spawners are used in the estimation of spawning frequency, e.g. Picquelle & Stauffer (1985)), or, to the average number of Day_1, Day_2, ... spawners when females with POFs can be assigned to three or more spawning nights, e.g. Quintanilla & Pérez, (2000):

$$N_0^* = \frac{\sum_{i=1}^{n} N_i}{n} \qquad 4.26$$

where:

N_0^* = the corrected number of Day_0 females, and,

N_i = number of Day-i spawners.

The precision of the spawning frequency estimate could generally be improved if more than one class of Day-$_i$ spawners can be identified and subsequently combined to produce a composite estimate (e.g. Quintanilla & Pérez, 2000; Ganias *et al.,* 2003b). A requisite of such a combination is that different spawners' classes have the same statistical distributions (Alheit, 1984). The generalized formula of a composite spawning fraction estimate is:

$$S = \frac{1}{n} \cdot \sum_{i=1}^{n} S_i \qquad 4.27$$

and the variance is given by (Ganias *et al.,* 2003b):

$$\hat{Var}(S) = \left(\frac{1}{n}\right)^2 \cdot [\sum_{i=1}^{n} \hat{Var}(S_i) + +2 \cdot \sum_{i<j} COV\,(S_i, S_j)] \qquad 4.28$$

where:

S = the composite spawning fraction estimate

S_i = the fraction of Day-i females.

4.5.3 The postovulatory follicle (POF) method

Postovulatory follicles (POF) are transitory remnants of the ovulated follicles which remain within the ovary after spawning, until they are fully resorbed. These structures are composed of the follicle cells (granulosa) surrounded by a connective tissue theca. Hunter & Goldberg (1980), based on the description of POF degradation in northern anchovy (*Engraulis mordax*) sampled at different time period after spawning induction, established a classification system for these structures. On the other hand, they observed in anchovy that spawning mainly occurs at a discrete period of the day, which allows the identification of POF daily cohorts in the ovaries. Therefore, they basically proposed two main POF stages according to the elapsed time from spawning: a) Day_0 (< 24 h after spawning) and b) Day_1 (between 24 and 48 h after spawning). 48 h after spawning, degeneration process advanced further and POF may be confused with intermediate atretic oocytes.

During the last 30 years several studies have been made in different species (pelagic and demersal fish) following the POF method proposed by Hunter & Goldberg (1980) to estimate the daily proportion of spawning females (Ganias, 2012). In some species, it was demonstrated that the rate of POF degradation is dependent upon temperature at spawning place. For this reason, before spawning frequency estimations, it is necessary to know the temperature range in the reproductive site and corroborate that it is similar to that previously used to validate the POF ageing. More recent studies have analysed the degeneration rate of POF both in captivity fish and in the field at different temperature ranges (Alday *et al.*, 2008) and confirmed that POF have a short life at moderate and high temperatures (< 60 h at 13° -19° C).

4.5.3.1 POF staging: an interspecific approach

The present section provides evidence for temperature related differences in the degeneration process of postovulatory follicles (POF) between fish species residing in the temperate waters of the Southwest Atlantic Ocean. Two groups of species were recognized: (A) those is which spawning occurs at moderate temperature range (10 – 16° C) including *Merluccius*

hubbsi (Macchi *et al.*, 2004), *Engraulis anchoita* (Pájaro *et al.*, 2009), *Brevoortia aurea* (Macchi & Acha, 2000), *Ramnogaster arcuata* (Rodrigues *et al.*, 2008), *Percophis brasiliensis* (Militelli & Macchi, 2001) and *Cynoscion guatucupa* (Macchi, 1998); (B) those where spawning occurs at higher temperatures (20° -25° C) including *M. fumieri* (Macchi *et al.,* 2003) and *Macrodon ancylodon* (Militelli and Macchi, 2004). Given that the first group of species spawns at temperatures that approximate the thermal habitat of northern anchovy, *Engraulis mordax*, POF ageing was based on Hunter & Goldberg (1980). In the second group of species POF degradation was faster than that reported for northern anchovy, as was observed by Macchi *et al.* (2003). These authors could analyze POF degradation in ovaries of *M. furnieri* sampled on board during its spawning peak, and they observed that a 24-h-old POF showed advanced signs of degeneration similar to those reported for *E. mordax* 48 h after spawning. Similar faster POF degeneration rates have been observed in engraulidae spawning in warm waters (Clarke, 1987; Funamoto & Aoki, 2002). Therefore, daily proportion of spawning females was estimated by taking the total of females with POFs less than 24 h old (Hunter *et al.*, 1986; Shaefer, 1996).

In general, the diagnosis of POF degeneration stages was similar for the different species analyzed (Table 4.3) and characterized by:

1. Reduction of lumen size
2. Occurrence of vacuoles between the granulosa cells
3. Occurrence of pycnotic nuclei inside the granulosa cells
4. Loss of the laminar structure of the granulosa cells by breakdown of the follicle
5. Cell alignment.
6. Shrinking and compacting of the POF structure
7. Reduction of the follicular lumen
8. No distinction between theca and granulosa

When the sampling design is limited to a discrete period of the day (morning-afternoon) and the spawning is also limited to a specific time period (for example midnight), then it is more easy to link the POF structure to the time elapsed after spawning. Therefore, in species that synchronize their spawning over a 24 cycle, it becomes easier to distinguish between Day_0 and Day_1 POF. In general, most of studies made since the beginning of

Table 4.3.

Main histological characteristics considered for the postovulatory follicle classification during the degradation process.

Stages	General aspect	Granulosa	Theca	Lumen
DAY 0	- Convoluted shape, with a folded structure - Large size (about 500µm) - Signs of degradation are not evident	- Columnar cells aligned as a cord-like - Nucleus commonly situated in the apex or at the base of the cell	- Evident layer clearly separated from the granulosa. - Flattened cells surrounded by capillaries	- Large and irregular - In some cases with eosinophilic granules
DAY 1	- Loss of cord-like appearance - Size reduction - More compact appearance - Signs of degradation	- Breakdown of alignment - Cells dispersed - Pycnotic nucleus	- Still visible but adhering to granulosa	- Great reduction in size - With many free granulosa cells
DAY 2	- Compact structure - Smaller than 50% of day-0 POF - High degradation	- Cells compacted - Many vacuoles and pycnotic nucleus	- No distinction between theca and granulosa	- Absent or occupied by cells in degradation

80s with the objective of validating the age of the POF in relation with its stage of degradation, agree that day-0 POF may be distinguished from the Day_1 stage by the breakdown of the granulosa cell alignment and compacting of POF, which precede the reduction of size and disappearance of the lumen (Hunter & Goldberg, 1980; Fitzhugh & Hettler, 1995; Alday *et al.*, 2010).

Figure 4.23 shows POF at different degradation stages for species characterized by spawning at moderate temperatures. The main morphological difference between these species during the day_0 POF stage was associated with the shape of the granulose cells and location of the nucleus. For example, in the case of *M. hubbsi* and *R. arcuata granulose* cells were columnar with the nucleus sited at the base, while in E. anchoita and B. aurea it was mainly observed in the apex (Fig. 4.23) P. brasiliensis showed the nucleus of the granulose cells in the apex too, but these cells were mainly cubical in shape. Species that spawn at higher latitudes as *Micromesistius australis* (Pájaro & Macchi, 2001) commonly exhibit POFs at different degradation stages in the same individual (Fig. 4.24). This fact

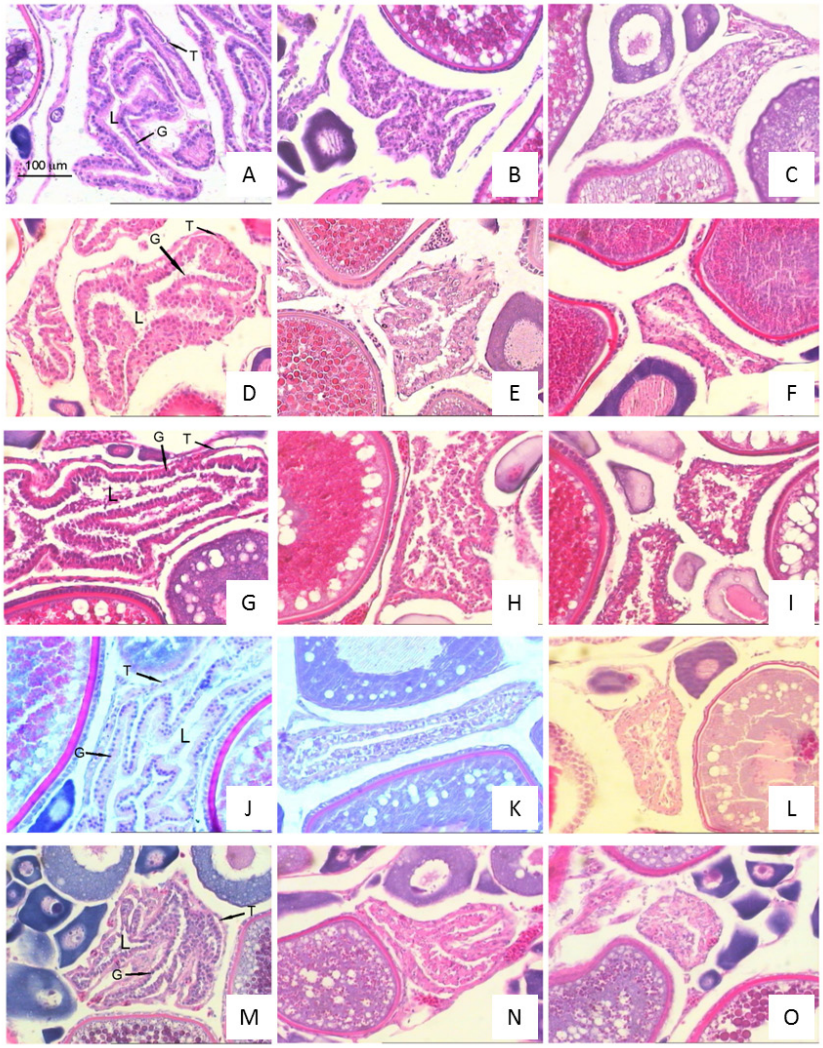

Figure 4.23.

Postovulatory follicles at different degradation phases, classified as $Day_1 0$(first column), Day_1 (second column) and Day_2 (third column) stages, for the species: M. hubbsi (A, B, C), E. anchoita (D, E, F), B. aurea (G, H, I), R. arcuata (J, K, L) and P. brasiliensis (M, N, O). G, granulosa; T , theca; L, lumen.

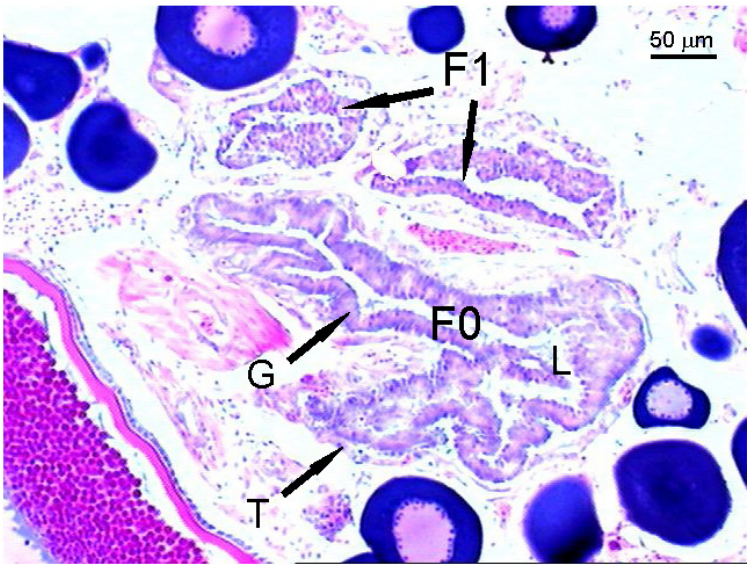

Figure 4.24.

Ovary of M. australis in spawning stage with postovulatory follicles (POF) at different degradation phase. : F0, Day0 POF; F1, Day1 POF; G, granulosa; T , theca; L, lumen. From Macchi et al. (2005).

may be associated with the low rate of POF resorption as consequence of low temperatures (< 6° C) in the reproductive area as suggested by Macchi *et al.* (2005).

Remarks:

- Day_0 POF of the species analyzed were mainly differentiated by the shape of the granulose cells and location of the nucleus in the granulosa cells.
- In species spawning at moderate temperatures (10° -16° C) a degradation period similar to that reported for *E. mordax* (Hunter & Goldberg, 1980) was considered, with two main POF daily cohorts.
- The degradation process was similar between species, considering the breakdown of the granulosa alignment as the feature more easily recognizable to differentiate Day_0 and Day_1 POF.
- In species spawning at higher temperatures (>20°C) POF degradation was faster, and all stages described were within a period of 24 h.
- In M. australis, a species spawning at low temperatures (<6°C), POF of consecutive degradation phases were detected adjacent to each other in the same ovary, possibly as a consequence of the low degeneration rate.

4.5.3.2 POF 3-D reconstruction: a quantitative validation of POF staging

To date, classification of POF stages is carried out based on the histological characteristics seen in two-dimensional (2-D) sections. Histological characteristics used to classify POF morphology, i.e, cell shape and organization, and evaluation of the vacuole abundance are essentially qualitative properties, and therefore, subject to sources of bias/subjectivity (Korta *et al.*, 2010b). Hence, the introduction of quantitative components in histology is essential to objectively relate the 2-D structure of POFs with its three-dimensional (3-D) structure and obtain data as volume, surface area or spatial relationship between different classes of POF. To a certain extent, volume is an appropriate measure to quantify POF stages as, the knowledge of the third dimension is important for better understanding and interpretation of results fromm the tissue level (Verbeek, 2000). However, there is a dimensional loss

of information within the 2-D histological sections used to characterized POF stages. The 3-D shape of 2-D structures from histology seems intuitive, but, actually, 2-D profiles fail to provide any sort of shape discriminator for the geometric solids which generated them (Mayhew, 1991). Consequently, a 3-D reconstruction process is required to obtain this volume data, which may add objectivity to the definition of POF stages. In short, the 3-D reconstructions from serial histological sectioning of POF stages provides an objective metric to verify the correctness of the 2-D histomorphological characteristics used to stage POFs.

The method is quite laborious to be added routinely to histological procedures. However, it could be useful to first apply to fish species that depend on POF histomorphological classification, adopted from a different species.

3-D reconstruction method

3-D reconstruction is the process of reproducing real structures, e.g., POF, while maintaining their physical characteristics (dimensions, volume and shape), by means of a computer. POF are reconstructed from planar images taken from 2-D histological slices in destructive testing, i.e., sectioning. Note that POF integrity is destroyed and distortion can occur due to compression during the cutting and the mounting process. Therefore, a good 3-D reconstruction system should have tools to correct these problems, at least to an acceptable level. Then, with specialised software for 3-D modelling, the user is able to trace POF profiles onto histological images, align them and measure the final structure automatically.

Sample preparation and serial image registration

Ovarian tissue from spawning females is used to conduct the 3-D reconstruction of POFs. A 0.5 cm thick cross section is cut from each ovary and dehydrated in ascending concentrations of alcohol and infiltrated in methyl-hydroxymethacrylate resin (Technovit 7100) prior to polymerisation into blocks. The block is serially sectioned at 5 µm.

Alternate sections are retained on slides for 3-D reconstruction. This introduces an acceptable error in the final reconstruction, but it is less laborious and time consuming than collecting all of the sections. All retained sections are mounted as being collected from the original block, that is, in order of collection to avoid any shape deformation during reconstruction. Next, these sections are stained with Haematoxylin & Eosin. The profile corresponding to the same POF is identified through the serial sections. They are photographed with a camera mounted on a microscope. The calibration of the magnification used is done by taking a photo to a 1 mm calibration slide at the same magnification of POF profile images. This process generates a stack of serial images of the 2-D POF profiles that covers the full depth of POF along the direction of sectioning (Z axis) (Fig. 4.25).

Manual tracing and alignment

Once all the POF profile images are captured a 3-D image can be reconstructed in a computer. In each POF image, the external boundary of the POF profile is digitized in X-Y plane by tracing around the POF's periphery (Fig. 4.26A). The traces should be aligned with the utmost precision; otherwise a progressive deviation would be produced through the serial sections due to the accumulative translational misalignments in X-Y axis and/or rotational misalignments in the Z axis (Quincoces, 1995) (Fig. 4.26B, C) realigned stack of outline traces is then produced (Fig. 4.26D), which is used to reconstruct 3-D wireframe surfaces by connecting the set of points representing the POF segments as surface elements - either triangles, squares or other geometric shapes (Fig. 4.26E, I).

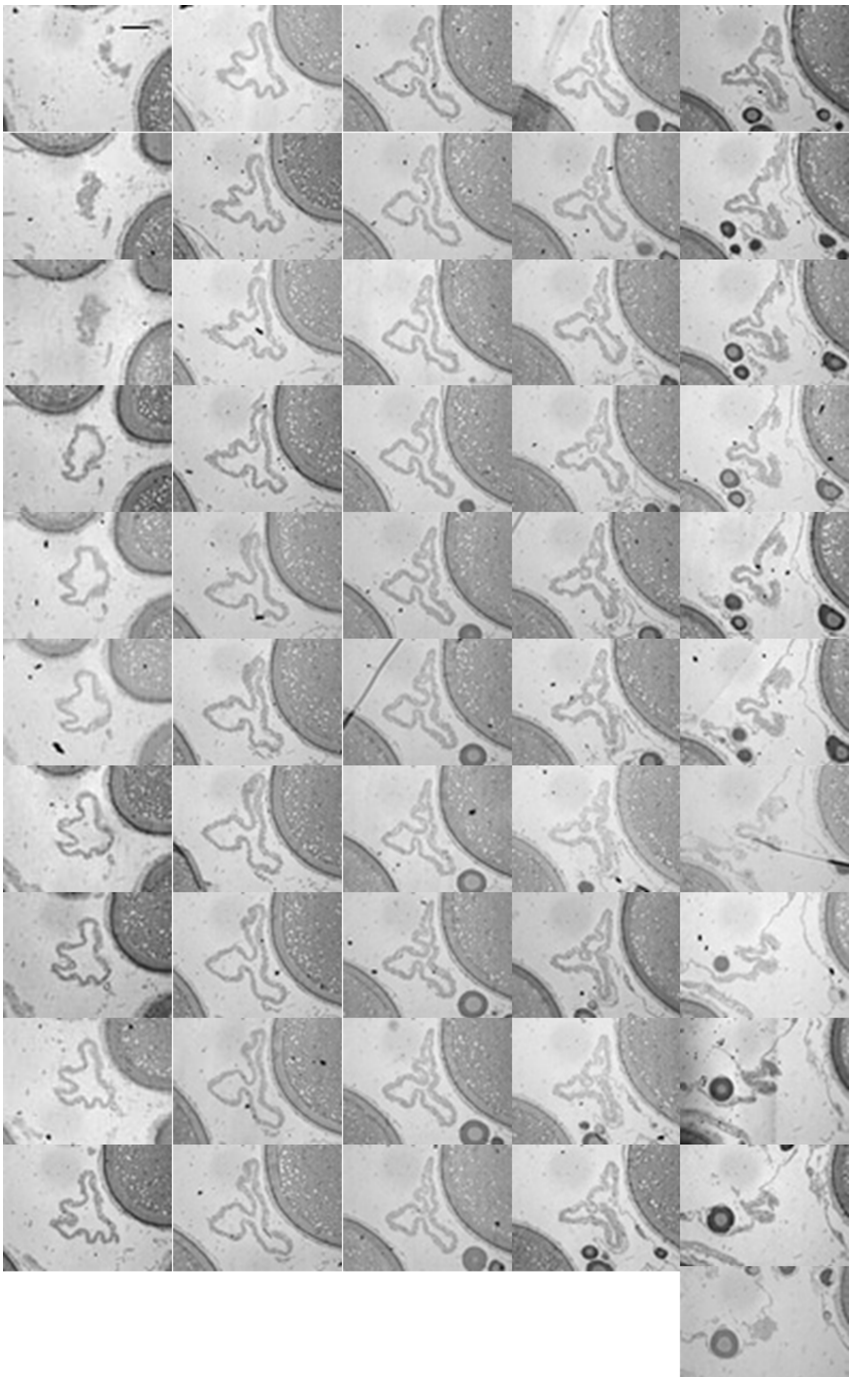

Figure 4.25.

From top to bottom and left to right a series of alternate histological sections from a postovulatory follicle (PDF) retained to generate a 3-D model.

Finally, the volume of the 3-D reconstruction of POF is estimated by integrating the volume of each pair of sections representing a unit depth of 10 µm (alternate sections) and based on the assumption that the serial section thickness is held uniform at 5 µm.

4.5.3.3 POF ageing: basic principles

The study of POF degeneration until full resorption with time can be made through the analysis of a collection of samples obtained throughout a 24-hour cycle (Alheit *et al.,* 1984; Macewicz *et al.,* 1996; Roumillat

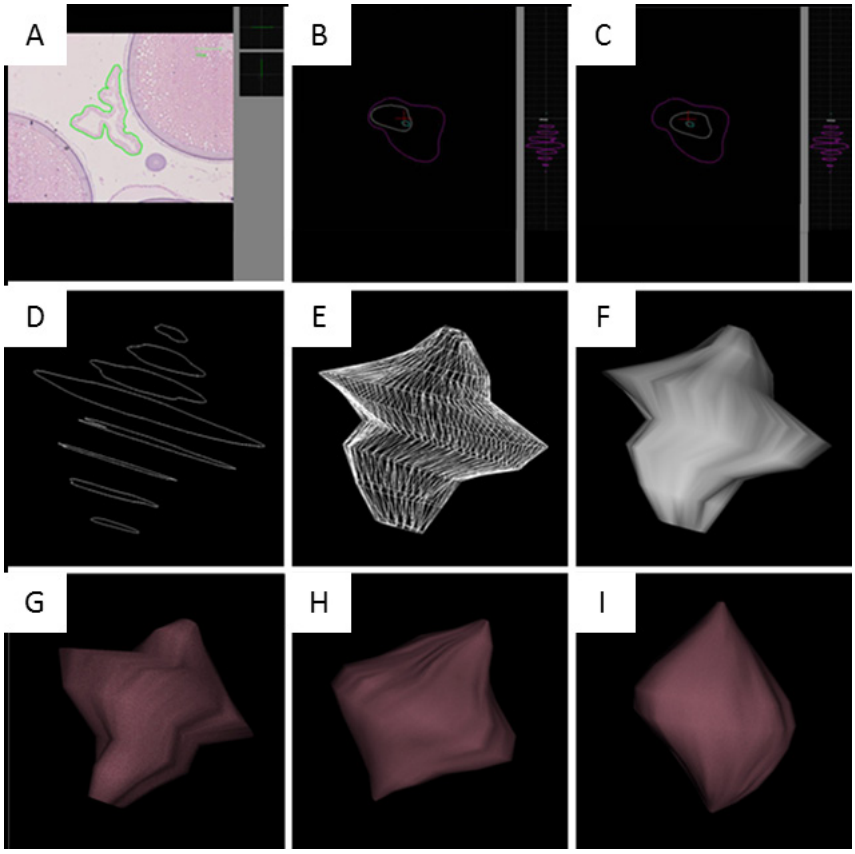

Figure 4.26.

Assembly and visualization of a 3-D reconstruction of a postovulatory follicle (POF) generated by image analysis. (A) Profile of POFs manually drawn; (B) Traces in all sections arranged in sequence; (C) Traces aligned with precision; (D) series of a digitized tracing profiles aligned according to the sequence; (E) triangular faces placed at midpoints of traces; (F) a surface drawn a wireframe; (G) a surface without smoothing; (H) a surface with a smooth shading; (I) lateral view of the complete aligned 3-D reconstruction.

& Brouwer 2004; Yoneda *et al.,* 2002). However, as POF can last for several days in the gonads (depending upon temperature; see Section 4.5.3.1) usually the analysis is restricted to a collection of samples obtained to a limited period of the day. This facilitates distinction of POFs pertaining to different daily spawning classes, as their differences in shape, size and histological indicators are enhanced (Funamoto and Aoki, 2002; Ganias *et al.,* 2003b, 2007a). In order to analyze POF degeneration with time it is necessary to use several histological markers including, POF size and shape the aspects of theca, granulose cells, lumen, etc. (see Sections 4.5.3.1 and 4.5.3.5). In addition to the examination of field samples, the degeneration of POF in time can be well established by inducing spawning in aquaria and sampling females at known time intervals after their synchronous spawning time (see Section 4.5.3.4). This was the method first applied to the study of the degeneration of POF for northern anchovy (Hunter & Goldberg, 1980; Hunter & Macewicz, 1985b) which guided most of the subsequent applications of the POF method. Validation of the pattern of POF degeneration with time in tank experiments is usually achieved through verification of the consistency of the occurrence in time of the different POF stages in field samples obtained at similar sea temperatures (see example in Alday *et al.,* 2008). Once the occurrence of different types of POFs (or stages) relative to peak spawning time is obtained for the range of temperatures inhabited by

spawning stock, the occurrence of the type of POF (or stage) at a given sampling time will give indication of the time passed since allocation to spawning daily classes will, in principle, be straightforward.

For species with a protracted daily spawning period, lasting for instance for half a day or more or without any distinct modal spawning time, the study of the degeneration of POF from field samples is more complicated. In these cases, synchronous induced spawning in aquaria or monitoring of concrete individuals in aquaria with known spawning time will be required for a good understanding of the dynamics of POF degeneration. To manage the monitoring of the final maturation and POF degeneration processes of individual females, small gonad tissue samples could be removed with catheter at short intervals (Kurita *et al.*, 2011, see also Fig. 4.27), although special care to reduce the stress on females is required. An alternative approach is to take ovary tissue from wild or captive fish and follow final maturation process of oocytes (e.g. Matsubara *et al.,* 1995) or degeneration process of POFs in vitro incubations in plastic culture dishes. If these studies are not available, the duration of the different POF stages can be used from well studied similar species, which show marked single daily spawning peak. Subsequently POF stages, which jointly may last for about a day, can be grouped and used for the estimation of spawning fraction from their mean incidence in the mature population. Kurita (2012) points out the convenience of grouping spawning markers so that their joint presence last for about 24 hours for the mean environmental temperature at sampling stations. Spawning fraction can be then accurately and robustly estimated based on those markers, with appropriate correction factors for deviation from 24 hours of their actual joint duration; regardless of the spawning time, frequency distribution, and sampling time. A good study of the process of oocyte maturation and POF degeneration in time would allow establishing the correspondences between the different degrees of oocyte maturity and of degeneration of POFs and the time left to, or past from, the ovulation or spawning. When sampling is restricted to a limited period of the day a direct description of the characteristics of POFs corresponding to spawning classes Day_0, Day_1 or Day_2 is feasible; as such POFs can be directly classified into Day_0 or Day_1 type etc., and this has been the most common procedure for the analysis of POFs; with existing examples for anchovy in Hunter & Macewicz et al. (1985); and Funamoto & Aoki (2002), and for sardine in Alarcón *et al.* (1984), Goldberg *et al.* (1984) Ganias *et al.* (2003b). However when sampling is widespread throughout the day the variety of different stages of oocyte maturation and/or POF degeneration that could belong to the same spawning class increases and description of POFs type Day_1 or Day_2 become more complicated, requiring a large experience in examining and ageing POF at the same time. In those cases a two steps procedure which splits the staging of oocyte maturation and POF degeneration from their ageing, or allocation to a spawning cohort, can be assayed. For the staging of oocyte maturation the usual

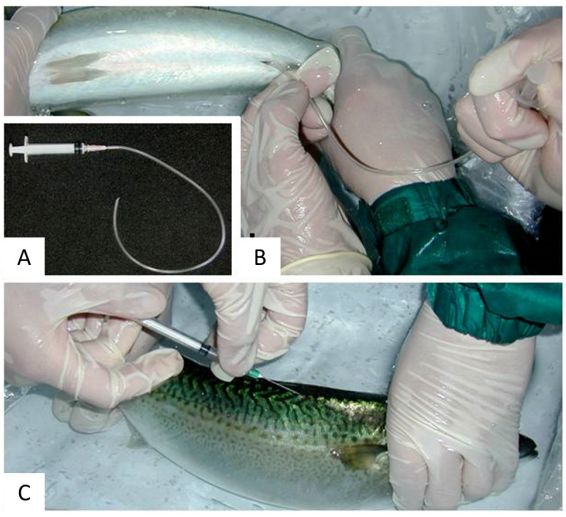

Fig. 4.27.
Egg sampling by using a flexible catheter (A, B) and GnRHa injection to the dorsal muscle of the chub mackerel (C).

identification of the maturing steps from germinal vesicle migration (GVM) and vesicle breakdown (GVB) to the hydration phases provides a sufficient well resolved staging system (Hunter & Macewicz, 1985b; Lowerre-Barbieri *et al.*, 2011b), while for the POFs a staging system based solely on the degeneration features of POFs is to be applied. An example of such a classification system of POFs (comprising 7 degeneration POF stages) is given in Alday *et al.* (2008 and 2010), which might be valid for many species (Ganias, 2012). For the ageing, a matrix system for allocating females to daily spawning cohorts based on time of capture and stage of oocyte maturation/ POF degeneration is to be defined according to the experimental sampling or aquaria designs mentioned above (see example in Uriarte *et al.,* 2012). The procedure of separating oocytes and POF staging from their ageing (or allocation to a daily spawning cohort) makes the process more objective, as staging describes only the observed maturity state of oocytes and the degeneration state of POF. In contrast ageing becomes a separate step, dealing only with the allocation of oocyte and POF stages to spawning daily classes by an automated procedure, based upon the biological knowledge of their maturation and degeneration process over time. The process becomes itself more repeatable for subsequent cross-checking of POF stages and for any potential future revision of the stage-cohort matrices according to new criteria, if required. Finally it is worth remembering that the ageing or allocation to daily spawning classes of females showing histological indicators of imminent (or recent) spawning requires a clear definition of the daily spawning classes. For example, if spawning is around midnight, usually daily classes are defined for a period comprising the peak spawning time, as for instance daily cycles starting and ending at 06:00 hours. The usual reason to comprise the peak spawning time well inside the limits of the spawning class definitions is to make that any potential oversampling of spawning females affect only to a single spawning cohort (the Day_0 females).

4.5.3.4 Spawning induction and POF ageing in tank experiments

As mentioned in the previous section, combining survey data with tank experiments should improve POF ageing and, in addition, improve the actual knowledge of wild stocks reproductive biology. However, a major problem in tank experiments is that the hatchery-reared broodstock of many commercial fish species fails to undergo final oocyte maturation and ovulation spontaneously. The major endocrinological dysfunction is due to a lack of luteinizing hormone (LH) secretion from the pituitary. The present section describes the procedure of inducing spawning and subsequently following the process of oocyte growth and POF degeneration in captive female chub mackerel, *Scomber japonicus*. During the spawning season (April-June), fish reared in 3-ton outdoor concrete tanks under natural photoperiod and temperature were anaesthetized with 2-phenoxyethanol (100 mg/l), and females with fully-grown oocytes at late yolk (LY) stage (600-650 μm in diameter) were selected by ovarian biopsy using a plastic catheter tube (Fig. 4.27A, B). Ovarian tissues were removed and preserved in Ringer's solution (135 mM NaCl, 2.4 mM KCl, 1.5 mM $CaCl_2$, 1 mM $MgCl_2$, 1 mM $NaHCO_3$, 0.5 mM NaH_2PO_4).

After measurement of the diameter of the most advanced oocytes, Ringer's solution was discarded and a few drops of Sera solution (ethanol:formalin:acetic acid = 6:3:1, v/v) were added to make the cytoplasm transparent which allowed the nucleus to be viewed (Fig. 4.28A, B, C). If the nucleus (GV, germinal vesicle) was not observed, this indicated the onset of oocyte atresia, and the fish were removed from the study.

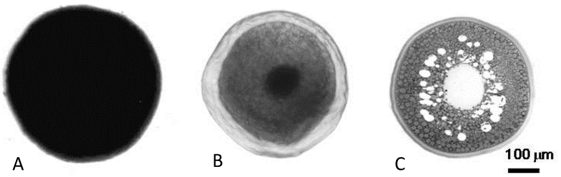

Fig. 4.28.

Photomicrographs of fully-grown oocytes at late yolk stage (LY) of the chub mackerel by simple transmitted light. (A), fresh oocyte preserved in Ringer's solution; (B) fixed oocyte with Sera solution; (C) histological section of same stage of oocyte.

Males oozing milt under gentle abdominal pressure were selected. After selection of required number of females and males, intramuscular injection with the GnRH analogue [des-Gly^{10}-(D-Ala^{6}) LHRH ethylamide, 400 µg/kg BW] was performed (Fig. 4.27C) to release the endogenous pituitary LH. The first ovulation occurred 34-36 h post-injection (Shiraishi *et al.*, 2008), and subsequent daily spawning was observed for 20-30 days when the water temperatwure ranged between 18-23°C. During spawning, fish were fed with commercial dry pellets. Using this system, it is possible to obtain a series of ovary samples at regular intervals from the time of ovulation. Through such study, a time table of Final Oocyte Maturation (FOM), ovulation and spawning may be revealed (Fig. 4.29). Fish sampling was usually performed after one week of GnRHa injection because the endogenous hormonal pathway of Brain-Pituitary-Gonad (BPG) axis is involved in the regulation of multiple spawning without the influence of externally administered GnRHa (Nyuji *et al.*, 2011). In the spawning stock, ovulation occurred synchronously among fish, and spawning was performed immediately following ovulation between 21:00-01:00, generally peaking at around 23:00. Fish with germinal vesicle migration (GVM)-stage ovaries caught before noon are capable of spawning on the night of that same day. Fish with germinal vesicle breakdown (GVBD)- and hydration (HY)-stage ovaries appeared during afternoon and continued until the evening.

The degenerative process of postovulatory follicles collected from fish reared at 19°C was also analyzed. The size of the follicular lumen was reduced over time (Fig. 4.30A, D) and in 24-h-old POFs, the lumen was either a remnant or closed completely (Fig. 4.30E). The POFs were distinguishable from other tissues up until 48 h (Fig. 4.30F), however, in 72-h-old ovaries, the POFs were completely resorbed. Refer to Shiraishi

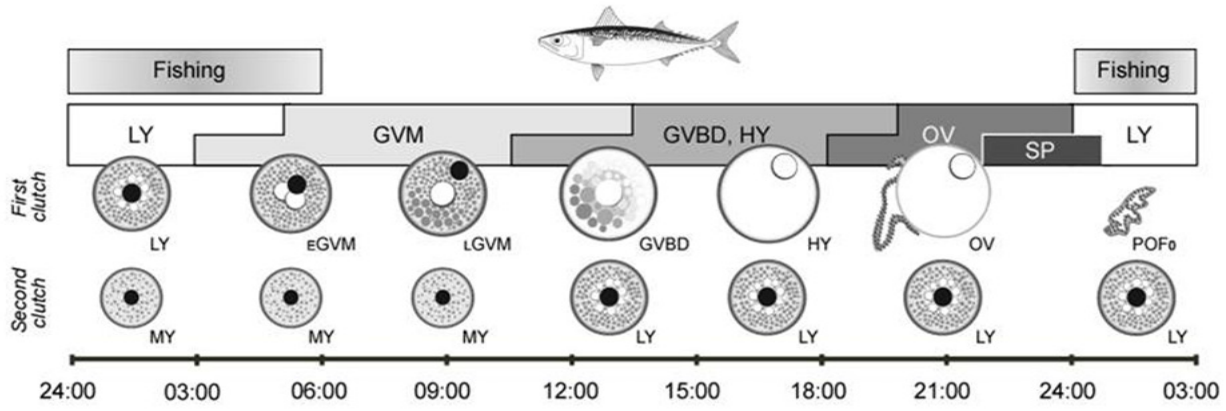

Fig. 4.29.

Time table of Final Oocyte Maturation, ovulation and spawning, and time zone of commercial catch in the chub mackerel in a day. $_{E}$GVM, early germinal vesicle migration; GVBD, germinal vesicle breakdown; HY, hydration; $_{L}$GVM, late germinal vesicle migration; LY, late yolk; MY, mid yolk; OV, ovulation; POF0, day 0 POF (age ≤6 h); SP, spawning.

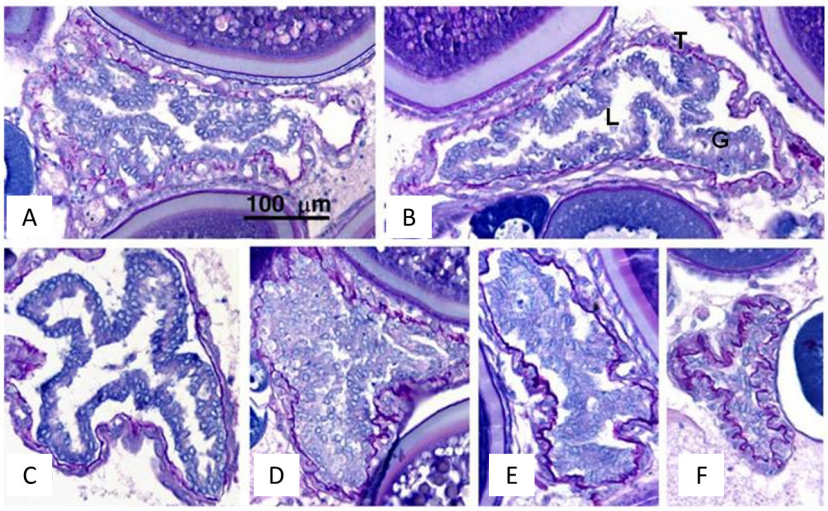

Figure. 4.30.

Photomicrographs of POFs of chub mackerel reared at 19°C and sampled at 0 (A), 6 (B), 12 (c), 18 (D), 24 (e), and 48 hours (F) after ovulation. G, granulose cell layer; T, thecal cell layer; L, follicular lumen. 4 µm-thick sections were cut and stained with 1 % toluidine blue solution followed by PAS (Periodic Acid and Schiff) reagent. Basement membrane between granulosa cell layer and thecal cell layer is clearly stained in purple-red with PAS.

et al. (2009) for detailed morphological changes of POF.

4.5.3.5 Using POF size in POF ageing

The method follows all the initial laboratory steps for histological analysis for fish maturity, atresia, and POFs studies. When POFs are detected, slides are scanned in detail to locate the largest follicle situated along the epithelium of the lamellae (Fig. 4.31A). These POFs are then photographed at an appropriate magnification so that the whole follicle fits into the photomicrograph (Fig. 4.31B). The cross-sectional area of the whole POF (POF_{xsa}) is then measured on-screen using image analysis software (Fig. 4.31B).

The first task in the analysis is to develop (or refine existing) staging criteria for POFs. A good way to accomplish this task is through analysing the frequency distribution of POF_{xsa} in females caught simultaneously and post-inspecting POFs in each size-age mode for differences in the cytomorphological characteristics (Fig. 4.32). Differences in the dimensional (size, shape) and fine

Table 4.5.

Summary of dimensional (shape, cross-sectional area) and fine histological (state of the granulosa layer) characteristics of different daily classes of sardine POFs.

Age (days)	Shape	Material	Surface área (µm2)	State of granulosa
<1	Irregular	paraffin resin	16404 ± 427 35486 ± 1472	Thick and looped
1-2	Rectangular	paraffin resin	9272 ± 255 17650 ± 468	One well formulated layer
2-3	Triangular	paraffin resin	5910 ± 187 12620 ± 303	A thin layer only some remnants
>3	Triangular	paraffin resin	4160 ± 197 7234 ± 373	Completely reabsorbed, only some residual vacuoles

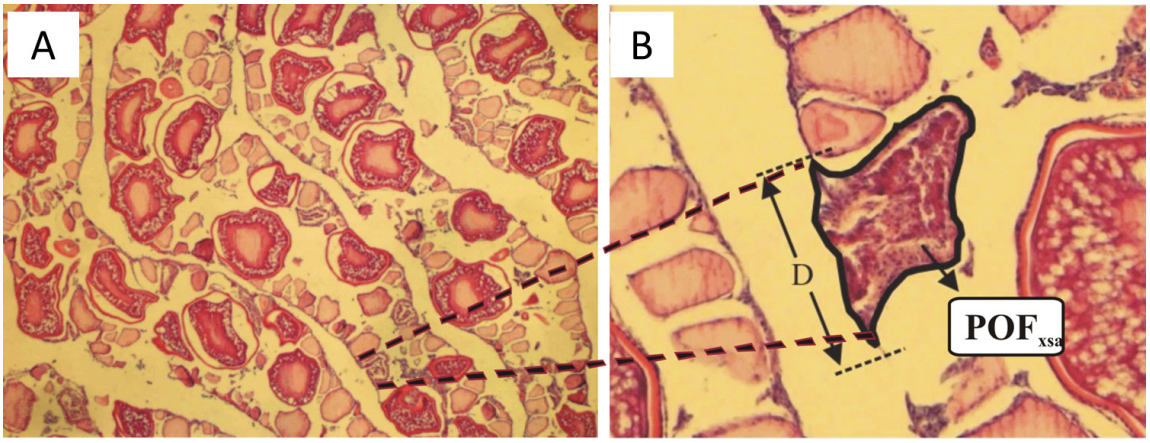

Figure 4.31.

Processing of photomicrographs from ovarian sections with POFs. A: allocation of the largest POF in the section; B: measurement of POF cross-sectional area (POF_{xsa}).

histological (deterioration of the granulosa layer) characteristics are subsequently used to describe the pattern of POF resorption. Table 4.5 summarizes some of the most important histomorphological criteria for sardine, *Sardina pilchardus*, POFs. After refining the staging criteria and classifying POFs into daily cohorts, the time of capture and the daily spawning hour are used to estimate the exact age of POFs, i.e., the time in hours elapsed between spawning and sampling. The effect of POF-age and other factors on POF_{xsa} could then be tested (e.g. by means of a generalized linear models GLM). Apart from POF-age, the GLM approach also allows to test for the effect of other explanatory variables, either continuous such as temperature, or discrete such as sampling year, the preservative type and the

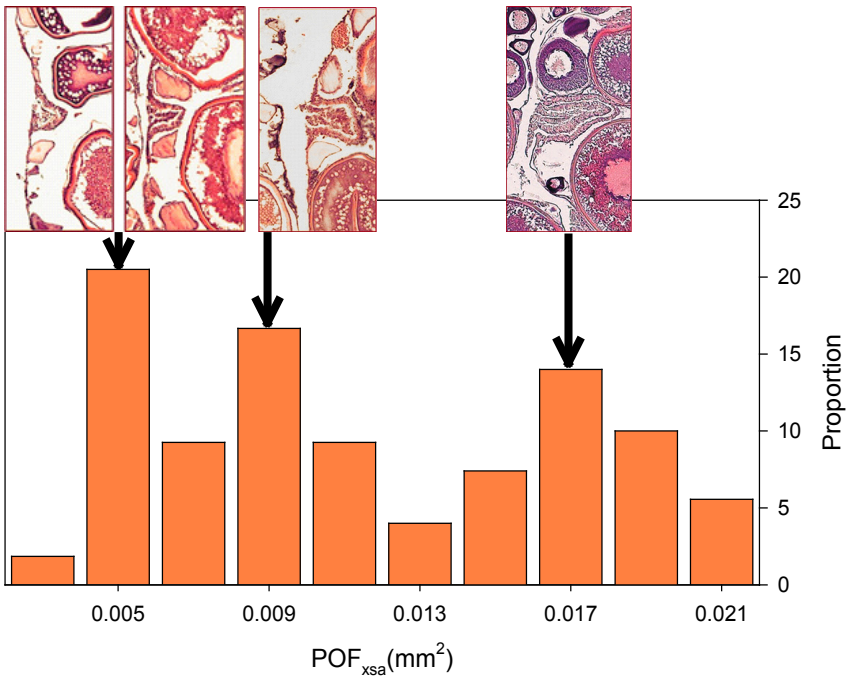

Figure 4.32.

Frequency distribution of POF cross-sectional areas (POFxsa) and corresponding histological appearance of POFs from each size class in paraffin sections.

embedding material. The latter is quite important because the laboratory processing of the ovaries may differ from year to year or between different labs or technicians. The explanatory power of the relationship between POF-age and POF_{xsa} indicates the accuracy of the devised staging and ageing criteria. For sardine, a highly significant log-linear relationship was found between POF_{xsa} and POF-age, the former decreasing by approximately 50% per day (Fig. 4.33A). POFs were also shown to shrink faster at higher temperatures (approximately 3% per degree) (Fig. 4.33B), but this temperature effect is unlikely to be an important source of bias in the assignment of females to daily spawning classes. The embedding material was also shown to influence the size of POFs, the latter being significantly larger in resin than in paraffin sections (Fig. 4.33A). These results indicate that the size of POFs provides an indirect, reliable estimation of the time elapsed from spawning and may thus be used to test both the validity of POF staging criteria for identifying daily cohorts of spawners and the effect of other factors (temperature, laboratory processing, etc.) in the classification of POFs Tests such as those described in the present section should be performed at least once for each species or population to assess bias in POF staging and ageing criteria. Moreover, the test would provide comparative information on POF resorption rates, impact of fixative, preservative or embedding material, and effects of temperature and other environmental parameters. In routine applications of the POF ageing method, the measurement of POF_{xsa} might increase the technical work, but not necessarily the precision in spawning fraction estimates since females are also classified into spawning daily cohorts as they were with the histological staging method. However, in cases where POF-age and POF_{xsa} relationships are already available, correspondence of POF sizes to daily spawning cohorts would be much more realistic compared to simple histological staging, which strongly depends on the experience of the observer and the quality of the slides.

4.5.4 Methods based on imminent spawners

Apart from females with markers of recent spawning activity, estimations of spawning fraction may also rely on the prevalence of females with

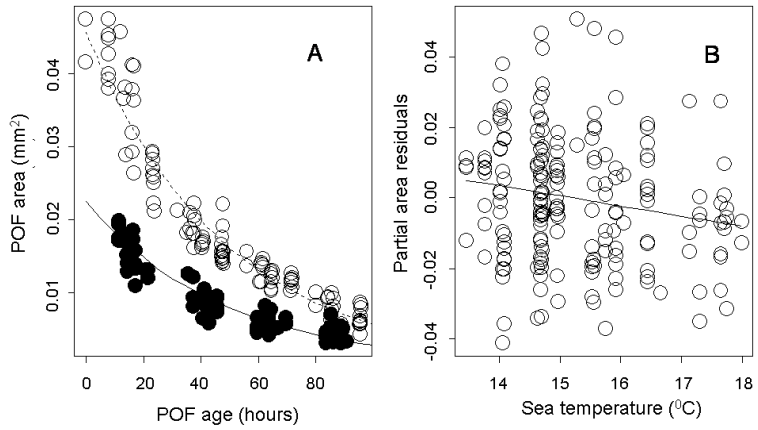

Figure 4.33.

A) Evolution of sardine POF cross-sectional area (POF-area) with time elapsed from spawning (POF age); ○: resin; •: paraffin. B) Effect of ambient temperature on sardine POF area.

preovulatory markers, e.g. females at the germinal vesicle migration or at the hydration stage.

4.5.4.1 The hydrated females method

The most significant advantage of the so-called hydrated oocytes or hydrated females, HF, method (DeMartini & Fountain, 1981) is that this stage is easily identified even with macroscopic inspection (Hunter & Macewicz, 2003) which makes S estimation rather quick and cheap. However, the method has several prerequisites to get an accurate estimation of S the most important being the distributional pattern of hydrated females both in space and time. In many species hydrated females exhibit segregating behavior which consequently leads to their over- or under-representation in samples of adult fish. In that respect, the HF method is only valid for species where hydrated females are evenly distributed within the adult population. Other prerequisites of the HF method is that the period from ovulation to spawning must be short, the longevity of hydration as a visible characteristic of the ovary is known and sampling is constrained within the daily period of its prevalence. Priede & Watson (1993) extended this approach by considering also the preceding stage of nuclear migration to estimate the spawning fraction of mackerel, *Scomber scombrus*, one of the few pelagic species without evidence of daily spawning synchronicity at the population level. One efficient way to test the validity of the HF method is to test its coherence with the POF method; for example, in several fish families, estimators based on imminent and recent spawners were shown to be coherent suggesting that the HF method may serve as a low-cost alternative to the POF method

4.5.4.2 The gonadosomatic index method

Claramunt & Roa (2001) and Claramunt *et al.* (2003) developed a theoretical and statistical argument for a new method, previously outlined in Claramunt & Herrera (1994), which has the same conceptual basis as the hydrated females method, but differs in that the proportion of hydrated females is an expected proportion under a normal frequency distribution of the population. The normal distribution is controlled by the mean and standard deviation, and the latter can be modeled as a linear function of the gonadosomatic index (GSI). Instead, the mean is a function of the distance between the hydrated oocyte diameter and the mean diameter of the more advanced yolked oocytes. The assumptions that should be satisfied are:

1. S is the daily proportion of females in which the mean diameter of the most advanced batch of oocytes is greater than or equal to the hydration diameter (Fig. 4.34).

2. Within the population of mature females, mean diameter of the most advanced oocyte mode, follows a normal distribution, ranging from resting and spent to spawning (left to right) (Fig. 4.34).

To check this assumption, it is necessary to randomly select females and measure mean diameter of the most advanced mode of oocytes. To estimate the mean diameter of the more advanced mode, disaggregated oocytes of ovary subsamples must be measured and grouped in a frequency distribution. The oocyte size distribution can be estimated by using a set of sieves in an appropriate range and intervals (e.g. 0.2-1 mm at 0.05 mm intervals) or through digital image analysis. For details on using image analysis see Section 4.2.5. The mean diameter of the most advanced oocyte mode can be estimated by using the MPA (Modal Progression Analysis of Bhattacharya) and NORMSEP routine of FiSat II v.1.2.0 (http://www.fao.org/) (Section 4.4.3). These females are then classified according to the mean diameter of the most advanced mode and used to check the assumption of a normal distribution.

Once assumptions 1 and 2 are satisfied, the daily spawning fraction ($S_{t,exp}$) is determined by calculating the area under the normal curve to the right of the hydration diameter (Fig. 4.34). This calculation includes two unknown parameters, the mean and the standard deviation, and one known parameter, the hydration diameter:

$$S_{t,exp} = \frac{1}{\sqrt{2\pi\sigma_t^2}} \cdot \int_{X_t=H_t}^{\infty} exp\left[-\frac{(X_t-\mu_t)^2}{2\sigma_t^2}\right] dx_t \quad 4.29$$

where X_t is the mean diameter of the most advanced stock of oocytes within the ovary of an individual female; H_t is the hydration diameter, and μ_t and σ_t are the mean and standard deviation of the oocyte diameter distribution in the female fish population respectively (t indicates time period). The frequency distribution of the oocytes in hydrated ovaries allows one to estimate the diameter at the start of hydration (Fig. 4.35). The problem is that three parameters are needed to estimate the expected proportion: a) the mean μ_t, b) the standard deviation σ_t, and c) the diameter at which hydration occurs H_t. Claramunt & Roa (2001) reduced the problem to one unknown parameter: the standard deviation, by assuming certain known cutoff values for quantiles in the normal curve, where the upper bound is constrained to be 3 units of σ_t greater than the mean (Fig. 4.34) and that the hydration diameter (H) is constant in the time period (t). Then, it can be demonstrated that the spawning fraction can be estimated by a simplified version:

$$S_{t,exp} = \frac{1}{\sqrt{2\pi\sigma_t^2}} \cdot \int_{d_t}^{\infty} exp\left[-\frac{(d_t-3\sigma_t)^2}{2\sigma_t^2}\right] dx_t \quad 4.30$$

in which the hydration diameter is not present and

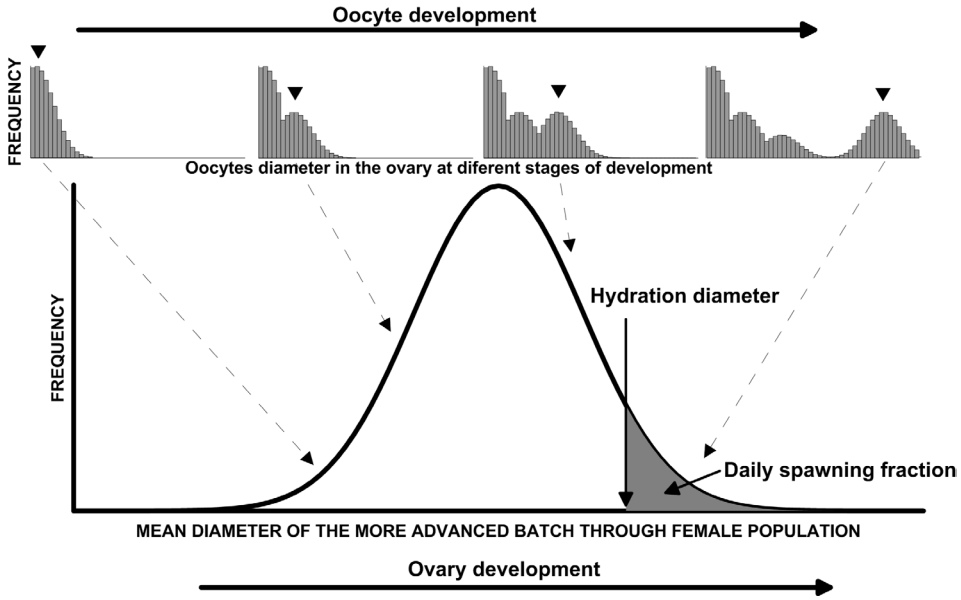

Figure 4.34.

Conceptualization of daily spawning fraction as the area under a normal distribution of the females classified by the mean diameter of the most advanced oocyte mode. Each observation represents mean oocyte diameter of the most advanced mode in the ovary of an individual female. The first line represents typical oocyte frequency distributions for different stages of maturation. Black inverted triangles indicate mean diameter of the most advanced mode, starting from partially yolked to hydrated oocytes (left to right). Arrows indicate approximately where the mean diameters of more advanced mode are located in the normal frequency distribution of the female population. The normal curve represents the proportion of females in the population by mean diameter of the most advanced oocyte mode (black inverted triangles in the first line). Grey area is the daily spawning fraction, which is equal to the proportion of females in which the most advanced oocyte mode is greater than or equal to the hydration diameter..

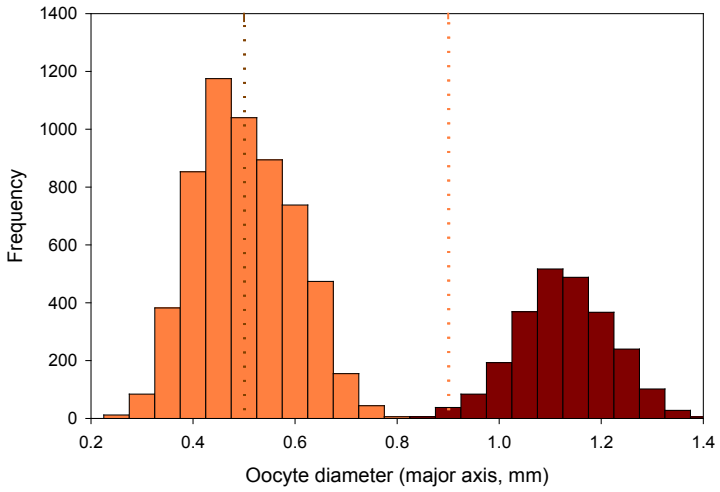

Figure 4.35.

Frequency distribution of the oocytes diameter in hydrated ovaries. Vertical lines indicate the separation of 0.4 mm between the mean of yolked oocytes and the start of hydration.

only the standard deviation remains as a parameter to estimate. The term d_t represents the difference between the diameter of yolked oocytes and the hydration diameter (Fig. 4.35) and can be obtained from the frequency distribution of the oocytes in hydrated ovaries. In practical terms the calculation is based on the area under a normal curve (i.e. with spreadsheet) with $X_t = d_t$; mean = $3*\sigma_t$ and standard deviation = σ_t. The authors use d_t = 0.4 mm for Sardinops sagax.

Application

Information from direct estimation of S (i.e. histology) from several months are necessary to calibrate the model. Using numerical optimization methods (e.g. Newton-Raphson; Routine Solver in Excel), the standard deviation values of equation (4.30) are estimated as those that would render $S_{t,exp}$ identical to estimates from histology. Finally it is observed that the calibrated standard deviation parameters are linearly related to the corresponding GSI observations from the same samples. Using monthly estimations of S by histology in Sardinops sagax Claramunt & Roa (2001) report the relationship:

$$\sigma_t = 64.257 + 4.806 \cdot GSI \quad (n = 11, r^2 = 0.78) \qquad 4.31$$

After this relationship is established and its parameters are known, it is possible to estimate daily spawning fraction for other samples, using the standard deviations (σ_t) estimated from Equation 4.31 in Equation 4.30.

Example: The mean GSI for August is 6.413. By using Equation 4.31 the estimated standard deviation is 95.078 µm. The area under the normal normal curve with X_t = 400 µm, mean = 3*95.078 µm, and standard deviation = 95.078 µm yields 0.114. Therefore 11.4% of females spawn each day.

4.5.4.3 The oocyte growth method

The present section presents a method to estimate the interspawning interval (ISI) based on oocyte growth rate (described in more detail in Ganias *et al.,* 2011). Figure 4.36 illustrates the conceptual model and the parameters required for this estimation. Given the rate of oocyte growth, G, and oocyte size at the beginning and the end of the batch cycle, O_b and O_e respectively then ISI can be estimated using the formula:

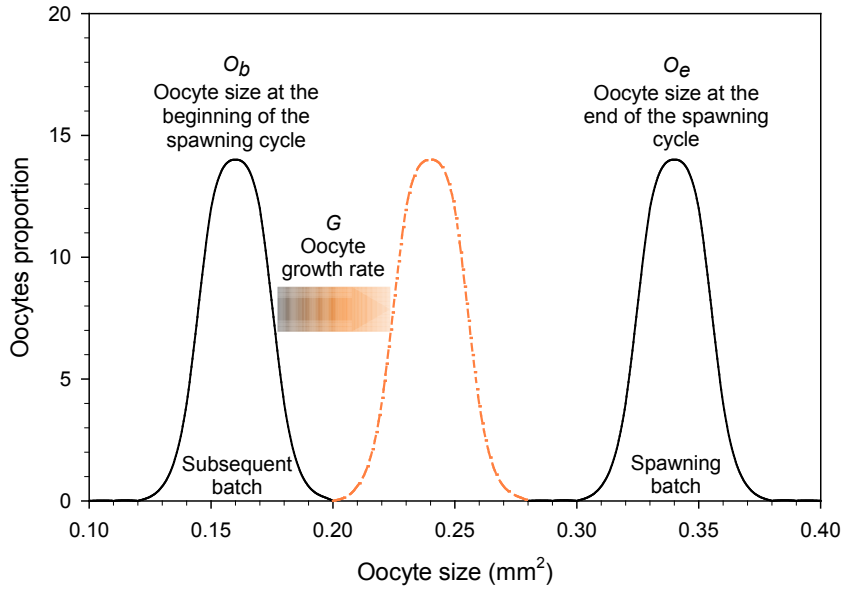

Figure 4.36.

Conceptual model for the estimation of individual spawning frequency exemplifying parameters used in Equation 4.31.

$$ISI = \frac{O_e - O_b}{G} \qquad 4.32$$

Equation 4.32 is only valid when G is stable throughout the batch cycle. However, most pelagic spawners undergo oocyte hydration which is known to alter G since oocyte size increases abruptly in a very short amount of time. In that case, Equation 4.32 should be transformed to:

$$ISI = \frac{O_v - O_b}{G_v} + \frac{O_H - O_v}{G_H} \qquad 4.33$$

or alternatively to:

$$ISI = \frac{O_v - O_b}{G_v} + t_H \qquad 4.34$$

where O_v and O_H is oocyte size at the end of vitellogenesis and hydration respectively, G_v and G_H is the rate of oocyte growth at vitellogenesis and hydration respectively and t_H is the time course of oocyte hydration To be valid the model should satisfy the following prerequisites: i) G_v should either be constant within the population or be a simple function of easily measured demographic or environmental parameters like body-size and temperature, ii) similarly, O_e (or O_v and t_H) should either be constant or predicted by easily measured life-history or physical parameters, iii) there should be no unpredictable pauses during the batch cycle, e.g. time lags between true vitellogenesis and hydration or 'ripe holding periods', and finally iv) female spawners at the beginning of their batch cycle should be easily and accurately identified in order to measure O_b. Given that all these prerequisites are met and that G, and O_e (or O_v and t_H) are known, ISI could be simply estimated by measuring O_b in female spawners at the beginning of their batch cycle. At each stage of oocyte development (e.g. true vitellogenesis, hydration) G could be estimated by regressing oocyte size, O, on spawning lag, t, i.e. the time lag before or after the spawning act in imminent and recent spawners respectively:

$$O_i = \beta_0 + G(t_i) + e_i \qquad 4.35$$

where O_i is oocyte size at spawning lag t_i, e_i is the

error term whilst β_0 expresses the average size of the oocytes of the spawning batch at the beginning of the batch cycle for the whole population. However, in order to measure O_b for each female separately, females should be caught exactly at the beginning of their batch cycle. An accurate and easy way to estimate O_b is through measuring the size of the oocytes of the subsequent batch in hydrated females (Fig. 4.37A). O_v could be estimated by measuring the size of oocytes of the advanced batch in a number of individuals at the transitional state between the completion of vitellogenesis and beginning of oocyte hydration. Finally, t_H could be estimated by following the time course of oocyte hydration from its very beginning to the mean daily spawning hour of the population. Since the process of oocyte hydration is usually quite ephemeral and most fish populations exhibit daily spawning synchronicity t for imminent spawners may be estimated from the lag between the time of capture and the average daily spawning time of the population. For recent spawners t could be estimated after ageing their POFs, e.g. by fitting POF_{xsa} to a fixed POF area/age curve (see Section 4.5.3.5). Knowing t, estimation of G_v and G_H would require measurements of oocyte size in recent and imminent spawners respectively. This task could be easily accomplished by means of particle analysis in digital photomicrographs of ovarian whole mounts using procedures described in Sections 4.2.5 and 4.4.2 (Fig. 4.37).

Application

The method was applied and the four prerequisites were tested for the Atlantic sardine, *Sardina pilchardus*. The slope of the oocyte size vs. spawning lag relationship did not differ significantly between four different groups of spawners (ANCOVA: P>0.1; Fig. 4.38A) suggesting that G_v was constant between different years and laboratory protocols (e.g. type of preservative).

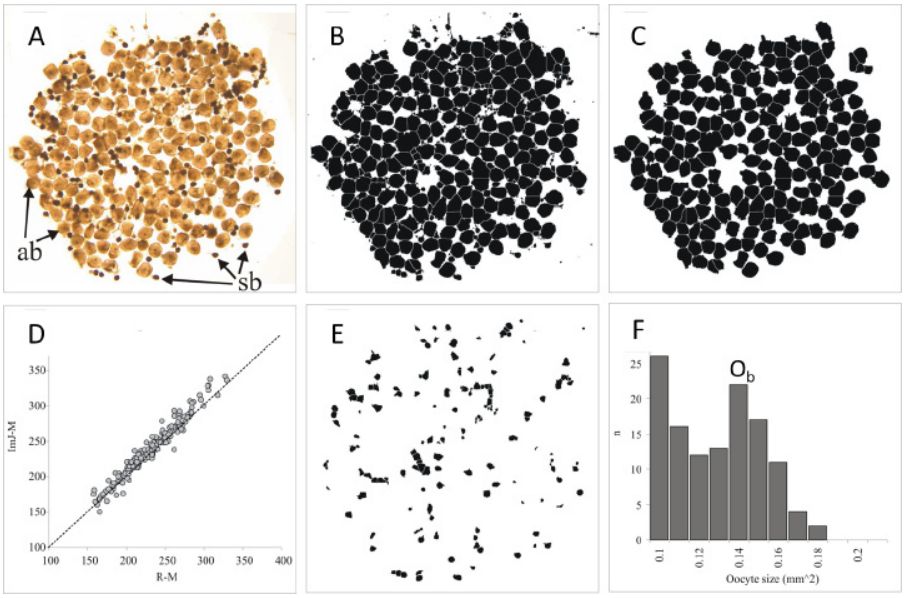

Figure 4.37.

A) micrograph of hydrated sardine ovarian whole mount illustrating oocytes of the advanced (ab) and subsequent (sb) batches; B) the same image after being subject to the ImageJ routine; C) separation of the spawning (hydrated) batch; D) manual oocyte counts (reference method; R-M) vs. counts provided by the ImageJ method (ImJ-M) plotted over the diagonal line; E) separation of non-hydrated oocytes; F) size distribution of non-hydrated oocytes illustrating overlapping between the subsequent batch and the smaller oocyte groups. O_b: the modal diameter of the subsequent batch..

This satisfies the first of the model prerequisites. Oocyte growth in imminent spawners is best described by the second order polynomial regression (Fig. 4.38B):

$$O = 0.177 - 0.010t + 0.003t^2 \quad 4.36$$

where t is set in hours. This together with the visual examination of Figure 4.38B indicated a shift in oocyte growth in imminent spawners which was attributed by means of histological observation to the onset of hydration at ca. 9:00. The most important histological marker for this transition was the fusion of all yolk globules into plates. Due to this abrupt change of G at hydration ISI was finally estimated using Equation 4.36. Consequently these results were used to estimate both t_H and O_v, i.e. the duration of oocyte hydration and oocyte size at the end of vitellogenesis respectively. The former was estimated to be 12h or 0.5d which is the time lag between the onset of hydration (9:00) to mean spawning time (21:00). O_v was estimated by predicting oocyte size at 9:00 using equation-5 (0.29 mm^2).

Given that G_v and O_v exhibited fairly constant values, and that sardine exhibits no pauses between true vitellogenesis and hydration and no 'ripe holding period' (which satisfies the third prerequisite) ISI in hydrated females was estimated as a factor of O_b, i.e. the size of oocytes of the subsequent batch in hydrated females using the formula:

$$ISI = \frac{0.29 - O_b}{0.018} + 0.5 \quad 4.37$$

Figure 4.39 illustrates the distribution of ISI values for a set of hydrated female sardines. The average ISI for these females was 11.50 days (CV=8.93%), corresponding to a spawning frequency of 0.086 which is within the range of yearly spawning fraction estimates derived from the POF method.

4.5.5 Methods for species with high spawning frequency

Many fishes including scombroids (Lowerre-Barbieri et al., 1996; Medina et al., 2002; Schaefer, 1996; Yamada et al., 1998; Yoneda et al., 2002) but also small pelagics (Clarke, 1987; Luo & Musik, 1991; Rogers et al., 2003; Takasuka et al., 2005; Uriarte et al., 2012; Wright, 1992 etc.) may have medium to high spawning fractions, with values of S between 0.25 and 0.5 or even higher. The reproductive dynamics of these fishes with

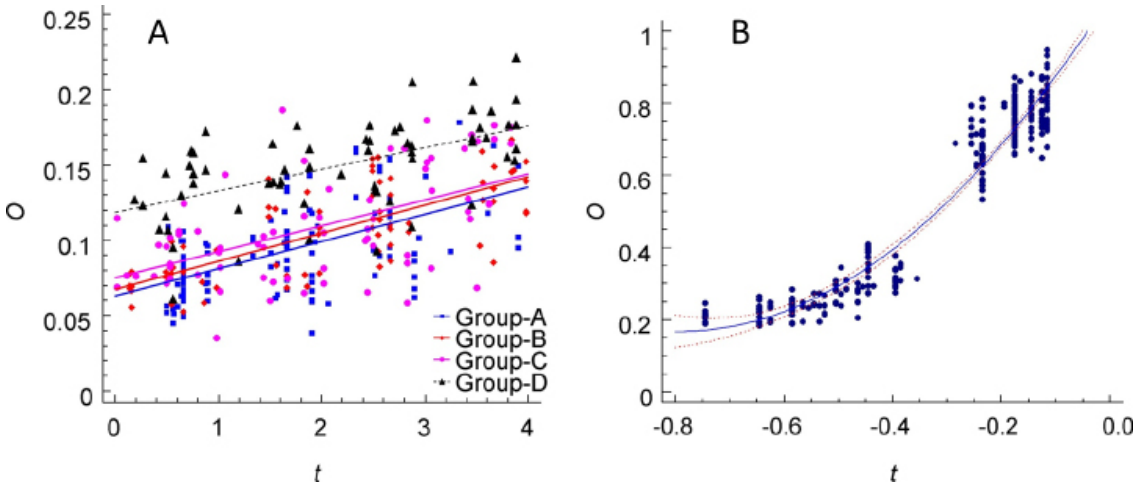

Figure 4.38

Relationship between the size of the oocytes of the advanced batch (O, in mm^2) with spawning lag (t, in days) for (A) the four different groups of recent spawners and (B) for imminent spawners.

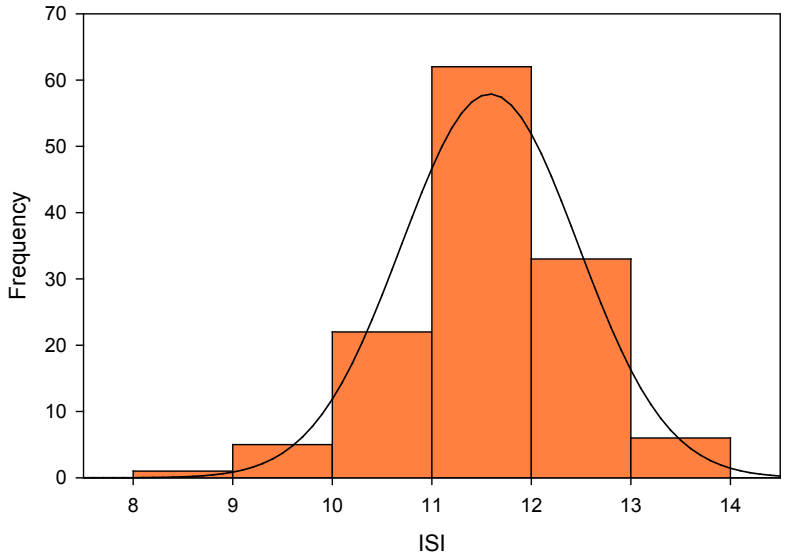

Figure. 4.39.

Frequency distribution of estimated interspawning intervals (ISI, in days) for hydrated females of the 2008 survey. ISI values were shown to come from a normal distribution (P>0.1; dotted line).

medium-high spawning fraction, have features of particular interest for the estimation of S, such as:

1. an increasing negative (complementary) relationship between the incidence of Day_0 and Day_1 spawners in the samples.

2. an increasing number of females displaying the co-occurrence of both pre- and post-spawning stages, allowing the direct estimation of spawning frequency (or interspawning intervals) on an individual basis.

4.5.5.1 Negative relationship between Day 0 and Day1 spawners

The increasing negative relationship between Day_0 and Day_1 spawners as S increases should be obvious, as for S=0.5 all Day_1 will spawn the following day and therefore will be Day_0 the following day and hence become completely complementary. This will confer some stable properties to an S estimator based on their combined incidence, given that a negative covariance should reduce the variance of a combined estimator (Ganias *et al.,* 2003b, see section 4.5.2 above). Effectively, the formula of a composite spawning fraction estimate based on Day_0 and Day_1 is:

$$S_{0+1} = \frac{(S_0+S_1)}{2} \qquad 4.38$$

And the expected variance from their individual variance and covariance is:

$$\hat{Var}(S_{0+1}) = \left(\frac{1}{2}\right)^2 \cdot [\hat{Var}(S_0) + \hat{Var}(S_1) + + 2COV(S_0, S_1)] \qquad 4.39$$

Hence, if the covariance is negative then the variance of this estimator is smaller than half the mean of the original individual variances of the estimators S_0 and S_1.

In addition S_{0+1} is an unbiased estimator whenever Day_0 is not oversampled in comparison to the other daily spawning classes. If some oversampling of Day_0 exist, for intermediate values of S the only

unbiased estimator of S will be the S_1 corrected for oversampling (as mentioned before), but the higher the S the smaller will be the biased for S_{0+1}. And at S=0.5, in the presence of oversampling of Day_0, the only unbiased estimator becomes S_{0+1} as the oversampling of day_0 will be compensated completely in the undersampling of Day_1 (repulsion effect of Day_0 on Day_1 cohort) (Uriarte *et al.,* 2012). So for high spawning frequencies applying S_{0+1}, in addition to the classical corrected S_1 estimate may be a worth pursuing. This estimator can be calculated on sample basis as:

$$S_{0+1} = \frac{(n_0+n_1)}{2n} \quad 4.40$$

For which the mean and variance from a group of samples from a survey can be directly computed applying equations 4.39 and 4.40 above.. And the relative expected mean bias for the samples taken at time t will be:

$$Rbias\left(\hat{S}(1+0)_t\right) = Rbias\left(\hat{S}(0)_t\right) \cdot \frac{1-2S}{2\cdot(1-S)} \quad 4.41$$

so that the bias of this estimator increases with the relative oversampling of Day0 and decreases with increasing S, becoming in fact 0 at S=0.5. (Uriarte et al. 2012). Note that in addition the S_{0+1} is robust to overlapping of Day_0 and Day_1 classes, whenever those females are included in both spawning classes. Such overlapping happens for population having a S in the range 0.5 to 1. Therefore for S values higher than 0.5 the bias of that estimator is expected to be 0. Uriarte *et al.* (2012) concluded that for species which have a high spawning fraction (usually above 0.33,

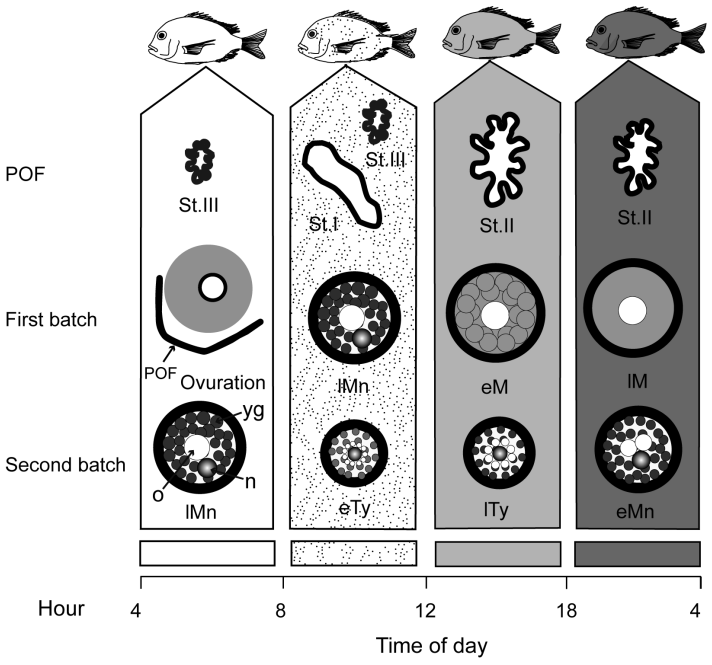

Fig. 4.40.

Diagrammatic representation of expected ovarian conditions in spawning Dentex hypselosomus with both maturing oocytes and degenerating postovulatory follicles at different times of the day. eM, early mature stage; eMn, early migratory nucleus stage; eTy, early tertiary yolk stage; lM, late mature stage; lMn, late migratory nucleus stage; lTy, late tertiary yolk stage; n, nucleus; o, oil droplet; yg, yolk globule; POF (postovulatory follicle): Stage I (St. I);Stage II (St. II); Stage III (St. III).

as many pelagic species –including small pelagics and scombroids in temperate and tropical areas), little oversampling of Day_0 and/or a strong negative correlation between Day_0 and Day_1 occurred and, thus, S_{0+1} can be considered as a robust and simple estimator of S. In their example (*European anchovy*), this estimator produced the most precise estimator of S with a negligible bias which could ultimately be corrected according to the formulae presented above (or by the mean relative bias across sampling times, when sampling is scattered throughout the day).

4.5.5.2 Co-occurrence of pre- and post-spawning stages

A second feature of the species having medium to high spawning frequencies is that there will be an increasing number of females displaying co-occurrence of both pre- and post-batch spawning stages. This co-occurrence has been reported for many scombroids and other groups (Dickerson et al., 1992; Lowerre-Barbieri et al., 1996; Macewicz & Hunter, 1993; McBride et al., 2002; Schaefer, 1996; Yamada, 1998; Yoneda et al., 2002) and also for some small pelagic species (Rogers et al., 2003; Motos, 1996; Uriarte et al., 2012)

Yoda & Yoneda (2009) examined the spawning season, spawning frequency and batch fecundity of yellow sea bream Dentex hypselosomus in the East China Sea to assess the spawning frequency and several other reproductive characteristics of the species. The time course of sampling showed that this species has a diurnal ovarian maturation rhythm: late tertiary yolk stage oocytes appeared 2 days before spawning, starting the process of germinal vesicle movement, breakdown, and ovulation, which occurs early in the morning on the day of spawning, and the postovulatory follicles (POFs) disappeared within about 24 hours of ovulation. These ovarian characteristics implied that the expected ovarian condition of spawning individuals was determined at different times of the day (Fig 4.40). In the early morning, three patterns were expected depending on the progression of ovulation. Before ovulation, the ovary contained both mature and migratory nucleus stages of oocytes in addition to stage III of POFs; in comparison, during or after ovulation, the ovary contained migratory nucleus stage oocytes as the most advanced batch, plus I and III POFs. From morning to afternoon, the largest oocytes in the ovary developed from the migratory nucleus to mature stage while the tertiary yolk stage (second largest) oocytes proceeded from early to late stage. At night, females had both mature and migratory nucleus stage oocytes and either stage II or III POFs. For the females which can receive double assignments to pre- and post-spawning daily classes an estimate of the individual spawning frequency can be obtained (measured in terms of inter-spawning intervals ISI, or days passed between successive spawning events). For example, in the case of yellow sea bream the spawning status of individual fish was determined from the expected ovarian conditions of the spawning females (Fig. 4.40). Females in which the most advanced batch in the ovary reached either the late tertiary yolk or migratory nucleus stage and who also had degenerating POF were defined as spawning repeatedly every other day (SPA1). The SPA1 group included females having oocytes at only one stage of maturation or degenerating POF, which were defined as spawning within 0 to 2 days before or after the day of collection. Females having oocytes at two different stages of maturation, including the late tertiary yolk stage (late morning), or a combination of mature stage oocytes and degenerating POFs were defined as spawning on two consecutive days. Females with a combination of oocytes at two different maturation stages and degenerating POFs in their ovaries were expected to spawn repeatedly on three consecutive days. According to Uriarte *et al.* (2012) this double

assignment allows an estimation of S for the population based upon the average of the individual spawning fraction of females, deduced from the reciprocal of the spawning frequencies (1/f), as follows:

$$S(f) = \sum_{f=1}^{\infty} \left(\frac{1}{f}\right) \cdot P(f) \qquad 4.42$$

where P(f) is the probability of a female having a spawning frequency of f days. With variance:

$$\hat{Var}(S(f)) = \sum_{f=1}^{\infty} \left(\frac{1}{f}\right)^2 \cdot \hat{Var}(P(f)) + \\ + 2 \cdot \sum_{f=1}^{\infty} \sum_{f'<f}^{\infty} \left(\frac{1}{f}\right)\left(\frac{1}{f'}\right) \cdot COV\,(P(f), P(f')) \qquad 4.43.$$

where,

f and f´refer to different spawning frequencies.

Certainly this formula cannot be applied unless any potential f can be detected on individual basis, so the preferred population for the application are those having S around 0.5 or above. For S in the range 0.33 to 0.5, the estimation of interspawning intervals higher than 3 days is very difficult unless POF last for 3 days or more in the ovaries (something that only happens for species spawning in cold waters). To apply this formula Uriarte *et al.* (2012) assumed that all females for which the ISI could not be estimated were going to spawn every third day and therefore had an ISI=3. As such the former expressions were restricted to the first three daily interspawning intervals. Under these circumstances, the estimator is simplified to:

$$S(f) = 1 \cdot P(f = 1) + 0.5 \cdot P(f = 2) + \\ +0.333 \cdot P(f = 3) \qquad 4.44$$

where P(f=1) is the probability (or frequency) of a female spawning every day, estimated by the conditional probability of being Day_0 and Day_1 at the same time within Day1 spawning cohort ($P(Day_0 | Day_1)$). And P(f = 3) is the probability of post-spawning females spawning every third day (the remaining fraction of females).

When an ISI estimate is directly available for all females, a direct calculation of the mean and variance of the 1/ISI of all sampled individual females will give the population mean spawning fraction S and its variance. This estimator is unbiased for any type of oversampling of Day_0 females.

4.5.6 Spatio-temporal effects on fecundity estimates

Most of the previously described methods for estimating S are based on the assumption that spawning sites are equally distributed throughout the sampled area and that there is no net movement into or out of the sampled area (Hunter & Macewicz, 1985b; Lowerre-Barbieri *et al.,* 2009). However, knowledge of the spatio-temporal distribution of spawning sites is needed to test these assumptions (Lowerre-Barbieri *et al.,* 2011b), as spawning activity may not be evenly distributed throughout a study site (Fig. 4.41). Methods to directly assess spawning behavior and location include: analysis of ovarian development in GPS-referenced females from capture-based surveys (Begg & Marteinsdottir, 2002; Ollerhead *et al.,* 2004); visual observations of spawning behavior (Domeier & Colin, 1997; Samoilys, 1997); acoustic surveys to detect and enumerate the size of spawning aggregations (Lawson & Rose, 2000; Macchi *et al.*, 2005); and passive acoustic surveys to detect biological sounds associated with spawning (Luczkovich *et al.*, 2008; Walters *et al.,* 2009). Telemetry has also been used in conjunction with other methods to evaluate

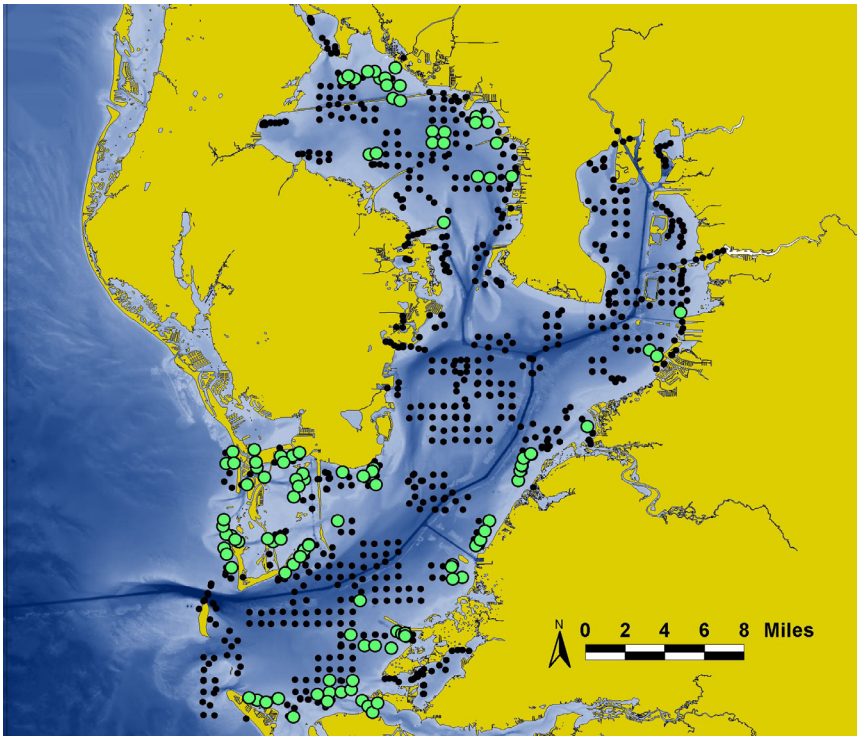

Figure 4.41.

Spatiotemporal patterns of spawning activity can be complex, as demonstrated here for spotted seatrout, which spawn near dusk in lower Tampa Bay, Florida (N=2034). Two reproductive patterns were observed based on samples taken in the afternoon (post meridian PM): (1) fish moving nightly to a high-intensity spawning site at the Inlet and (2) low-intensity spawning in three of four estuarine zones. Pie charts indicate the proportion of active spawners collected in the PM by sampling zone. Zone-specific markers indicate individual sampling sites. In before noon (ante meridian AM) sampling, no females were collected at the inlet and the proportion of females with POFs in estuarine zones ranged from 13-23%. OM: oocyte maturation and POF:postovulatory follicle.

movements and residence time on the spawning grounds (Zeller, 1998; Robichaud & Rose, 2002; Svedang *et al.,* 2007; Lowerre-Barbieri *et al.*, 2013).

To use capture-based methods to assess the spatial distribution of spawning, it is necessary to first assess the diel periodicity of spawning and develop sampling times appropriately. This is because fish at the time of spawning may aggregate at spawning sites and spawning females will not be randomly distributed (Hunter & Macewicz, 1985b; Ganias, 2008). Thus, to assess spatial variability in the proportion of spawning females, sampling designs should include collection of fishes over a wide spatial distribution and both at spawning and nonspawning times (Murua *et al.*, 2003). Logistic regression can then be used to evaluate how sampling location and time impacted the probability of sampling spawning females (Lowerre-Barbieri *et al.,* 2009). Passive acoustic methods to assess spawning sites based on courtship sound production have several advantages over capture-based methods, including: no need to sacrifice fish; their ease of deployment, meaning they can be used over any bottom type, and can survey large geographic areas in a fraction of the time needed with capture gear (Fig. 4.42), and minimal to no interruption in spawning behavior (Roundtree *et al.,* 2006; Walters *et al.,* 2009). Nevertheless, although fishers have known for centuries that spawning aggregations of soniferous species could be located based on sound production, only recently has this method been more commonly incorporated into scientific studies (Gannon 2008). In soniferous species,

typically the male fish, makes sounds associated with spawning (Rountree *et al.,* 2006; Luczkovich *et al.,* 2008). Thus underwater microphones deployed from a boat or remotely with a recording mechanism can be used to assess diel periodicity and spawning seasonality (Rountree *et al.,* 2006; Walters *et al.,* 2007; Fudge & Rose, 2009), as well as the spatial distribution of spawning aggregations based on the categorization of the number of fish calling and the duration of sound production (Luzkovitch *et al.,* 2008; Lowerre-Barbieri *et al.*, 2008; Walters *et al.,* 2009). In addition, long-term acoustic recording devices allow for acoustic monitoring of spawning sites throughout the spawning season, greatly improving our ability to assess diel periodicity (Walters *et al.,* 2007; Lowerre-Barbieri *et al.,* 2013). .

Telemetry, or the monitoring of fish with acoustic tags, is also increasing our understanding of reproductive spatio-temporal behavior. Robichaud & Rose (2002) were able to demonstrate that there is a turn-over rate of individual fish at cod spawning grounds leading to acoustic surveys underestimating the spawning population. Telemetric methods have also been used to assess sex-specific behavior on the spawning grounds (Robichaud & Rose 2002; Lowerre-Barbieri *et al.*, 2013), spawning migratory routes (Rhodes & Sadovy, 2002), and the timing of arrival on spawning grounds (Douglas *et al.,* 2009). If a known spawning site is identified, telemetry can also be used to assess how often individuals return to this site within a spawning season, or site-specific spawning frequency (Lowerre-Barbieri *et al.,* 2013).

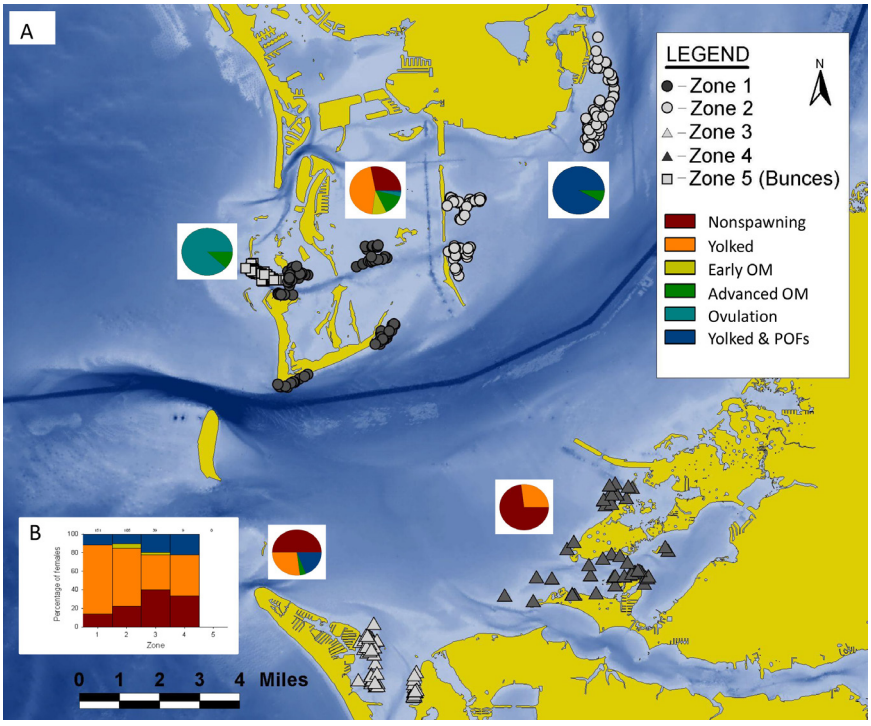

Figure 4.42.

Spatial distribution of Spotted Seatrout (Cynoscion nebulosus), spawning aggregation sites in Tampa Bay, Florida in 2004 based on a passive acoustic survey. Male spotted seatrout make sounds associated with courtship, making it possible to detect spawning aggregation sites based on sound production. Sites sampled are indicated by black dots (random stratified site selection). Sites with spawning aggregations are indicated by blue dots.

4.6 Annual fecundity

Fish spawn their eggs at various temporal scales (Lowerre-Barbieri 2011b), spanning from semelparity, i.e. one spawning event in a lifetime like some salmons and eels, to extreme iteroparity, i.e. species that spawn continuously throughout their entire adult life. Species can then be broadly classified by fecundity pattern, according to the lag between oocyte recruitment and spawning. A continuum of intermediate patterns, with determinacy and indeterminacy as end-points, is generally recognized (see Box 4.1). Extreme determinacy is observed & in semelparous species, or single spawners like herring, where oocyte recruitment & spawning periods are rather short and clearly distinguished among them. Extreme indeterminacy is seen in species that spawn year round and where oocyte recruitment and spawning periods completely overlap. The position of a population along the determinacy-indeterminacy continuum will be influenced by the degree of overlap between the oocyte recruitment and spawning periods, with determinate spawners having all their annual stock of oocytes recruited before the onset of the spawning period. Due to these differences in the pattern of batch recruitment, estimation of annual fecundity is quite different for indeterminate and determinate spawners.

4.6.1 Determinate fecundity species

In determinate fecundity, as previously described in the BOX 4.1, the estimated number of vitellogenic oocytes present in the ovary (total fecundity) prior to the commencement of spawning is considered equivalent to the potential annual fecundity. This is because the recruitment of oocytes to the vitellogenic pool ended before spawning commences. In species which exhibit determinate fecundity, annual realized fecundity is estimated by discounting oocyte atresia (the process of oocyte and follicle resorption altering the oocyte structure indicating that the oocyte will not complete the maturation process) from total fecundity. For estimating the total fecundity or the number of vitellogenic oocytes in the ovary before the onset of the spawning, apart from general methods described in Sections 4.2 and 4.3, the following specific methods can be used.

4.6.1.1 The autodiametric method

The auto-diametric fecundity method (Thorsen & Kjesbu, 2001) is based on the fact that there exists a relationship between the mean diameter of the vitellogenic oocytes and the oocyte density (oocyte number/g ovary) (Fig. 4.43). For determinate spawners this relationship is typically very tight (see section 4.3.2.2) which means that once this relationship has been established oocyte density can be accurately estimated by measuring the mean diameter of vitellogenic oocytes. This again means that the standing stock of maturing oocytes can be estimated from mean oocyte diameter and the ovary weight.

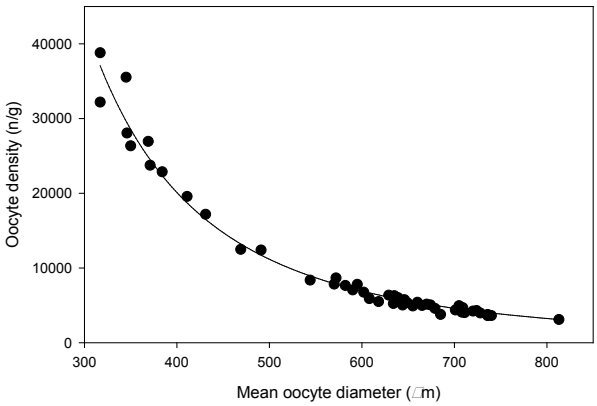

Figure 4.43.
Relationship between mean oocyte diameter and oocyte density (n/g) for cod (Gadus Morhua L.). From Thorsen & Kjesbu, 2001.

Compared to traditional gravimetric fecundity counting this has two major advantages; sampling simplicity and sample work-up speed. Although gonad weight should be accurately weighted for estimating the total number of vitellogenic oocytes in the ovary, sampling is more straightforward since the sub-sample does not have to be accurately weighed or volume measured, it is enough to simply take a small piece of ovary material and put it in a tube with buffered formalin. This is particularly important when doing sampling at sea, - in a rolling ship it is often not possible to do accurate subsample weighing. Sample work-up is also much easier; measuring mean oocyte diameter is usually very quick using particle analysis on digital images (see Section 4.2.5). Typically it takes 1-2 minutes to measure mean oocyte diameter of a cod ovary sample, - including all sample handling.

Establish the mean oocyte diameter versus oocyte density relationship

To establish the regression or calibration curve between the mean oocyte diameter and the oocyte density it is necessary to do both gravimetric counting and diameter measurement on a chosen set of samples. For doing so, the selection of samples should cover fish that are in all maturation stages; from early vitellogenesis (vitellogenesis) to pre-spawning. This will assure an accurate regression line to be established that works for the whole range of maturation stages. Usually 20-50 samples are enough.

The subsamples used for building up the calibration curve should preferably contain several hundreds of maturing oocytes, but usually not thousands since that would imply much extra work without significant increase in precision. The subsamples should be accurately weighed, usually with mg precision. Alternatively the subsamples can be taken volumetrically by a micropipette (Witthames et al., 2009) and then convert to weight units (Fig. 4.44). Repeated volumetric sampling and subsequent weighing can establish the volume/weight conversion factor. The most efficient way to work up gravimetric subsamples is probably by using a combination of automatic particle analysis and manual counting (see Section 4.2.5). First the sample is spread out in one or more photographic chambers and pictures are taken that include all the oocytes in the subsample. Then automatic particle analysis is applied on the pictures. Usually some of the oocytes will not be measured by the automatic procedure due to presence of oocyte clumps etc. The number of oocytes remaining will vary with the degree of separation of the oocyte material in the photographic chamber, but it has been found that this selection is random (Thorsen & Kjesbu, 2001). Thus the automatic measurements can be considered representative and the mean oocyte diameter can be calculated as such. To measure oocyte density the total number of vitellogenic oocytes has to be counted; after the automatic particle analysis has finished the remaining oocytes are counted manually on the pictures using a counting tool in the image analysis software. The relationship between mean oocyte diameter and oocyte density can usually be established using a

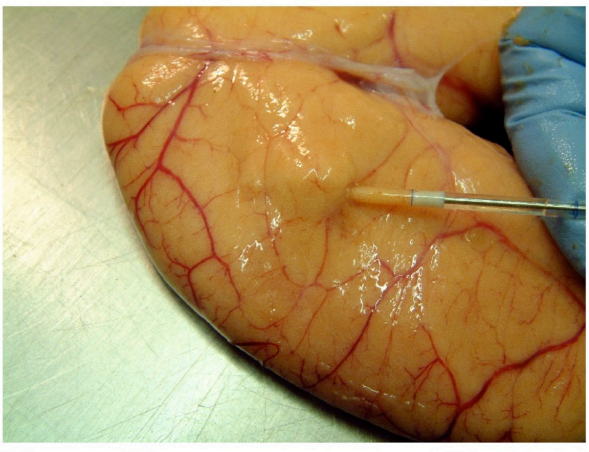

Figure 4.44.
Volumetric sampling of ovary using a micropipette.

power regression or a polynomial regression. Species with a narrow vitellogenic (maturing) oocyte size distribution typically have a tighter relationship between mean oocyte diameter and oocyte density than species with broad size distributions. Determinate fecundity type species typically have relatively narrow vitellogenic oocyte size distributions with a clear gap to the pre-vitellogenic pool (Fig. 4.45). On the other hand indeterminate spawners typically have broader distributions with no size gap to the previtellogenic pool (Fig. 4.45). This means that clearly determinate fecundity species like herring, plaice, redfish and cod are well suited for the auto-diametric method, while indeterminate species as hake and horse mackerel are not suited (Witthames *et al*., 2009). Mackerel is an example of a species that do not fall clearly into either the determinate or indeterminate group. However, mackerel have a very broad vitellogenic oocyte size distribution and are regarded as not suitable for the Auto-diametric method.

Comparative studies (Witthames *et al*. 2009) have shown that different species/stocks of fish in general fit into the same mean oocyte diameter – oocyte density relationship. However, small differences between species probably exist; therefore, it is recommended to use a species specific relationship. Furthermore, since different labs have different optics and cameras this may result in small lab specific differences on the measured mean diameters. For the most accurate fecundity work it is therefore recommended to use oocyte diameter versus oocyte density relationships that are both lab and species/stock specific.

4.6.1.2 Atresia and fecundity down-regulation

In many fecundity studies, the standing stock of vitellogenic oocytes (potential fecundity) is assumed to equal the realised fecundity (actual number of eggs spawned); however, this is not always the case. Failure to account for changes in potential fecundity as ovary development proceeds can result

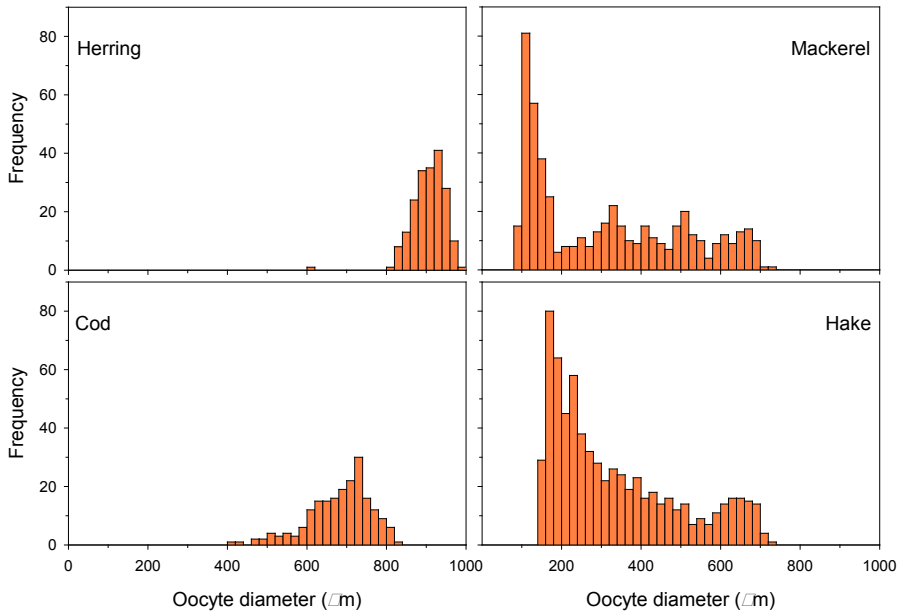

Figure 4.45.

Oocyte size frequency histograms for Atlantic Herring (Clupea harengus), Atlantic Cod (Gadus morhua), Atlantic Mackerel (Scomber Scombrus), and European hake (Merluccius merliccius). All samples taken from pre-spawning fish in late maturation stage. Lower size measuring thresholds were 250 µm for cod and herring, 100 µm for mackerel and 185 µm for Hake.

in erroneous conclusions on perceived differences in fecundity between years or areas which may be a result of development stage rather than a temporal or spatial difference in fecundity (Thorsen *et al.,* 2006). In addition, failure to account for down-regulation by atresia may lead to errors in the calculation of spawning stock biomass (SSB) during application of the annual egg production method for SSB (Witthames *et al.,* 2009). The apparent first mention of the effect of maturity stage on fecundity was by (Vladykov, 1956) who described the decrease in fecundity with oocyte development in wild speckled trout (*Salvelinus fontinalis*). Despite this early description, the effect of maturity stage on fecundity has rarely been considered in fecundity studies until recently (Kurita *et al.,* 2003; Thorsen *et al.,* 2006; Kennedy *et al.,* 2007).

There are several studies which have shown that ration related differences in fecundity are more closely tied to differences in production rates of oocytes rather than atretic rates (Tyler & Dunn, 1976; Wootton, 1979). Up until 1984, ovarian atresia had never been used for quantitative estimation of any reproductive processes in marine fish populations (Hunter & Macewicz, 1985a). After atresia became a common consideration during fecundity studies, several laboratory experiments on effects of feeding on reproductive traits showed a significant effect of food level on the intensity of atresia in several species: Atlantic cod (*Gadus morhua*) (Kjesbu *et al.,* 1990), Atlantic herring (*Clupea harengus*) (Ma *et al.,* 1998), turbot (*Psetta maxima*) (Bromley *et al.*, 2000) and European plaice (*Pleuronectes platessa)* (Kennedy *et al.,* 2008).

Investigations into the down-regulation of fecundity have been carried out for only a few species. The most complete account is for Atlantic herring where fecundity has been estimated throughout the entire vitellogenic phase of ovary development for Norwegian spring-spawning (NSS) herring (Kurita *et al.,* 2003; Kennedy *et al.,* 2011) and North Sea herring (van Damme *et al.,* 2009). The greatest reduction in the number of developing oocytes occurs during the early stages of development as can be seen by the changes in fecundity between months and development stage (Kennedy *et al.,* 2011; Kurita *et al.,* 2003) or the non-linear negative correlation between relative fecundity (fecundity/body weight) and average oocyte diameter (van Damme *et al.,* 2009). The difference in fecundity between autumn and winter spawning herring is brought about by greater down-regulation in the winter spawners compared to the autumn spawners. Current estimates of down-regulation are in the range of 20-50 % and appear to be the dominating mechanism in producing annual fluctuations in fecundity for herring (van Damme *et al.,* 2009; Kennedy *et al.,* 2011; Kurita *et al.,* 2003). The only other species in which fecundity has been documented through the complete ovary development cycle are European plaice (Kennedy *et al.,* 2007) and Atlantic cod (Skjæraasen *et al.,* 2010). These two species have a similar development pattern, but this differs from Atlantic herring. The recruitment of oocytes to the developing cohort in these species continues until the average oocyte diameter is approximately 600 µm (spawning occurs when oocytes reach 800-900 µm and 1100-1200 µm for Atlantic cod and European plaice respectively). Fecundity is then reduced through atresia as vitellogenesis continues. Annual variations in fecundity for NEA cod are driven by a combination of variations in the down-regulation of fecundity (Kjesbu *et al.,* 1990) and by variations in the number of oocytes recruited to the developing cohort (Kjesbu, O.S. pers. comm. Institute of Marine Research, Norway). Spatial variations in fecundity of European plaice in the Irish Sea are driven by differences in the down-regulation of atresia; however, is not clear whether annual variations are driven by differences in oocyte recruitment.

The importance of atresia in fecundity regulation appears to be greater in the determination of fecundity in species with long period of oocyte development i.e. Atlantic herring versus Atlantic cod. The time needed to develop oocytes to full maturity is primarily a function of temperature and oocyte size. Thus, the time between oocyte recruitment and spawning, for species living at a similar temperature, will be greater for species with larger eggs. As the time until spawning increases, the ability to predict the energy reserves which will be available at spawning decreases. In that respect, species which have a long ovary development period will be unable to recruit an appropriate number of oocytes which closely reflects their energy reserves at spawning. This is especially true if oocyte recruitment occurs before the peak feeding season e.g. herring (Kurita *et al.,* 2003; Slotte, 1999).

Methods for estimating the down-regulation by atresia

In order to assess the degree of down-regulation by a specific population, it is advisable to estimate fecundity using the autodiametric method (Section 4.6.1.1) which provides a measurement of oocyte sizes. The leading cohort oocyte diameter (average of the largest 10% of oocytes) can then be used as a proxy for the progression of ovary development. If oocyte size is unavailable, oocytes per gram of ovary can also be used as this is inversely proportional to oocyte size (Kjesbu, 1994; Thorsen & Kjesbu, 2001; Kennedy *et al.,* 2009). Fish should be collected for fecundity estimation on several occasions throughout the ovary development cycle with at least one occasion very close to spawning. The number of sampling occasions will depend on the time taken for oocyte development and also the oocyte development rate but will depend on the aims (s)of the study. Greater numbers of sampling occasions will give a better temporal resolution of the discerned pattern of down-regulation. There are indications that the down-regulation pattern can vary between years (Kennedy *et al.,* 2011). Thus any documented pattern should be examined for temporal stability if it is to be used to identify possible sampling periods which are far from the spawning season for annual variations in fecundity. The number of individuals sampled on each occasion should be high enough to include the entire range of development stages present in the population at the sampling occasion.

It is essential to know that when sampling is close to the spawning season the potential fecundity is equal, or very close to, the realised fecundity. This can be done by investigating the intensity and prevalence of atresia (Óskarsson & Taggart, 2006). This can be done using whole mount images for some species (Óskarsson *et al.,* 2002) or using the profile counting technique on histological sections, calibrated with the unbiased disector method (Kjesbu *et al.,* 2010).

When attempting to quantify the level of down-regulation in a population, it is important to have an accurate estimation of the timing of peak fecundity i.e. when oocyte recruitment has ended and the number of vitellogenic oocytes present in the ovary is at its highest. This occurs at different points in different species (Kurita *et al.*, 2003; Kennedy *et al.,* 2007). Individuals which have reached their peak fecundity can be identified by the hiatus between the previtellogenic and vitellogenic oocytes within the oocyte size distribution (Fig. 4.46).

There are many problems associated with attempts to link down-regulation in fecundity with energy levels. The level of down-regulation may be linked to changes in energy levels as opposed to energy levels per se (Kennedy *et al.,* 2008). This makes it difficult to investigate such processes in the field except at the population level. To perform such investigations

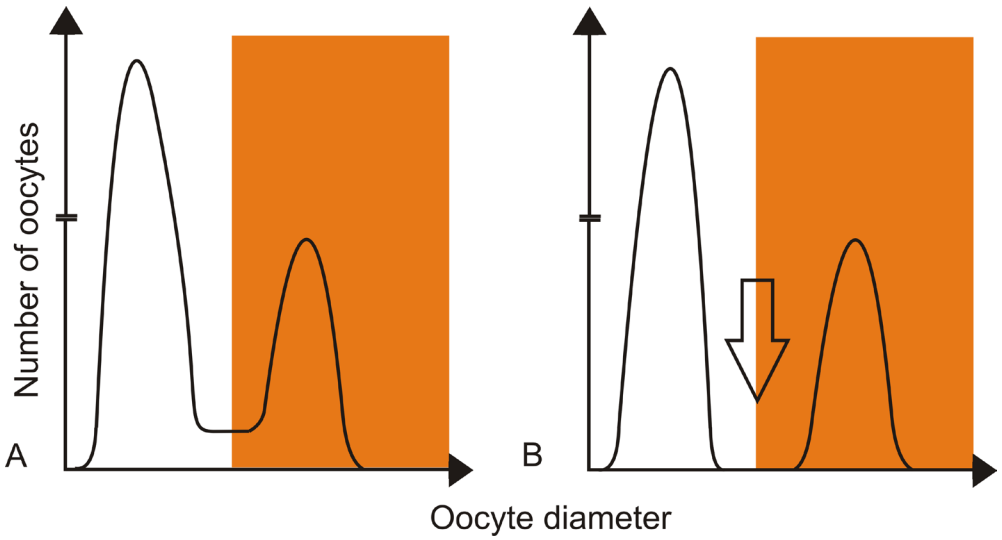

Figure 4.46.

Oocyte size distribution in a determinate fecundity species during (A) oocyte recruitment and after its completion (B). White area refers to previtellogenic oocytes, shadow area refers to vitellogenic oocytes. Vertical arrow shows hiatus. The number of pre-vitellogenic oocytes is extremely high explaining the broken y-axis scale. Adapted from Kjesbu (2010).

at the individual level, laboratory experiments are required, where individual fish can be monitored in response to variable levels of food intake. It is currently not possible to estimate fecundity in live fish, however, atresia can be monitored by taking gonad biopsies through the experiment (Kennedy *et al.,* 2008; Witthames *et al.,* 2010).

Potential errors can creep into the analysis of fecundity data due to differing patterns in down-regulation in addition to those brought above by the down-regulation itself. Examples of such scenarios have been described by (Kjesbu, 2009) (Fig. 4.47).

These scenarios mainly focus on the timing of the down-regulation due to atresia but other scenarios could have included different stabilisation plateaus, different temporal patterns for down-regulation (different 'atretic windows'), or another shape than linear (e.g. exponential) for the down-regulation curve (Kjesbu, 2009). All of these scenarios highlight the need for the estimation of fecundity close to spawning for comparison with fecundity estimates taken earlier.

It is recommended that sampling schemes for fecundity should sample fish from the same spawning grounds each year (however, this can be problematic due to geographical shifts in spawning areas) (Kjesbu, 2009). This ensures that the same part of the population is sampled between years as many fish stocks are heterogeneous in respects to fish size, condition or maturity stage which will affect fecundity estimates at different sampling locations. For this reason, the same part of the population should be sampled throughout the migration to spawning sites (if exist) or, in other words, throughout the same maturation development stages when investigating the pattern or degree of down-regulation. Alternatively, and more desirable, a representative sample could be taken from throughout the main areas of distribution but this is not always possible.

4.6.1.3 Skipped spawning

Current knowledge of reproductive systems in

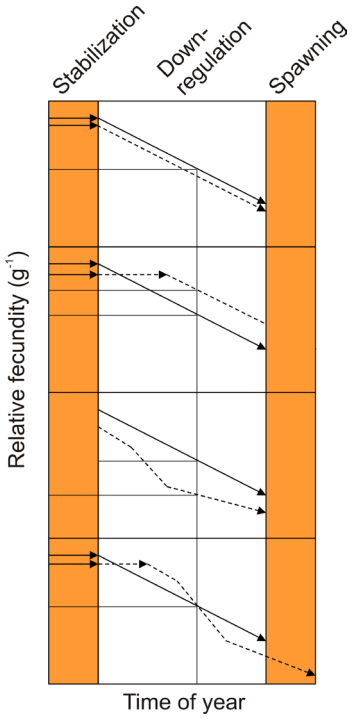

Figure 4.47.

Different scenarios for how sampling at a specific point of time in the year may influence the understanding of relative potential fecundity (RFP) in two contrasting groups (populations) of fish, depending on the temporal changes in the degree of down-regulation. Vertical and horizontal thin line, sampling time and corresponding RFP; solid line, reference (control) group; dashed line, response group, i.e. after a change in environmental or experimental conditions. (A) Same degree of down-regulation and spawning time; correct conclusion. (B) Delayed spawning time in response group but equal degree of down-regulation; overestimated RFP in response group. (C) Same spawning time but larger degree of down-regulation in response group: correct conclusion. (D) Delayed spawning time and larger degree of down-regulation in response group: type II error (accepted false null hypothesis). Note for (C) and (d) that the response group was assumed to undertake a steep decline in RFP during a specific part of the maturation cycle, i.e. showed a clear atretic window. Source: Kjesbu (2009).

fishes suggests a high degree of plasticity, where reproductive output can be scaled down to meet individual or environmental conditions. Under challenging circumstances gamete development can be abandoned completely, resulting in skipped spawning. The objective here is to provide a concise overview of methods used to identify skipped spawning in fishes. Readers interested in further details regarding methodologies or the causes and consequences of skipped spawning in fishes should consult reviews by Rideout *et al.* (2005) and Rideout & Tomkiewicz (2011) and the references cited therein.

Identification of skipped spawning requires an understanding of the three general forms of skipped spawning that have been described: retaining, reabsorbing, and resting (Fig. 4.48). Retaining–nonreproductive fish produce fully developed gametes that are never released. Reabsorbing–nonreproductive fish begin oocyte development but growth is arrested at some point prior to completion and all developing oocytes are reabsorbed via follicular atresia. Reabsorbing individuals can be divided into those that arrest development during the cortical alveoli stage of development (Reabsorbing-CA) and those that arrest development during true exogenous vitellogenesis (Reabsorbing-Vtg). Resting-nonreproductive fish do not commence secondary growth of oocytes and thus maintain only primary growth oocytes of various sizes throughout the entire year. Understanding the form of skipped spawning that a fish is undergoing can give insight into the potential causes of skipped spawning and when it is initiated. Such categorizations, however, can only be made via lethal sampling of fish and direct observations on the gonad (or potentially via live fish biopsies).

Methodology: Lethal sampling

Standard sampling procedures employed during fisheries research assessment surveys and other types of field work usually include the macroscopic maturity staging of fish gonads. Such approaches are generally directed at evaluating the spawner biomass or other indices of population reproductive potential. They have less utility when it comes to identifying skipped spawning. However, there are some notable

exceptions. For example, macroscopic observations may be sufficient to identify the retaining form of skipped spawning since such individuals retain fully developed oocytes that are usually visible to the naked eye (Lam *et al.*, 1978; Trippel & Harvey, 1990). The criteria required to reliably identify resting and reabsorbing ovaries cannot be identified with the naked eye and require histology. In some cases, however, comparison of detailed histological results with detailed macroscopic observations on the appearance of the corresponding ovaries has led to the identification of ovary size and colour characteristics that are indicative of skipped spawning. For example, non-reproductive ovaries in winter flounder can be extensive in size, like ripening ovaries, but are flaccid, dull grayish-red and flat. Immature ovaries are small, firm and yellowish. Reabsorbing non-reproductive Atlantic cod ovaries are small, red to grayish-red in colour and often very similar in appearance to recently spent ovaries. However, because spent individuals of this species are only encountered on a seasonal basis, the occurrence of small, red ovaries at other times of the year may be indicative of skipped spawning. When skipped spawning cannot be reliably identified macroscopically it is relatively common to consider fish with 'undeveloped ovaries' as skipped spawners when the fish are above a specified size at maturity and immature when they are smaller than the specified cut-off size. Unfortunately, these approaches do not allow for individual variation in size at maturity and therefore may erroneously classify non-reproductive fish as immature and vice versa. The appearance of 'immature' fish above some species-specific size is a good preliminary indicator of potential spawning omission but results should be confirmed histologically. Likewise ovaries that bear macroscopic characteristics that are suggestive of skipped spawning should be analyzed histologically for confirmation. The strict definition of skipped spawning implies that a fish that has spawned in previous reproductive cycles

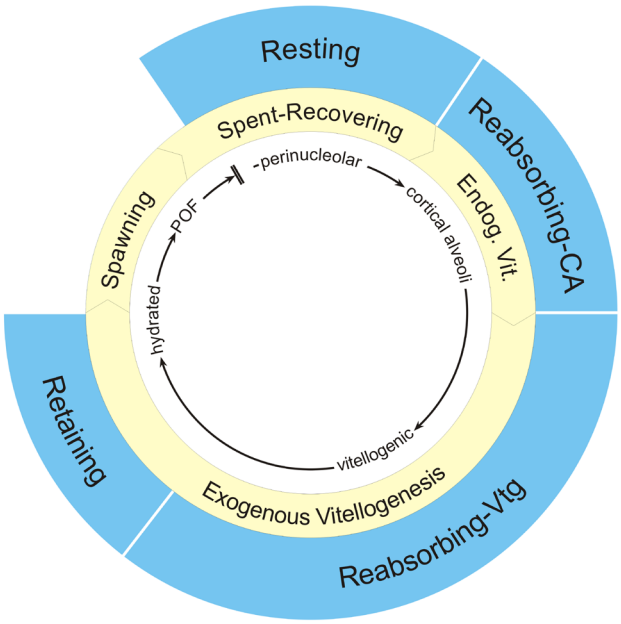

Figure 4.48.

Schematic representation of various aspects of the reproductive cycle of a determinate fecundity fish including: sequential stages of oocyte and follicular development (inner circle); sequential stages of ovarian development (i.e. reproductive status; yellow circle); and forms of skipped spawning based on when oocyte/ovarian development is interrupted. From Rideout & Tomkiewicz (2011).

(years) will fail to spawn in the current reproductive cycle. From this perspective, identification of skipped spawning requires evidence that no spawning would have occurred in the current year but that spawning did occur in the previous year. In a more general sense, skipped spawning is sometimes used to refer to any fish that is erroneously included as reproductive (i.e. part of the SSB) when in fact the fish would not have spawned. Under such a definition fish that start developing oocytes for the first time but ultimately fail to complete development may be included as skipped spawners. The focus here is on the more strict definition of skipped spawning and determining if a fish (1) will spawn in the current cycle and (2) has spawned previously. The latter is less crucial under the broader definition.

The morphological characters that are used to confirm failure to spawn in the current reproductive cycle and whether or not a fish spawned in the previous cycle are not visible to the naked eye and therefore reliable identification of skipped spawning requires gonadal histology. The histological criteria used in the identification of skipped spawning are presented below.

Evidence that a fish would have failed to spawn

Atresia–Follicular atresia refers to the active resorption of the oocyte via the cells of the follicle. The role of atresia in regulating oocyte production to suite environmental and nutritional conditions was discussed in Section 4.6.1.2. Some level of atresia is normal in fish ovaries and typically does not interfere with spawning. However, atresia can also be used to halt the development of all developing oocytes (Fig. 4.49) and thus result in skipped spawning. In fish with determinate oocyte recruitment patterns, mass atresia of developing oocytes is confirmation of impending skipped spawning since no additional recruitment of oocytes can occur. Conclusions are not so clear cut when it comes to fish with indeterminate fecundity type fishes (see Rideout & Tomkiewicz, 2011).

Lack of oocyte development–Skipped spawning does not always occur via atresia. Sometimes the annual recruitment of oocytes into vitellogenesis does not even begin (i.e. Resting – see Fig. 4.48). Such ovaries have oocyte size frequency distributions very similar to an immature fish but have characteristics to indicate that they are in fact mature. For resting ovaries, proving that they would have skipped spawning is a matter of timing of sample collection relative to the spawning season and detailed knowledge of the timing and duration of reproductive development. When a species has a well-defined spawning season it is possible to identify these fish as skipped spawners when they are detected close to the spawning season (i.e. the fish could not possibly have developed gametes in time to spawn in the given year). Such an approach requires detailed knowledge of the timing of the reproductive cycle of a species/population. For example, Atlantic cod require 5-6 months to complete vitellogenesis so females with old POFs but no developing oocytes sampled within a couple of months before (and even after) the spawning season can be reliably identified as skipped spawners. In a situation such as this (i.e. a protracted period of vitellogenesis), it is even possible

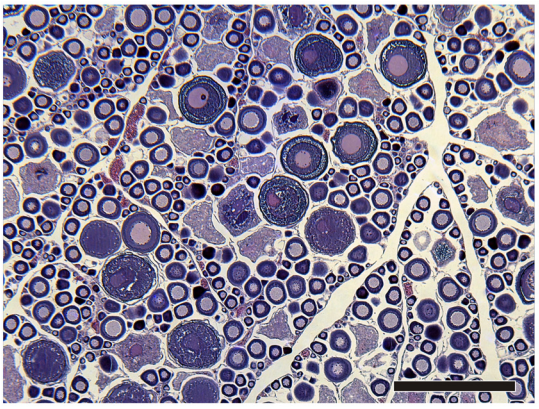

Figure 4.49.

Mass atresia of Atlantic cod oocytes entering the cortical alveoli stage of development. Arrows indicate atretic oocytes at different stages of resorption. Scale bar = 500 µm.

to identify skipped spawners several months before the spawning season. The certainty of the skipped spawning identification, however, will become reduced as one gets further away from the start of the spawning season (i.e. the potential increases that the fish still would have had time to develop for the current cycle).

Evidence that a fish is mature (i.e. spawned in the past)

Post-ovulatory follicles–As seen previously in Section 4.5.3, the identification and staging of POFs plays an important role in estimating spawning fraction, particularly for small pelagic species. POFs in such species are considered transitory structures that degenerate and disappear within a few days (e.g. Hunter & Goldberg, 1980). In some coldwater determinate fecundity type demersal species, however, POFs can persist in the ovary for several months to a year (Saborido-Rey & Junquera, 1998; Rideout *et al.*, 2005; Witthames *et al.*, 2010). As such, these structures can remain in the ovaries well into the next reproductive cycle (Fig. 4.50) and are the best indicator of reproductive activity in the previous year. A fish with POFs is always considered mature.

Residual oocytes–Residual oocytes are another fail-safe indicator of reproductive activity in the previous year. These are late vitellogenic or hydrated oocytes

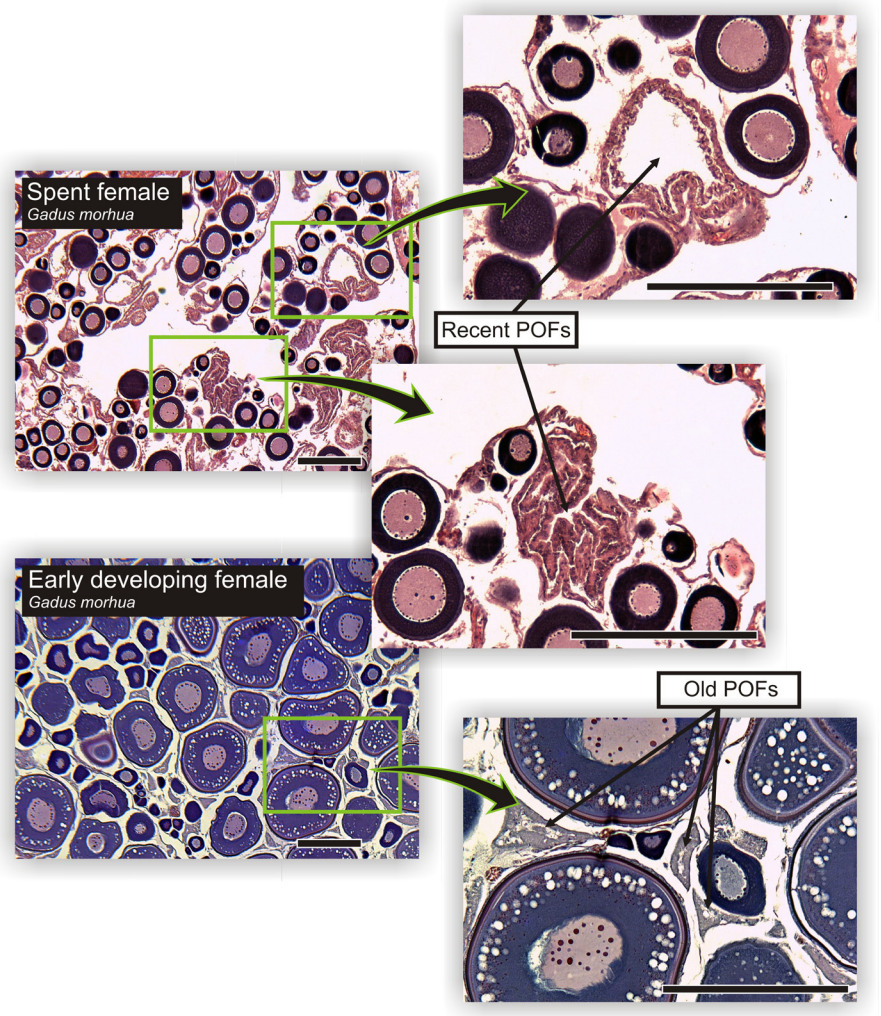

Figure 4.50.

Demonstration of recent and old post-ovulatory follicle (POF) structure in Atlantic cod. POFs are the most prominent structure in the recently spent ovary. POFs degenerate with time but remain identifiable in the ovary well into the next reproductive cycle and are a reliable indicator of past reproductive history. Scale bars = 250 µm.

remaining from the previous reproductive cycle that are eventually resorbed. Residual oocytes can be observed either in the ovarian lumen (i.e. ovulation occurred) or still within the follicle (Fig. 4.51). Late vitellogenic and hydrated oocytes that remain in their follicles may form into atretic cysts (Fig. 4.51). These structures are noteworthy since they appear to be quite persistent once formed and can last long into the next reproductive cycle (Witthames *et al.*, 2010; Domínguez-Petit *et al.*, 2011). As such, they can be useful for indicating past reproductive activity when identifying skipped spawning.

Tunica thickness – In some species, POFs are not of sufficient temporal duration to be useful in the identification of skipped spawning. And often no residual oocytes are observed. In such cases, tunica thickness can be used to indicate past reproductive history (i.e. whether or not an individual has spawned previously). Evidence suggests that tunica thickness increases during the maturation process (i.e. when a fish develops and spawns for the first time) and that measuring tunica thickness can therefore be useful in distinguishing immature fish from those that spawned in a previous year but would not do so in the current year (Fig. 4.52) (Burton & Idler, 1984; Rideout *et al.*, 2000; Witthames *et al.*, 2010). In terms of methodology it is important to make multiple measurements in order to quantify tunica thickness since thickness is not necessarily uniform (even within a single ovary section). The utility of using tunica thickness as an indicator of past reproductive history should also be confirmed on a species-specific basis since there is some indication that tunica thickness also increases with fish size and not just reproductive history (Holdway & Beamish, 1985). It should be noted that the use of tunica thickness as a tool for determining past reproductive history may only be applicable for species with cystovarian ovary types and not those with gymnovarian ovaries (Rideout *et al.*, 2005).

Otoliths - While reproductive status (including whether or not a fish is skipping spawning) is typically determined via inspection of fish ovaries, information stored within fish otoliths may also be useful for identifying skipped spawning. Chemical elements present in a fish's environment often become incorporated into the otoliths in levels indicative

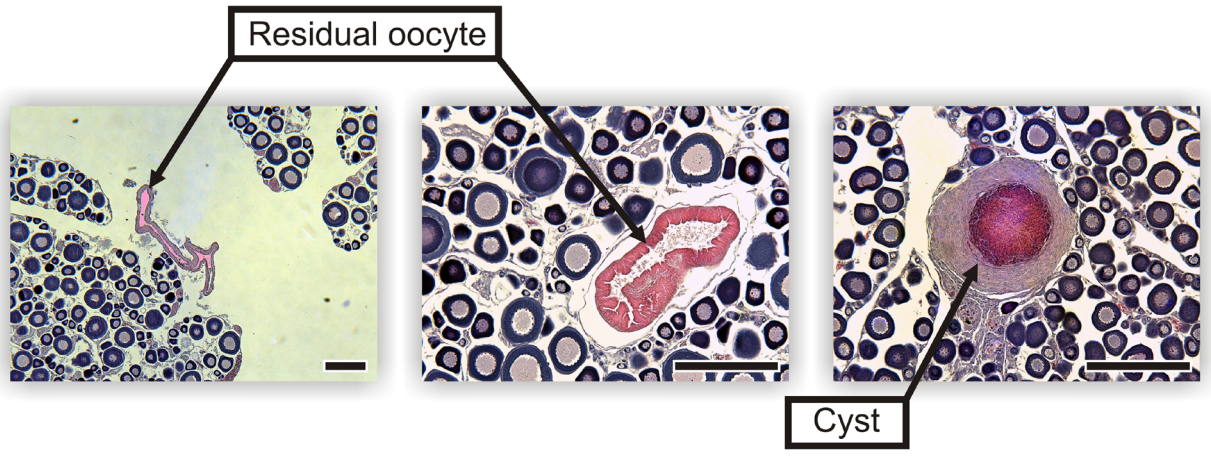

Figure 4.51.

Evidence for previous spawning in Atlantic cod can be obtained by the presence of residual oocytes in the lumen (left) or remaining within their follicle (middle) or by the presence of late stage oocytes being resorbed via cyst formation (right). Scale bars = 250 µm.

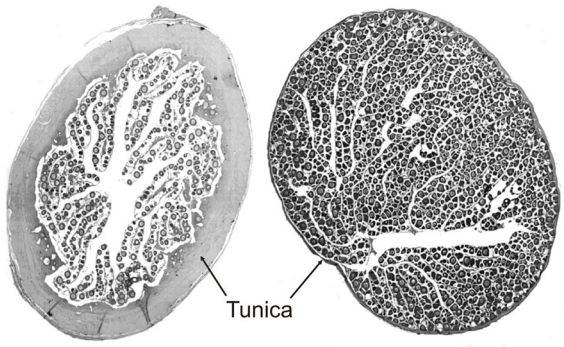

Figure 4.52.
Comparison of winter flounder ovaries categorized as skipped spawning (left) and immature (right). Note the difference in tunica thickness. Modified from Burton (2008).

of environmental concentrations. When spawning areas have clearly different chemical signatures than feeding areas it becomes possible to identify years when fish did and did not spawn by analyzing the chemical composition of the various annuli. Such an approach has been used to study skipped spawning in diadromous species based on ^{87}Sr:^{86}Sr and Sr/Ca ratios (Milton & Chenery, 2005; Secor & Piccoli, 2007), which differ significantly between marine and freshwater. The examination of otolith elemental signatures thus provides the potential to determine the number of times a fish skipped spawning over its entire life, something that cannot be done through the examination of ovaries.

Methodology: Non-Lethal Sampling

The methods to identify skipped spawning described above require direct observations to be made on fish ovaries and therefore typically require lethal sampling. It should be pointed out, however, that some of the same approaches could likely be used to identify skipped spawning based on non-lethal collection of ovarian biopsies (e.g. Skjæraasen *et al.*, 2009). There are other situations as well where observations on skipped spawning can be made without lethally sampling fish. For example, failure of captive broodstock to release eggs can be used as direct evidence of skipped spawning (Hislop *et al.*, 1978). Such direct observations of spawning (or lack of spawning) are not likely possible for wild fishes but inferences about skipped spawning can be made through careful monitoring of fish movements. For example, conventional tagging methods have been used to suggest high levels of skipped spawning in white sucker (Olson & Scidmore, 1963; Geen *et al.*, 1966; Quinn & Ross, 1985) Such studies typically monitor fish movements to a spawning area or presence at a spawning site and assume that two or more years between appearances for an individual fish is indicative of skipped spawning. This approach relies heavily on an assumption of spawning site fidelity (i.e. the assumption that a 'missing' fish is not spawning elsewhere).

Newer tagging methodologies rely on tags that continually collect and store environmental information (depth, temperature, etc.). Such methods provide high resolution data regarding fish movements and can be used to identify skipped spawning, i.e. fish that fail to visit known spawning areas/conditions are considered to skip spawning (Loher & Seitz, 2008; Hüssy *et al.*, 2009). Data can also be combined with knowledge of spawning behaviour. For example, many demersal fishes undertake sharp vertical rises during spawning and a lack of vertical rises might be indicative of skipped spawning (Loher & Seitz, 2008).

In some cases fish scales can act as 'natural data storage tags', providing information about past reproductive history. For example, Atlantic salmon are an anadromous iteroparous species that do not feed during their upstream spawning migration, instead relying on stored energy reserves. The lack of feeding results in some degree of resorption of the scale, which leaves a distinct spawning mark (Fig. 4.53). These spawning marks can then be used to determine the

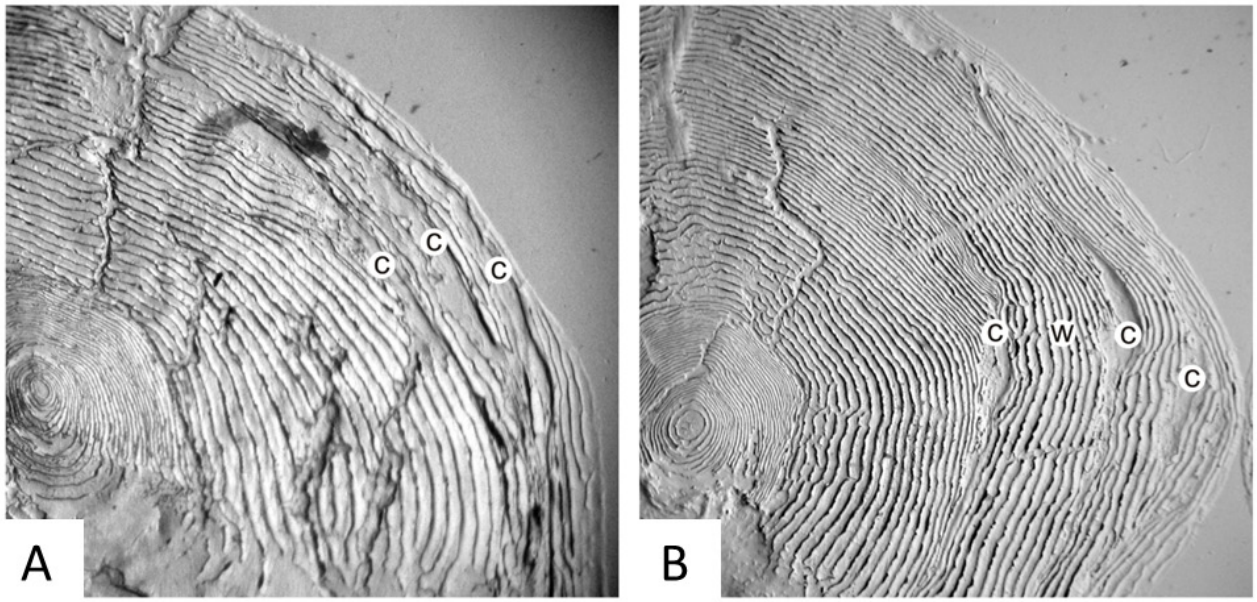

Figure. 4.53.

Demonstration of the use of scales to identify skipped spawning in Salmo salar: (A) a fish that spawned in three consecutive years; (D) a fish that skipped its second potential spawning season (i.e. spent complete year at sea) followed by two consecutive years of spawning. C, spawning check; W, winter spent at sea. Modified from Rideout and Tomkiewicz (2011)

reproductive history of the fish. Spawning episodes separated by one or more years at sea indicate skipped spawning (commonly referred to as alternate spawning for this species), whereas no such extended sea period between spawning episodes would indicate spawning in consecutive years (Fig. 4.53).

4.6.2 Indeterminate fecundity species

As previously described in BOX 4.1, in indeterminate fecundity fish species, potential annual fecundity [defined as the total number of advanced vitellogenic oocytes matured per year uncorrected for atretic losses (Hunter *et al*, 1992)] is not fixed before the onset of spawning, because previtellogenic oocytes are recruited into the vitellogenic oocytes pool during the spawning season. In these species the potential annual fecundity cannot be considered as the realized annual fecundity and, thus, a different approach should be taken to estimate annual fecundity.

4.6.2.1 Annual fecundity

In indeterminate fecundity fish species (sardine, anchovy, hake, etc.), annual fecundity (AF) should be calculated from the number of oocytes released by females at each spawning event (batch fecundity, BF), and the number of spawning events taking place during the spawning season (Nunes et al., 2011a). The latter may be derived by multiplying daily spawning fraction (S) by the duration of the spawning season in days (n). Therefore, AF can be estimated using the formula:

$$AF = n \cdot BF \cdot S \qquad 4.45$$

The duration of the spawning season, may be determined by regular sampling over the year, e.g. from the commercial fleet, and estimation of the seasonal variation in reproductive activity, i.e. the proportion of reproductively active females in the samples collected. As such, the duration of spawning season can be appraised as the time elapsed from 50

% of the population in prespawning condition to 50 % of females in postspawning condition (Murua *et al.*, 2003). Reproductive activity (pre- and post-spawning) can be assessed by means of histological analysis of the sampled ovaries, or in case this is not possible, from the macroscopic maturity stage of the ovaries, or from the gonadosomatic index (GSI: ratio of the gonad weight over the female weight). The use of GSI can be validated by establishing a relationship between GSI and gonad activity (assessed histologically): a logistic curve is fitted, a GSI_{50} (i.e. the value of GSI for which 50% of the females are reproductively active) is identified, and the latter is then applied to the individual GSI data from the samples collected to estimate the proportion of reproductively active females (e.g. Ganias *et al.,* 2007a).

As described in Section 4.4.1, individual batch fecundity, BF, is commonly measured by the gravimetric method applied to the hydrated ovaries with no signs of recent spawning (post-ovulatory follicles, POFs). In species where the spawning batch is already clearly distinguishable in size and shape from the subsequent batches, e.g. at the migratory nucleus stage, the gravimetric method can also be applied using methods described in Section 4.4.2.

As described in Section 4.5.3, S is commonly estimated in indeterminate fecundity species by means of the POF method. This parameter is the most complex to obtain, as it requires the collection of a significant number of samples (Picquelle et al., 1985) and an accurate knowledge of POF degeneration rate and unbiased POF staging/ageing system. Bias in this parameter estimation may exist due to particular fish behaviours (e.g., spatial segregation of spawning schools), and thus the selection of fishing gear and sampling timing of the day are important for obtaining samples representative of the population. Batch fecundity and spawning fraction are known as well to vary during the spawning season (Zwolinski *et al.*, 2001, Claramunt *et al.,* 2007; Korta *et al.,* 2010a). Thus samples should be collected regularly throughout the spawning season to assess seasonal variation of these parameters and correctly determine the production of eggs over the entire spawning season. In indeterminate species, the incidence of oocyte atresia is usually low during the spawning season, and becomes important only at the cessation of spawning, with the reabsorption of the oocyte surplus production (Hunter & Macewicz 1985a, Ganias *et al.,* 2003a; Murua & Motos, 2006; Nunes *et al.,* 2011b). Atresia is thus not directly used in the calculation of annual fecundity in such species. However, females with highly atretic ovaries (assessed histologically) sampled during the main spawning season but clearly in post-spawning stage, should be excluded from the calculation of annual fecundity.

4.6.2.2 Total egg production

The stock-recruitment (S-R) relationship is a key tool for fisheries managers and allows predicting the R based on a given level of reproductive stock or spawning stock biomass (SSB). Traditionally SSB has been used to fit models, nevertheless, there is increasing evidence that Total Egg Production (TEP) is a better index of stock reproductive potential because it includes the size-dependent capacity of females to produce eggs and the demographical structure of the spawning stock. (Morgan et al., 2011; Pérez-Rodríguez et al., 2013)

Currently, S-R models assume a direct proportionality between egg production and SSB. However, this assumption is increasingly criticized (Marshall *et al.*, 1998, 2003; De Lara *et al.*, 2007) and may fail for several reasons. It has been reported that large/old females' contribution to reproductive output is

higher than small/young females' (Marshal *et al.*, 1998). In addition, egg quality varies with female size (Vallin & Nissling, 2000) and spawning experience (Trippel, 1998). For many stocks, no distinction is made between males and females in the reproductive stock (Marshall *et al.*, 2006), even though stock reproductive potential depends mainly on females attributes. These questions have led us to reconsider the suitability of using SSB as accurate index of R.

Determining the most appropriate method to estimate TEP depends on characteristics of the target species, including reproductive habits (e.g., migrations, feeding activity, accessibility to fishing gears), seasonality of spawning activity (i.e., number of spawning events throughout the year), and reproductive strategy (e.g., determinate vs indeterminate fecundity, total vs multiple spawner). In addition, logistical factors like desired levels of accuracy and precision, costs of obtaining data, and availability of existing biological information must be considered.

For fish with indeterminate fecundity, TEP is estimated similarly to individual annual fecundity (see section 4.6.2.1) based on batch fecundity and the annual number of spawnings (Murua *et al.*, 2003; 2006). This model was developed for the European hake and indeterminate fecundity fish species (Murua *et al.*, 2006). However, as will be discussed later, estimates of TEP also take into account the demographic composition of the assessed stock and the seasonality and size-dependency of the relevant reproductive variables.

Traditionally, TEP methods do not include egg quality parameters; recently, some researchers have included these parameters in TEP estimates (Mehault *et al.*, 2010) because recruitment is directly affected by offspring survivorship that depends on its quality (Brooks *et al.*, 1997; Trippel, 1998; Marteinsdottir and Steinarsson, 1998; Rideout *et al.*, 2005). Nevertheless, this method makes important assumptions and has advantages and disadvantages that must be considered for results interpretation. For example, it assumes that estimated TEP is equal to the total number of fertilized eggs, however the number of eggs released is estimated but some of them will not be fertilized. It also assumes that offspring mortality rates are constant (Claramunt *et al.*, 1997). Advantages and disadvantages of using batch fecundity to estimate TEP are summarized in Stratoudakis *et al.* (2006). A general limitation of all TEP models based on fecundity is that reproductive parameters are often estimated from data of commercial catches that may represent mixed stocks or be biased because of commercial targets and fishing gears. In this situation, it is assumed that reproductive parameters do not change between stocks. Due to those issues, some authors suggest using icthyoplankton surveys to estimate egg production. The most relevant icthyoplankton methods are summarized by Hunter and Lo (1993).

The first step to estimate TEP (for further details see Murua *et al*,2003; 2006) is to estimate relative monthly fecundity (EP_{rel}) as the product of the mean number of batches per month (NB), relative batch fecundity (BF_{rel}), and percentage of active females (AF) in the population:

$$EP_{rel} = NB \cdot BF_{rel} \cdot AF \qquad 4.46$$

The mean number of batches per month was estimated as:

$$NB = \frac{No.days\ of\ each\ month}{S} \qquad 4.47$$

where S is the spawning fraction estimated using methods described in Section 4.5.2. For the estimation of TEP, Mehault *et al.,* (2010)

further took into account the quarterly variation of egg production and egg quality (i.e. dry mass and diameter of hydrated oocytes). As indeterminate fish species usually show a protracted spawning season it is important to consider a whole year sampling for the estimation of TEP.

In this model the TEP index was estimated for each age group (a) by quarter (q) and year (y) based on the assumption that the batch fecundity is proportional to the realized fecundity (Murua *et al.*, 2003):

$$TEP_{a,q,y} = N_{a,y} + SR_{a,y} + M_{a,y} + \\ + BF_a + S_{a,q} + Q_a \qquad 4.48$$

Where $N_{a,y}$ is the number of individuals at a given age at the beginning of the year obtained from VPA (ICES, 2008); $SR_{a,y}$ is the sex ratio at a given age; $M_{a,y}$ is the expected proportion of mature females at a given age from annual logistic regressions; BF_a is the pooled mean absolute batch fecundity at a given age obtained from linear model; $S_{a,q}$ is the mean spawning fraction by quarter obtained from the four-quarterly linear regressions; and Q_a is the mean hydrated oocyte dry mass at a given age obtained from a linear model.

Thus, the TEP for a given year is expressed as:

$$TEP_y = \sum_{q=1}^{4} \sum_{a=0}^{i} TEP_{a,q,y} \qquad 4.49$$

This TEP index does not represent the real egg production because the oocyte dry mass at a given age is included as a factor in the model. In addition, dry weights are only rough estimates because dry weight may be reduced by up to 30% due to leaching during formaldehyde storage (Hislop & Bell, 1987). To compensate for leaching, oocytes may be rehydrated until they reach stabilization.

The aforementioned model for estimating TEP could be subject to several improvements. For example, samples usually came from wild fish populations whose reproductive history was unknown. Trippel (1998) reports that repeat spawners produce more and higher quality eggs than first-time spawners; thus, this information could be included in the model. Additionally, both egg diameter and dry mass can change as the individual spawning season progresses (Wlodarczyk & Horbowa, 1997; Trippel, 1998; Saborido-Rey *et al.*, 2003). Finally, hydrated oocytes are subject to an abrupt change in their size few hours before spawning and thus the effect of sampling time on the size of hydrated oocytes should also be considered. Despite technical considerations, this method facilitates estimating the impact of female stock structure on the TEP of the stock, as well as modeling quarterly variation of egg production.

4.7 References

Alarcón, V.H., Goldberg, S.R., Alheit, J. 1984. Histologia de foliculos postovulatorios de la sardina (*Sardinops sagax*) del Perú. *Boletin del Instituto del Mar Perú-Callao*. 8(1): 1-16.

Alday, A., Santos, M., Uriarte, A., Martín, I., Martínez, U., Motos, L. 2010. Revision of criteria for the classification of postovulatory follicles degeneration, for the Bay of Biscay anchovy (*Engraulis encrasicolus L.*). *Revista de Investigación Marina*. 17(8): 166-171.

Alday, A., Uriarte, A., Santos, M., Martín, I., Martínez de Murguia A, Motos L. 2008. Degeneration of postovulatory follicles degeneration of Biscay anchovy (*Engraulis encrasicolus L.*). *Scientia Marina*. 72(3): 565-575

Alheit, J. 1993. Use of the daily egg production method for estimating biomass of clupeoid fishes: a review and evaluation. *Bulletin of Marine Science.* 53: 750–767.

Alheit, J., Alarcon, V.H., Macewicz, B.J. 1984. Spawning frequency and sex ratio in the Peruvian anchovy, *Engraulis ringens*. *CalCOFI reports* 25: 43-52

Alonso-Fernández, A. 2011. Bioenergetics approach to fish reproductive potential: case of *Trisopterus luscus (Teleostei)* on the Galician Shelf (NW Iberian Peninsula). Ph D Thesis Dissertation. University of Vigo, Spain.

Alonso-Fernández, A., Vallejo, A.C., Saborido-Rey, F., Murua, H., Trippel, E.A. 2009. Fecundity estimation of Atlantic cod (*Gadus morhua*) and haddock (*Melanogrammus aeglefinus*) of Georges Bank: Application of the autodiametric method. *Fisheries Research*. 99: 47–54.

Aragón, L. 2010. Estudio comparativo de la biología reproductora del atún rojo atlántico, *Thunnus thynnus (L.)*, en poblaciones salvajes y en cautividad. Ph D Thesis Dissertation. University of Cádiz, Spain.

Aragón, L., Aranda, G., Santos, A., Medina, A. 2010. Quantification of ovarian follicles in bluefin tuna *Thunnus thynnus* by two stereological methods. *Journal of Fish Biology*, 77: 719–730.

Armstrong, M., Shelton, P., Hampton, I., Jolly G., Melo, Y.C. 1988. Egg production estimates of anchovy biomass in the Southern Benguela System. *CalCOFI Reports*. 29: 137-156.

Begg, G.A., Marteinsdottir, G. 2002. Environmental and stock effects on. spawning origins and recruitment of cod *Gadus morhua*. *Marine Ecology Progress Series*. 229: 263-277.

Bromley, P.J., Ravier, C., Witthames, P.R. 2000. The influence of feeding regime on sexual maturation, fecundity and atresia in first-time spawning turbot. *Journal of Fish Biology*. 56: 264–278.

Brooks, S., Tyler, C.R., Sumpter, J.P. 1997. Egg quality in fish: what makes a good egg? Reviews in *Fish Biology and Fisheries*, 7(4): 387-416.

Brown-Peterson, N.J., Wyanski, D.M., Saborido-Rey, F., Macewicz, B.J.,owerre-Barbieri, S.K. 2011. A Standardized Terminology for

Describing Reproductive Development in *Marine and Coastal Ficheries*. 3: 52-70.

Bucholtz, R.H., Tomkiewicz, J., Nyengaard, J.R., Andersen, J.B., 2013. Oogenesis, fecundity and condition of Baltic herring (*Clupea harengus L.*): A stereological study. *Fisheries Research.* 145: 100–113.

Burton, M. 2008. Reproductive omission and skipped spawning: detection and importance. Cybium 32: 315-316.

Burton, M.P., Idler, D.R. 1984. The reproductive cycle in winter flounder, *Pseudopleuronectes americanus (Walbaum).* Canadian *Journal of Zoology.* 62: 2563-2567.

Cailliet, G.M., Love, M.S., Ebeling, A.W. 1986. Fishes. Wadsworth Publ. Co., Belmont CA, 194 p.

Christiansen, H.E., Brodsky, S.R., Cabrera, M.E. 1973. La microscopía aplicada con criterio poblacional en el estudio de las gónadas de los vertebrados e invertebrados marinos. *Physis*, 32: 467–480.

Christiansen, H.E., Weiss, G. 1974. Nuevo método para la determinación de la fecundidad en peces con técnicas estereométricas mediante cortes por congelación. Su comparación puntual con otros métodos. *Physis*, 33: 453–458.

Claramunt, G., Herrera, G. 1994. A new method to estimate the fraction of daily spawning females and the numbers of spawnings in *Sardinops sagax* in northern Chile. *Scientia Marina* 58(3), 169-177.

Claramunt, G., Herrera, G., Pizarro, P., Pizarro, J., Escribano, E., Oliva, M., Zuleta, A. 1997. Evaluación del stock desovante de anchoveta por el método de la producción de huevos en la I y II Regiones. Informe Final FIP 96-01. Informes Técnicos FIP–IT/96-01.

Claramunt, G., Roa, R. 2001. An indirect approach to estimate spawning fraction as applied to *Sardinops sagax* from northern Chile. *Scientia. Marina*. 65: 87-94.

Claramunt, G., Roa, R., Cubillos, L. 2003. Estimating daily spawning fraction using the gonadosomatic index: application to three stocks of small pelagic fish from Chile. In: Reports of the Workshop "Modern approaches to assess maturity and fecundity of warm- and cold-water fish and squids" (eds O.S. Kjesbu, J.R. Hunter & P.R. Witthames), *Fisken Og Havet, Bergen, Norway*. pp. 43-49.

Claramunt, G., Serra, R., Castro, L.R., Cubillos, L. 2007. Is the spawning frequency dependent on female size? Empirical evidence in S*ardinops sagax* and *Engraulis ringens* off northern Chile. *Fisheries Research*. 85: 248–257.

Clarke, T.A. 1987. Fecundity and spawning frequency of the Hawaiian anchovy or nehu, *Encrasicholina purpurea*. *Fishery Bulletin.* 85: 127-138.

Cooper, D.V., Pearson, K.E., Gunderson, D.R. 2005. Fecundity of shortspine thornyhead (*Sebastolobus alascanus*) and longspine thornyhead (*S. altivelis*) (*Scorpaenidae*) from the northeastern Pacific Ocean, determined by stereological and gravimetric techniques. *Fishery Bulletin*, 103: 15–22.

Coward, K., Brogman, N. R. 2002 Quantification of ovarian condition in fish: a safer, more precise alternative to established methodology. *Aquatic Living Resources* 15 (04): 259-261.

De Lara, M., Doyen, L., Guilbaud, T., Rochet, M.L.2007. Is a management framework based on spawning-stock biomass indicators sustainable? A viability approach. *ICES Journal of Marine Science,* 64: 761–767.

DeMartini, E.E., Fountain, R.K. 1981. Ovarian cycling frequency and batch fecundity in the queenfish, *Seriphus politus*: attributes representative of serial spawning fishes. *Fishery Bulletin*. 79: 547-559

Dickerson, T.L., Macewicz, B.J., Hunter, J.R. 1992. Spawning frequency and batch fecundity of chub mackerel, *Scomber japonicus*, during 1985. *CalCOFI Reports*. 33: 130-140.

Domeier, M.L., Colin, P.L. 1997. Tropical reef fish spawning aggregations: Defined and reviewed. *Bulletin of Marine Science.* 60: 698-726.

Dorph-Petersen, K.-A., Nyengaard, J.R., Gundersen, H.J.G. 2001. Tissue shrinkage and unbiased stereological estimation of particle number and size. *Journal of Microscopy*, 204: 232–246.

Douglas,S.G.,Chaput,G.,.Hayward,J.,Sheasgreen,J.2009. Prespawning,spawning, and postspawning behavior of striped bass in the Miramichi River. *Transactions of the American Fisheries Society* 138:121–134.

Emerson, L.S., Greer Walker, M., Witthames, P.R. 1990. A stereological method for estimating fish fecundity. *Journal of Fish Biology*, 36: 721–730.

Fitzhugh, G.R., Hettler W.F., 1995. Temperature influence on postovulatory follicle degeneration in Atlantic menhaden, *Brevoortia tyrannus*. *Fishery Bulletin* 93: 568-572.

Fleming, I.A., S.Ng. 1987. Evaluation of techniques for fixing, preserving and measuring salmon eggs. *Canada Journal of Fisheries and Aquatic Science*. 44: 1957-1962.

Friedland, K.D., Ama-abasi, D., Manning, M., Clarke, L., Kligys, G., Chambers, R.C. 2005. Automated egg counting and sizing from scanned images: rapid sample processing and large data volumes for fecundity estimates. *Journal of Sea Research*. 54: 307–316

Fudge, S.B., Rose, G.A. 2009. Passive- and active-acoustic properties of a spawning Atlantic cod (*Gadus morhua*) aggregation. *ICES Journal of Marine Science*. 66: 1259–1263.

Funamoto, T., Aoki, I. 2002. Reproductive ecology of Japanese anchovy off the Pacific coast of eastern Honshu, Japan. *Journal of Fish Biology.* 60: 154-169.

Ganias, K. 2008. Ephemeral spawning aggregations in the Mediterranean sardine, *Sardina pilchardus*: a comparison with other multiple-spawning clupeoids. *Marine. Biology*. 155: 293-301.

Ganias, K. 2012. Thirty years of using the postovulatory follicles method: Overview, problems and alternatives. *Fisheries Research*. 117: 63-74.

Ganias, K. 2013. Determining the indeterminate:

Evolving concepts and methods on the assessment of the fecundity pattern of fishes. *Fisheries Research.* 138, 23-30.

Ganias, K., Nunes, C., Stratoudakis, Y., 2007a. Degeneration of postovulatory follicles in the Iberian sardine *Sardina pilchardus*: structural changes and factors affecting resorption. *Fishery Bulletin.* 105: 131-139.

Ganias, K., Nunes, C., Vavalidis, T., Rakka, M., Stratoudakis, Y. 2011. Estimating Oocyte Growth Rate and Its Potential Relationship to Spawning Frequency in Teleosts with Indeterminate Fecundity. *Marine and Coastal Fisheries*. 3: 119-126.

Ganias, K., Rakka, M., Vavalidis, T., Nunes, C. 2010. Measuring batch fecundity using automated particle counted. *Fisheries Research*. 106: 570 – 574

Ganias, K., Somarakis, S., Koutsikopoulos, C., Machias, A. 2007b. Factors affecting the spawning period of sardine in two highly oligotrophic Seas. *Marine Biology.* 151(4): 1559-1569.

Ganias, K., Somarakis, S., Koutsikopoulos, C., Machias, A., Theodorou, A. 2003a. Ovarian atresia in the Mediterranean sardine, *Sardina pilchardus sardina*. Journal Marine *Biological Association U.K.* 83: 1327-1332

Ganias, K., Somarakis, S., Machias, A., Theodorou, A., 2003b. Evaluation of spawning frequency in a Mediterranean sardine population (*Sardina pilchardus sardina*). *Marine Biology*. 142, 1169–1179.

Ganias, K., Somarakis, S., Machias, A., Theodorou, A. 2004. Pattern of oocyte development and batch fecundity in the Mediterranean sardine. *Fisheries Research*. 67: 13-23.

Gannon, D. 2008 . Passive a coustic techniques in fisheries science: a review and prospectus.*Transactions of the American Fisheries Society.* 137: 638-656

Gayanillo, F.C.Jr, Soriano, M.L., Pauly, D. 1988. A draft guide to the Compleat ELEFAN. ICLARM Software 2, 65p. International Center for Living Aquatic Resources Management, Manila, Philippines.

Gayanillo, F.C. Jr., Sparre, P., Pauly, D. 1996. FAO-ICLARM Fish Stock Assessment (FiSAT) User's Guide. FAO Computerized Information Series (Fisheries) 7. FAO of the United Nations, Rome, Italy. 180p.

Geen, G.H., Northcote, T.G., Hartman, F., Lindsey, C.C. 1966. Life histories of two species of Catastomid fishes in Sixteenmile Lake, British Columbia, with particular reference to inlet stream spawning. *Journal of the Fisheries Research Board of Canada* 23: 1761-1788.

Goldberg, S.R., Alarcon, V., Alheit, J. 1984. Postovulatory follicle histology of the Pacific sardine, *Sardinops sagax*, from Peru *Fishery Bulletin*. 82: 443-445.

Gonçalves, P., Costa, A.M., Murta, A.G. 2009. Estimates of batch fecundity, and spawning fraction for the southern stock of horse mackerel, *Trachurus trachurus,* ICES Division IXa. ICES *Journal of Marine Science*. 66: 617–622.

Greer-Walker, M., Witthames, P.R., Bautista De Los Santos, J.I. 1994. Is the fecundity of

the Atlantic mackerel (*Scomber scombrus: scombridae*) determinate? *Sarsia* 79: 13-26.

Gundersen, H.J.G. 1986. Stereology of arbitrary particles. A review of unbiased number and size estimators and the presentation of some new ones, in memory of William R. Thompson. *Journal of Microscopy*, 143: 3–45.

Gundersen, H.J.G., Bagger, P., Bendtsen, T.F., Evans, S.M., Korbo, L., Marcussen, N., Møller, A., Nielsen, K., Nyengaard, J.R., Pakkenberg, B., Sørensen, F.B., Vesterby, A., West, M.J. 1988. The new stereological tools: Disector, fractionator, nucleator and point sampled intercepts and their use in pathological research and diagnosis. *APMIS* 96: 857–881.

Heins, D.C., Baker, J. A. 1999. Evaluation of ovum storage techniques for reproductive studies of fishes, *Ecology of Freshwater Fish* 8: 65-69.

Hiemstra, W.H. 1962. A correlation table as an aid for identifying pelagic fish eggs in plankton samples. *Journal du Conseil. Conseil International pour l'Exploration de la Mer* 27:100-108.

Hislop, J.R.G., Bell, M.A. 1987. Observations on the size, dry weight and energy content of the eggs of some demersal fish species from British marine waters. J*ournal of Fish Biology*, 31: 1–20.

Hislop, J.R.G., Hall, W.B. 1974. The fecundity of whiting, *Merlangus merlangus* (L.), in the North Sea, the Munch and at Iceland. *Journal du Conseil. Conseil International pour l'Exploration de la Mer* 36: 162-165.

Hislop, J.R.G., Robb, A.P., Gauld, J.A. 1978. Observations on effects of feeding level on growth and reproduction in haddock, *Melanogrammus aeglefinus* (L.) in captivity. *Journal of Fish Biology* 13: 85-98.

Holdway, D.A., Beamish, F.W.H. 1985. The effect of growth rate, size, and season on oocyte development and maturity of Atlantic cod (*Gadus morhua L.*). Experimental *Marine Biology and Ecology* 85: 3-19.

Howard, C.V., Reed, M.G. 1998. Unbiased Stereology, Three-Dimensional Measurement in Microscopy. Oxford: *BIOS Scientific Publishers.*

Howard, C.V., Reed, M.G. 2005. Unbiased Stereology: Three-Dimensional Measurement in Microscopy. 2nd ed. Abingdon, Oxon, UK: *Garland Science/BIOS Scientific Publishers.*

Hunter, J.R., 1985. Preservation of Northern Anchovy in Formaldehyde Solution. In Lasker R. (ed.) An Egg Production Method for Estimating Spawning Biomass of Pelagic Fish: Application to the Northern Anchovy, *Engraulis mordax*. *NOAA Technical Report. NMFS* 36: 63-65.

Hunter, J.R., Goldberg, S.R. 1980. Spawning incidence and batch fecundity in northern anchovy, *Engraulis mordax. Fishery Bulletin,* 77: 641-652.

Hunter, J.R., Lo, N.H. 1993. Ichthyoplankton methods for estimating fish biomass introduction and terminology. *Bulletin of Marine Science,* 53(2): 723-727.

Hunter, J.R., Lo, N.C.H., Leong, H.J. 1985. Batch fecundity in multiple spawning fishes. pp. 67-77. In: R. Lasker (ed.). An Egg Production Method

for Estimating Spawning Biomass of Pelagic Fish: Application to the Northern Anchovy, *Engraulis mordax*. *NOAA Technical Rep* NMFS 36.

Hunter, J. R., Macewicz, B. 1985a. Rates of atresia in the ovary of captive and wild northern anchovy, *Engraulis mordax*. *Fishery Bulletin*, 83: 119–136.

Hunter, J.R., Macewicz. B.J., 1985b. Measurement of spawning frequency in multiple spawning fishes. .*NOAA Technical Report. NMFS* 36: pp. 79-94.

Hunter, J.R. , Macewicz, B.J. 2003. Improving the accuracy and precision of reproductive information used in fisheries. In: Reports of the Workshop "Modern approaches to assess maturity and fecundity of warm- and cold-water fish and squids" (eds O.S. Kjesbu, J.R. Hunter & P.R. Witthames), Fisken Og Havet, Bergen, Norway. 57-68.

Hunter, J. R., Macewicz, B. J., Kimbrell, C. A. 1989. Fecundity and other aspects of the reproduction of sablefish, Anaplopoma fimbria, in Central California waters, *California Cooperative Oceanic Fisheries Investigations Reports* 30: 61-72

Hunter, J.R., Macewicz, B.J., Lo, N.C.H., Kimbrell, C.A, 1992. Fecundity, spawning, and maturity of female Dover sole, *Microstomus pacificus*, with an evaluation of assumptions and precision. *Fishery Bulletin*. 90: 101-128.

Hunter, J.R., Macewicz, B.J., Sibert, J.R. 1986. The spawning frequency of Skipjack Tuna, Katsuwonus pelamis, from the South Pacific. *Fishery Bulletin*. 84: 895-903.

Hüssy, K., Nielsen, B., Mosegaard, H., Clausen, L. W. 2009. Using data storage tags to link otolith macrostructure in Baltic cod *Gadus morhua* with environmental conditions. *Marine Ecology Progress Series.* 378: 161-170.

ICES, 2008. Report of the Working Group on the Assessment of Southern Shelf Stocks of Hake, Monk and Megrim (WGHMM). *ICES CM 2008\ACOM:07*. 613 pp.

Isaac-Nahum, V.J., Cardoso, R.d.D., Servo, G., Rossi-Wongtschowski, C.L.d.B. 1988. Aspects of spawning biology of the Brazilian sardine, *Sardinella brasiliensis* (Steindachner, 1879), (Clupeidae). *Journal of Fish Biology.* 32: 383-396.

Joseph, J. 1963. Fecundity of yellowfin tuna (*Thunnus albacares*) and skipjack (*Katsuwonus pelamis*) from the eastern Pacific Ocean. *Inter-American Tropical Tuna Commission Bulletin*. 7: 255-292.

Kennedy, J., Gundersen, A.C., Boje, J. 2009. When to count your eggs: Is fecundity in Greenland halibut (*Reinhardtius hippoglossoides W.*) down-regulated? *Fisheries Research*. 100: 260–265

Kennedy, J., Nash, R.D.M., Slotte, A., Kjesbu, O.S. 2011. The role of fecundity regulation and abortive maturation in the reproductive strategy of Norwegian spring-spawning herring (*Clupea harengus*). *Marine Biology.*

Kennedy, J., Witthames, P. R., Nash, R. D. M. 2007. The concept of fecundity regulation in plaice (*Pleuronectes platessa*) tested on three Irish Sea spawning populations. Canadian *Journal of Fisheries and Aquatic Sciences,* 64(4): 587–601.

Kennedy, J., Witthames, P.R., Nash, R.D.M., Fox, C.J.

2008. Is fecundity in plaice *(Pleuronectes platessa L.*) down-regulated in response to reduced food intake during autumn? *Journal of Fish Biology.* 72: 78–92.

Kjesbu, O.S. 1994. Time of start of spawning in Atlantic cod (*Gadus morhua*) females in relation to vitellogenic oocyte diameter, temperature, fish length and condition. *Journal of Fish Biology.* 45: 719–735.

Kjesbu, O.S. 2009. Applied fish reproductive biology: contribution of individual reproductive potential to recruitment and fisheries management. pp. 293-332. In: T. Jakobsen, M. Fogarty, B.A. Megrey and E. Moksness (ed.). Fish reproductive biology: implications for assessment and management. Blackwell Science Ltd., Oxford, U.K.

Kjesbu, O.S., Fonn, M., Gonzáles, B.D., Nilsen, T. 2010. Stereological calibration of the profile method to quickly estimate atresia levels in fish. *Fisheries Research*. 104: 8–18.

Kjesbu, O.S., Witthames, P.R., Solemdal, P., Greer Walker ,M. 1990. Ovulatory rhythm and a method to determine the stage of spawning in Atlantic cod (*Gadus morhua*). *Canadian Journal of Fisheries and Aquatic Sciences*, 47: 1185–1193.

Kjesbu, O.S., Witthames, P.R., Solemdal, P. , Greer Walker, M. 1998. Temporal variations in the fecundity of Arcto-Norwegian cod (*Gadus morhua*) in response to natural changes in food and temperature. *Journal of Sea Research.* 40: 303–321.

Klibansky, N., Juanes, F. 2007. Species-specific effects of four preservative treatments on oocytes and ovarian material of Atlantic cod (*Gadus morhua*), haddock (*Melanogrammus aeglefinus*), and American plaice (*Hippoglossoides platessoides*). *Fishery Bulletin*. 105: 538-547.

Klibansky, N., Juanes, F. 2008. Procedures for efficiently producing high-quality fecundity data on a small budget. *Fisheries Research*. 89: 84-89.

Korta, M. 2010. New methodologies applied to quantify the dynamics of the ovary in indeterminate fecundity species. Ph D Thesis Dissertation, University of Basque Country.Spain

Korta, M., Dominguez-Petit R., Murua, H., Saborido-Rey, F. 2010a. Regional variability in reproductive traits of European hake Merluccius merluccius L. populations . *Fisheries Research,*.104 : 64-72.

Korta, M., Murua, H., Kurita, Y. , Kjesbu, O.S. 2010b. How are the oocytes recruited in an indeterminate fish? Applications of stereological techniques along with advanced packing density theory on European hake (*Merluccius merlucssius L.*). *Fisheries Research*. 104: 56-63.

Korta, M., Murua, H., Quincoces, I., Thorsen A. , Witthames P. 2010c. Three-dimensional reconstruction of postovulatory follicles from histological sections. *Fisheries Research* 104: 38-44.

Kucera, P. A., Kennedy, J. L. 1977. Evaluation of a sphere volume method for estimating fish fecundity. T*he Progressive Fish-Culturist*, 39: 115-117.

Kurita, Y. 2012. Revised concepts for estimation of spawning fraction in multiple batch spawning fish considering temperature-dependent duration of spawning markers and spawning time frequency

distribution. *Fisheries Research*. 117: 121-129

Kurita, Y., Fujinami, Y., Amano, M., 2011. The effect of temperature on the duration of spawning markers —migratory-nucleus and hydrated oocytes and postovulatory follicles— in the multiple-batch spawner Japanese flounder (*Paralichthys olivaceus*). *Fishery Bulletin*. 109: 79–89.

Kurita, Y., Kjesbu, O.S. 2009. Fecundity estimation by oocyte packing density formulae in determinate and indeterminate spawners: theoretical considerations and applications. *Journal of Sea Research.* 61: 188–196.

Kurita, Y., Meier, S., Kjesbu, O.S. 2003. Oocyte growth and fecundity regulation by atresia of Atlantic herring (*Clupea harengus*) in relation to body condition throughout the maturation cycle. *Journal of Sea Research*. 49: 203–219.

Lam, T.J., Nagahama, Y., Chan, K., Hoar, W.S. 1978. Overripe eggs and postovulatory copora lutea in the *threespine stickleback, Gasterosteus aculeatus L.*, form *trachurus. Canadian Journal of Zoology*. 56: 2029-2036.

Lawson, G.L., Rose G.A. 2000. Small-scale spatial and temporal patterns in spawnign of Atlantic cod (*Gadus morhua*) in coastal Newfoundland waters. C*anada Journal of Fisheries and Aquatic Science*. 57: 1011-1024

Loher, T., Seitz, A.C. 2008. Characterization of active spawning season and depth for Eastern Pacific halibut (*Hippoglossus stenolepis*) and evidence of probable skipped spawning. J*ournal of Northwest Atlantic Fishery Science*. 41: 23-36.

Lowerre-Barbieri, S.K., Barbieri, L.R. 1993. A new method of oocyte separation and preservation for fish reproduction studies. *Fishery Bulletin* 91:165-170.

Lowerre-Barbieri, S.K., Barbieri, L.R., Flanders, J., Woodward, A., Cotton C., Knowlton, M.K. 2008. Use of passive acoustics to determine red drum spawning in Georgia waters. *Transactions of the American Fisheries Society.* 137:562-575.

Lowerre-Barbieri, S.K., Brown-Peterson, N.J., Murua, H., Tomkiewicz, J., Wyanski, D.M., Saborido-Rey, F. 2011a. Emerging issues and methodological advances in fisheries reproductive biology. *Marine and Coastal Fisheries*. 3: 32–51

Lowerre-Barbieri, S.K., Chittenden, M.E., Barbieri, Jr., Barbieri, L.R. 1996. Variable spawning activity and annual fecundity of weakfish in Chesapeake Bay. *Transactions of American Fisheries. Society*. 125: 532-545.

Lowerre-Barbieri, S.K., Ganias, K. , Saborido-Rey, F., Murua, H., Hunter, J.R. 2011b. Reproductive Timing in Marine Fishes: Variability, Temporal Scales, and *Methods. Marine and Coastal Fisheries*. 3: 71-91.

Lowerre-Barbieri, S.K., Henderson, N., Llopiz, J., Walters, S., Bickford, J., Muller, R., 2009. Defining a spawning population (*spotted seatrout Cynoscion nebulosus*) over temporal, spatial, and demographic scales. *Marine Ecology Progress Series*. 394: 231-245.

Lowerre-Barbieri, S.K., Walters, S., Bickford, J., Cooper, W., Muller, R. 2013. Site fidelity and reproductive timing at a spotted seatrout

spawning aggregation site: individual versus population scale behavior. *Marine Ecology Progress Series.* 481:181-197.

Luczkovich, J.J., Mann, D.A., Rountree, R.A. 2008. Passive acoustics as a tool in fisheries science. Transactions of the *American Fisheries Society* 137: 533–541.

Luczkovich, J.J., Pullinger, R.C., Johnson, S.E., Sprague, M.W. 2008 Identifying sciaenid critical spawning habitats by the use of passive acoustics. *TAFS* 137:576-605

Luo, J., Musick, J. 1991. Reproductive biology of the Bay Anchovy, *Anchoa mitchilli,* in Chespeake Bay. *Transactions of American Fisheries Society*. 120: 801-710.

Ma, Y., Kjesbu, O.S., Jørgensen, T. 1998. Effects of ration on the maturation and fecundity in captive Atlantic herring (*Clupea harengus*). *Canadian Journal of Fisheries and Aquatic Sciences*, 55: 900–908.

Macchi, G.J. 1998. Preliminary estimate of spawning frequency and batch fecundity of striped weakfish, *Cynoscion striatus,* in coastal waters off Buenos Aires province. *Fishery Bulletin*. 96: 375-381.

Macchi, G.J., Acha, E.M. 2000. Spawning frequency and batch fecundity of Brazilian menhaden, Brevoortia aurea, in the Río de la Plata estuary off Argentina and Uruguay. *Fishery Bulletin.* 98: 283-289

Macchi, G.J., Acha, E.M., Militelli, M.I. 2003. Seasonal egg production of whitemouth croaker (*Micropogonias furnieri*) of the Río de la Plata estuary, Argentina -Uruguay. *Fishery Bulletin*. 101(2): 332-342.

Macchi, G.J., Estrada, M., Renzi, M., Abachian, V. 2010. Estructura y producción potencial de huevos del efectivo desovante de merluza (*Merluccius hubbsi*) al sur de 41° S durante diciembre de 2008 marzo de 2009. *Technical Report INIDEP N° 01/1*

Macchi, G.J., Gustavo J., Eduardo M. Acha, and Carlos A. Lasta. 2002 Reproduction of black drum (*Pogonias cromis*) in the Río de la Plata estuary, Argentina. *Fisheries research* 59(1) : 83-92.

Macchi, G.J., Pájaro, M., Ehrlich, M. 2004. Seasonal egg production pattern of the Patagonian stock of Argentine hake (*Merluccius hubbsi). Fisheries Research.* 67: 25–38.

Macchi, G.J., Pájaro, M., Wöhler, O., Acevedo, M., Centurión, R., Urteaga, D. 2005. Batch fecundity and spawning frequency of southern blue whiting (*Micromesistius australis Norman*, 1937) in the South-west Atlantic Ocean. New Zealand *Journal of Marine and Freshwater Research.* 39(5): 993-1000.

Macchi, G.J., Wöhler, O.C. 1994. Fecundidad parcial de la castañeta, *Cheilodactylus* bergi Norman, 1937. Comparación entre los métodos gravimétrico y estereométrico. *Boletín Instituto Español de Oceanografía*, 10: 41–49.

Macewicz, B.J., Castro-Gonzalez, J.J., Cotero-Altamirano, C.E., Hunter, J.R. 1996. Adult reproductive parameters of Pacific sardine (*Sardinops sagax*) during 1994. *CalCOFI Reports*. 37: 140-151.

Macewicz, B., Hunter, J.R., 1993. Spawning frequency and batch fecundity of jack mackerel, *Trachurus symmetricus*, off California during 1991. *CalCOFI Reports*. 34: 112-121.

Matsubara, T., Adachi, S., Ijiri, S., Yamauchi, K., 1995. Changes of lipovitellin during in vitro oocytes maturation in Japanese flounder *Paralichthys olivaceus*. *Fisheries Science*. 61: 478–481

Marshall, C.T., Kjesbu, O.S., Yaragina, N.A., Solemdal, P., Ulltang, Ø. 1998. Is spawner biomass a sensitive measure of the reproductive and recruitment potential of Northeast Arctic cod? *Canadian Journal of Fisheries and Aquatic Sciences,* 55(7): 1766-1783.

Marshall, C.T., Needle, C.L., Thorsen, A., Kjesbu, O.S., Yaragina, N.A. 2006. Systematic bias in estimates of reproductive potential of an Atlantic cod (*Gadus morhua*) stock: implications for stock recruit theory and management. *Canadian Journal of Fisheries and Aquatic Sciences,* 63(5): 980-994.

Marteinsdottir, G., Steinarsson, A. 1998. Maternal influence on the size and viability of Iceland cod *Gadus morhua* eggs and larvae. *Journal of Fish Biology*, 52(6): 1241-1258.

Mayhew, T., 1991. The new stereological methods for interpreting functional morphology from slices of cells and organs. *Experimental Physiology* 76: 639-665.

McBride, R.S., Stengard, F.J., Mahmoudi, B., 2002. Maturation and diel reproductive periodicity of round scad (*Carangidae: Decapterus punctatus*). *Marine Biology*. 140, 713–722.

McDermott, S.F., Maslenikov, K.P., Gunderson, D.R. 2007. Annual fecundity, batch fecundity, and oocyte atresia of Atka mackerel (*Pleurogrammus monopterygius*) in Alaskan waters. U.S. National Marine *Fisheries Service Fishery Bulletin.* 105:19–29.

Mayhew, T.M., Gundersen, H.J.G. 1996. 'If you assume, you can make an ass out of you and me': a decade of the disector for stereological counting of particles in 3D space. *Journal of Anatomy*, 188: 1–15.

Medina, A., Abascal, F.J., Aragón, L., Mourente, G., Aranda, G., Galaz, J.M., Belmonte, A., de la Serna, J.M., García, S. 2007. Influence of sampling gear in assessment of reproductive parameters for bluefin tuna in the western Mediterranean. *Marine Ecology Progress Series*, 337: 221–230.

Mayhew, T., 1991. The new stereological methods for interpreting functional morphology from slices of cells and organs. *Experimental Physiology* 76: 639-665.

Medina, A., Abascal, F.J., Megina, C., García, A., 2002. Stereological assessment of the reproductive status of female Atlantic northern *bluefin tuna* during migration to Mediterranean spawning grounds through the Strait of Gibraltar. J*ournal of Fish Biology.* 60: 203–217.

Mehault S., Domínguez-Petit R., Cerviño S., Saborido-Rey F. 2010. Variability in total egg production and implications for management of the southern stock of European hake. *Fisheries Research,* 104(1): 111-122.

Militelli, M.I., Macchi, G.J. 2001. Spawning

frequency and batch fecundity of Brazilian flathead, Percophis brasiliensis in coastal waters off the Buenos Aires Province. *Scientia Marina*. 65 (2): 169-172.

Militelli, M.I., Macchi, G.J. 2004. Spawning and fecundity of king weakfish, *Macrodon ancylodon*, in the Rio de la Plata estuary, Argentina-Uruguay. *Journal of the Marine Biological Association UK*. 84: 1-5

Michel, R.P., Cruz-Orive, L.M. 1988. Application of the Cavalieri principle and vertical sections method to lung: estimations of volume and pleura surface area. J*ournal of Microscopy*, 150: 117–136.

Milton, D.A., Chenery, S.R. 2005. Movement patterns of barramundi Lates calcarifer, inferred from $^{87}Sr/^{86}Sr$ and Sr/Ca ratios in otoliths, indicate non-participation in spawning. *Marine Ecology Progress Series*. 301: 279-291.

Morgan, M. J., Pérez-Rodríguez, A., Saborido-Rey, F. 2011. Does increased information about reproductive potential result in better prediction of recruitment? *Canadian Journal of Fisheries and Aquatic Sciences,* 68(8): 1361-1368.

Motos, L. 1996. Reproductive biology and fecundity of the Bay of Biscay anchovy population (*Engraulis encrasicolus L.*) *Scientia. Marina* 60 (suppl. 2): 195-207.

Murua, H., Kraus, G., Saborido-Rey, F., Witthames, P.R., Thorsen, A., Junquera. S. 2003. Procedures to estimate fecundity of marine fish species in relation to their reproductive strategy. *Journal of Northwest Atlantic Fishery Science.* 33: 33-54.

Murua, H., Lucio, P., Santurtun, M., Motos, L. 2006. Seasonal variation in egg production and batch fecundity of European hake *Merluccius merluccius (L.)* in the Bay of Biscay. *Journal of Fish Biology,* 69(5): 1304–1316.

Murua, H., Motos, L. 2006. Reproductive strategy and spawning activity of the European hake *Merluccius merluccius* (L.) in the Bay of Biscay. *Journal of Fish Biology*. 69: 1288-1303.

Murua, H., Saborido-Rey, F. 2003. Female reproductive strategies of marine fish species of the North Atlantic. *Journal of Northwest Atlantic Fishery Science*. 33: 23-31.

Myers, M., Britt, K.L., Wreford, N.G.M., Ebling, F.J.P., Kerr, J.B. 2004. Methods for quantifying follicular numbers within the mouse ovary. *Reproduction*, 127: 569–580

Nunes, C,, Silva, A., Marques, V., Ganias, K. 2011a. Integrating fish size, condition, and population demography in the estimation of Atlantic sardine annual fecundity. *Ciencias Marinas*. 37(42): 565-584.

Nunes, C., Silva, A., Soares, E., Ganias, K.. 2011b. The use of hepatic and somatic indices and histological information to characterize the reproductive dynamics of Atlantic sardine *Sardina pilchardus* from the Portuguese coast. *Marine and Coastal Fisheries* 3(1): 127-144.

Nyuji, M., Shiraishi, T., Selvaraj, S., Vu, V.I., Kitano, H., Yamaguchi, A., Okamoto, K., Onoue, S., Shimizu, A., Matsuyama M. 2011. Immunoreactive changes in pituitary FSH and LH cells during seasonal reproductive and spawning cycles of female chub mackerel *Scomber*

japonicus. Fisheries Science. 77: 731-739.

Ollerhead, L.M. N., Morgan, M.J., Scruton, M.J., Marrie, B. 2004. Mapping spawing times and locations for 10 commercially important fish species foundon the Grand Banks of Newfoundland. *Canadian technical report of fisheries and aquatic sciences St. Johns, Science, Oceans and Enviroment Branch*: 1 - 45.

Olson, D.E., Scidmore, W.J. 1963. Homing tendency of spawning white suckers in Many Point Lake, Minnesota. *Transactions of the American Fisheries Society* 92: 13-16.

Orfanidis, G., Ganias, K. 2011. Measuring batch fecundity in non-hydrated anchovies, *Engraulis encrasicolus*, using digital patricle analysis. *Book of abstracts of the FRESH final conference: Fish Reproduction and Fisheries*, *Vigo 15-22 May* 2011, 34.

Óskarsson, G.J., Kjesbu, O.S., Slotte, A. 2002. Predictions of realised fecundity and spawning time in Norwegian spring-spawning herring (*Clupea harengus). Journal of Sea Research.* 48: 59–79.

Óskarsson, G.J., Taggart, C.T. 2006. Fecundity variation in Icelandic summer-spawning herring and implications for reproductive potential. *ICES Journal of Marine Science*, 63: 493–503.

Pájaro, M., Macchi, G.J. 2001. Spawning pattern, length at maturity and fecundity of the southern blue whiting (*Micromesistius australis Norman*, 1937) in the Southwest Atlantic Ocean. New Zealand *Journal of Marine and Freshwater Research*. 35: 375-385.

Pájaro, M., Macchi, G.J., Leonarduzzi, E., Hansen, J. 2009. Spawning biomass of Argentine anchovy (*Engraulis anchoita)* from 1996 to 2004 using the Daily Egg Production Method. *Journal of the Marine Biological Association UK*. 89 (4): 829-837.

Pérez-Rodríguez, A., Morgan, M. J., Rideout, R. M., Domínguez-Petit, R., Saborido-Rey F. 2011. Study of the relationship between total egg production, female spawning stock biomass and recruitment in Flemish Cap cod (*Gadus morhua*). *Ciencias Marinas,* 37(4B): 675-687.

Picquelle, S., Stauffer, G., 1985. Parameter estimation for an egg production method of anchovy biomass assessment. In: Lasker R. (ed) An Egg Production Method for Estimating Spawning Biomass of Pelagic Fish: Application to the Northern Anchovy, *Engraulis mordax*. *NOAA Technical Report. NMFS* 36, pp. 7-16.

Plaza, G., Claramunt, G., Herrera, G. 2002. An intra-annual analysis of intermediate fecundity, batch fecundity and oocyte size of ripening ovaries of Pacific sardine *Sardinops sagax* in northern Chile. *Fisheries Science*, 68: 95-103.

Priede, I.G., Watson, J.J. 1993. An Evaluation of the Daily Egg Production Method for Estimating Biomass of Atlantic Mackerel (*Scomber scombrus*). *Bulletin of Marine Science*. 53: 891-911.

Quinn, S.P., Ross, M.R. 1985. Non-annual spawning in the white sucker. *Copeia* 1985, 613-618.

Quincoces, I. 1995. Un nuevo modelo morfofuncional de la glándula digestiva de *Mytillus galloprovincialis (Bilvalvia, Eulamellibranchia)*: reconstrucción tridimensional asistida por

ordenador y microscopia electrónica de barrido. University Degree Dissertation. Leioa, University of the Basque Country. pp. 112.

Quintanilla, L.F., Pérez, N. 2000. Spawning frequency of *Sardina pilchardus* (Walb.) off the Spanish North Atlantic coast in 1997. *Fisheries Research*, 45: 73-79.

Raja, D. S., Sultana, B. 2012. Potential Health Hazards for Students Exposed to Formaldehyde in the Gross Anatomy Laboratory. *Journal of Environmental Health* 74: 36-40.

Ramon, D., Bartoo, N. 1997. The effects of formalin and freezing on ovaries of albacore, *Thunnus alalunga*. *Fishery Bulletin.* 95: 869-872.

Rheman, S., Islam, M.L., Shah, M.M.R., Mondal, S., Alam, M.J. 2002. Observation on fecundity and gonadosomatic index (GSI) of grey mullet Liza parsian (Ham.). Online *Journal of Biological Sciences*. 2(10): 690 – 693

Rhodes, K.L., Sadovy, Y. 2002. Temporal and spatial trends in spawning aggregations of camouflage grouper, *Epinephelus polyphekadion*, in Pohnpei, Micronesia.» Enviromental *Biology of Fishes*. 63: 27-39.

Rideout, R.M., Burton, M.P.M., Rose, G.A. 2000. Observations on mass atresia and skipped spawning in northern Atlantic cod, from Smith Sound, Newfoundland. *Journal of Fish Biology* 57: 1429-1440.

Rideout, R.M., Rose, G.A., Burton, M.P.M. 2005. Skipped spawning in female iteroparous fishes. *Fish and Fisheries.* 6: 50-72.

Rideout, R.M., Tomkiewicz, J. 2011. Skipped spawning in fishes: More common than you might think. *Marine and Coastal Fisheries*. 3: 176-189.

Robichaud, D., Rose, G.A. 2002. Assessing evacuation rates and spawning abundance of marine fishes using coupled telemetric and acoustic surveys. ICES *Journal of Marine Science*. 59: 254-260.

Rodrigues, K.A., Macchi, G.J., Acha, E.M., Militelli, M.I. 2008. Reproduction of Jenyns´s sprat, Ramnogaster arcuata, a winter spawner in the temperate waters of the Río de la Plata estuary (Argentina – Uruguay). *Journal of the Marine Biological Association UK*. 88 (2): 423-428.

Rogers, P.J., Geddes, T., Ward, T.M., 2003. Blue sprat Spratelloides robustus (Clupeidae: *Dussumieriinae*): a temperate clupeoid with a tropical life history strategy? *Marine Biology*. 142: 809-824.

Roumillat, W.A., Brouwer, M.C., 2004. Reproductive dynamics of female spotted sea trout (*Cynoscion nebulosus*) in South Carolina. *Fishery Bulletin*. 102: 473-487.

Rountree, R.A., Gilmore, R. G., Goudey, C.A., Hawkins, A.D., Luczkovich, J.J., Mann, D.A. 2006. Listening to fish: applications of passive acoustics to fisheries science. *Fisheries.* 31(9): 433-442.

Rumohr, H. 1999. Soft bottom macrofauna: collection, treatment, and quality assurance of samples. *ICES Techniques in Marine Environmental Science* Nº. 8, pp.18

Saborido-Rey, F., Kjesbu, O.S., Thorsen, A. 2003.

Buoyancy of Atlantic cod larvae in relation to developmental stage and maternal influences. *Journal of Plankton Research*, 25: 291–307.

Saborido-Rey, F., Junquera, S. 1998. Histological assessment of variations in sexual maturity of cod (*Gadus morhua L.*) at the Flemish cap (north-west Atlantic). ICES *Journal of Marine Science* 55: 515-521.

Samoilys, M.A. 1997. Periodicity of spawning aggregations of coral trout *Plectropomus leopardus* (Pisces: *Serranidae*) on the northern Great Barrier Reef. *Marine Ecology Progress Series* 160: 149-159.

Sánchez, R.P., de Ciechomski, J.D., Acha, E.M. 1986. Estudios sobre reproducción y fecundidad de la polaca (*Micromesistius australis* Norman 1937) en el Mar Argentino. *Revista de Investigación y Desarrollo Pesquero*, 6: 21–43.

Schaefer, K., 1996. Spawning time, frequency and batch fecundity of yellowfin tuna, *Thunnus albacares*, near Clipperton Atoll in the eastern Pacific Ocean. *Fishery Bulletin*. 94: 98-112.

Schaefer, M.B., Orange, C.J. 1956. Studies of the sexual development and spawning of yellowfin tuna (*Neothunnus macropterus*) and skipjack (*Katsuwonas pelamis*) in three areas of the eastern Pacific Ocean, by examination of gonads. *Inter-American Tropical Tuna Commission Bulletin*. 1: 283-320.

Sanz, A., Motos L., Uriarte A.. 1992. Daily fecundity of the Bay of Biscay anchovy, *Engraulis encrasicolus (L.)*, population in 1987. *Boletin del Instituto Español de Oceanografia* 8: 203-214.

Seber, G. A. F. 1973. The estimation of animal abundance and related parameters. Charles Griffin, London, England. 506p.

Secor, D.H. , Piccoli, P.M. 2007. Oceanic migration rates of Upper Chesapeake Bay striped bass (*Morone saxatilis*), determined by otolith microchemical analysis. *Fishery Bulletin* 105: 62-73.

Shiraishi, T., Ketkar, S.D., Katoh, Y., Nyuji, M., Yamaguchi, A., Matsuyama, M. 2009. Spawning frequency of the Tsushima current subpopulation of chub mackerel *Scomber japonicus* off Kyushu, Japan. *Fisheries Science*, 75: 649-655.

Shiraishi, T., Ketkar, S.D., Kitano, H., Nyuji, M., Yamaguchi, A., Matsuyama M. 2008. Time course of final oocyte maturation and ovulation in the chub mackerel Scomber japonicus induced by hCG and GnRHa. *Fisheries Science*, 74: 764-769.

Simpson, A.C. 1951. The fecundity of the plaice. *Fishery Investigations London Series* II Vol. XVII: 27pp

Skjæraasen, J.E., Kennedy, J., Thorsen, A., Fonn, M., Njøs Strand, B., Mayer, I., Kjesbu, O.S. 2009. Mechanisms regulating oocyte recruitment and skipped spawning in Northeast Arctic cod (Gadus morhua). Canadian Journal of Fisheries and Aquatic Sciences, 66:1582-1596.

Skjæraasen, J.E, Nash, R.D.M., Kennedy, J., Thorsen, A., Nilsen, T., Kjesbu, O.S. 2010. Liver energy, atresia and oocyte stage influence fecundity regulation in Northeast Arctic cod. *Marine Ecology Progress Series*, 404: 173–183.

Slotte, A. 1999. Differential utilization of energy during wintering and spawning migration

in Norwegian spring-spawning herring. *Journal of Fish Biology*, 54: 338–355.

Stéquert, B., Ramcharrun, B. 1995. La fécondité du listao (*Katsuwonus pelamis*) de l'ouest de l'océan Indien. *Aquatic Living Resources*, 8: 79–89.

Sterio, D.C. 1984. The unbiased estimation of number and sizes of arbitrary particles using the disector. *Journal of Microscopy*, 134: 127–36.

Stratoudakis, Y., Bernal, M., Ganias, K., Uriarte, A. 2006. The daily egg production method (DEPM): recent advances, current applications, and future challenges. *Fish and Fisheries*, 7: 35 - 57.

Svedang, H., Righton, D. et al. 2007 . Migratory behaviour of Atlantic cod *Gadus morhua*: antal homingistheprimestock-separatingmechanism. *Marine Ecology Progress Series* 345: 1-12.

Svåsand, T., Jorstad, K.E., Otterø, H., Kjesbu, O.S. . 1996. Differences in growth performance between Arcto-Norwegian and Norwegian coastal cod reared under identical conditions. *Journal of Fish Biology*. 49: 108-119.

Takasuka, A., Oozeki, Y., Kubota, H., Tsuruta, Y., Funamoto, T., 2005. Temperature impacts on reproductive parameters for Japanese anchovy: comparison between inshore and offshore waters. *Fisheries Research.* 76: 475-482.

Tan-Fermin, J.D. 1991. Suitability of different formalin-containing fixatives for the eggs of freshwater Asian catfish *Clarias macrocephalus* (Gunther). The Israeli *Journal of Aquaculture.-Bamidgeh*. 43: 57-61.

Thorsen, A., Kjesbu, O.S. 2006. A rapid method for estimation of oocyte size and potential fecundity in Atlantic cod using a computer-aided particle analysis system, *Journal of Sea Research*. 46: 295–308.

Thorsen, A., Marshall, C.T., Kjesbu, O.S. 2006. Comparison of various potential fecundity models for north-east Arctic cod *Gadus morhua*, L. using oocyte diameter as a standardizing factor. *Journal of Fish Biology*. 69: 1709–1730.

Trippel, E.A. 1998. Egg size and viability and seasonal offspring production of young Atlantic cod. *Transactions of American Fisheries Society*, 127: 339–359.

Trippel, E. A., Harvey, H. H. 1990. Ovarian atresia and sex ratio imbalance in white sucker, *Catostomus commersoni*. *Journal of Fish Biology* 36(2): 231-239.

Tyler, A.V., Dunn, R.S. 1976. Ration, growth, and measures of somatic and organ condition in relation to meal frequency in winter flounder, *Pseudopleuro nectes americanus*, with hypotheses regarding population homeostasis. *Journal of the Fisheries Research Board of Canada*. 33: 63–75

Uriarte, A., Alday, A., Santos, M., Motos, L. 2012. A re-evaluation of the spawning fraction estimation procedures for Bay of Biscay anchovy, a species with short interspawning intervals. *Fisheries. Research*. 117: 96-111.

Vallin, L., Nissling, A. 2000. Maternal effects on egg size and egg buoyancy of Baltic cod, *Gadus morhua*: implications for stock structure effects

on recruitment. *Fisheries Research*, 49: 21–37.

Van-Damme, C.J.G., Dickey-Collas, M., Rijnsdorp, A.D., Kjesbu, O.S. 2009. Fecundity, atresia, and spawning strategies of Atlantic herring (*Clupea harengus). Canadian Journal of Fisheries and Aquatic Sciences.* 66: 2130–2141.

Verbeek, F.J. 2000. Theory and Practice of 3D-reconstructions from serial sections. In Image Processing, A Practical Approach. Baldock RA and Graham J eds., pp. 153-195.

Vladykov, V.D. 1956. Fecundity of wild speckled trout (*Salvelinus fontinalis*) in Quebec lakes. *Canadian Journal of Fisheries and Aquatic Sciences*. 13: 799–841.

Wallace, R.A., Selman, K. 1981. Cellular and dynamic aspects of oocyte growth in teleosts. *American Zoology.* 21: 325–343.

Walters, S., Lowerre-Barbieri, S.K., Bickford, J., Crabtree, L., Mann, D. 2007. Preliminary results on seasonal and diel periodicities of a resident *Cynoscion nebulosus* spawning aggregation in Tampa Bay, Florida. Gulf and Caribbean Fisheries Institute.

Walters, S., Lowerre-Barbieri, S., Bickford, J., Mann, D. 2009. Using a passive acoustic survey to identify spotted seatrout spawning sites and associated habitat in Tampa Bay, Florida. *Transactions of the American Fisheries Society*. 138(1): 88-98.

Weibel, E.R. 1969. Stereological principles for morphometry in electron microscopy cytology. International *Review of Cytology,* 26: 235–302.

Weibel, E.R., Gomez, D.M. 1962. A principle for counting tissue structures on random sections. *Journal of Applied Physiology*, 17: 343–348.

Weibel, E.R., Kristler, G.S., Scherle, W.F. 1966. Practical stereological methods for morphometric cytology. *Journal of Cell Biology*, 30: 23–38.

Witthames, P.R. 2001. A manual for the estimation of fecundity and atresia in Mackerel and Horse mackerel. Lowestoft: *CEFAS*.

Witthames, P.R., Greer Walker, M. 1987. An automated method for counting and sizing fish eggs. *Journal of Fish Biology*. 30: 225–235.

Witthames, P.R., Thorsen, A., Kjesbu, O.S. 2010. The fate of vitellogenic follicles in experimentally monitored Atlantic cod *Gadus morhua* (L.): Application to stock assessment. *Fisheries Research*. 104: 27-37.

Witthames, P.R, Thorsen, A., Murua, H., Saborido-Rey, F., Greenwood, L.N., Domínguez-Petit, R., Korta, M., Kjesbu, O.S. 2009. Advances in methods for determining fecundity: application of the new methods to some marine fishes. *Fishery Bulletin*. 107: 148–164.

Wootton, R.J. 1979. Energy costs of egg production and environmental determinants of fecundity in teleost fishes. Symposium of the Zoological Society of London, 44: 133–159.

Wlodarczyk, E., Horbowa, K. 1997. Size-specific vertical distribution of Baltic cod (*Gadus morhua L.*) eggs in the Bornholm Basin in 1993 and 1994. *ICES Journal of Marine Science*, 54: 206–212.

Wroblewski, J.S., Hiscock, H.W., Bradbury, I.R. 1999. Fecundity of Atlantic cod *Gadus morhua* farmed for stock enhancement in Newfoundland bays. *Aquaculture,* 171: 163–180.

Wright, P.J. 1992. Ovarian development, spawning frequency and batch fecundity in *Encrasicholina heteroloba* (Ruppell, 1858) *Journal of Fish Biology.* 40, 833-844.

Yamada, T., Aoki, I., Mitani, I., 1998. Spawning time, spawning frequency and fecundity of Japanese chub mackerel, *Scomber japonicus*, in the waters around the Izu Islands, Japan. *Fisheries Research*. 38: 83-89.

Yoda, M., Yoneda, M. 2009. Assessment of reproductive potential in multiple-spawning fish with indeterminate fecundity: a case study of yellow sea bream (*Dentex hypselosomus*) in the East China Sea. *Journal of Fish Biology*. 74: 2338–2354.

Yoneda, M., Futagawa, K., Tokimura, M., Horikawa, H., Matsuura, S., Matsuyama, M., 2002. Reproductive cycle, spawning frequency and batch fecundity of the female whitefin jack, *Kaiwarinus equula*, in the East China Sea. *Fisheries Research*. 57: 297-309.

Zeldis, J.R., Francis, R.I.C.C. 1998. A daily egg production method estimate of snapper biomass in Hauraki Gulf, New Zealand. ICES *Journal of Marine Science*, 55: 522–534.

Zeller, D.C. 1998. Spawning aggregations: patterns of movement of the coral trout *Plectropomus leopardus (Serranidae)* as determined by ulrasonic telemetry. *Marine Ecology Progress Series* 162: 253-263.

Zwolinski, J., Stratoudakis, Y., Soares, E. 2001. Intra-annual variation in the batch fecundity of sardine off Portugal. *Journal of Fish Biology*, 58: 1633-1645.

4.8 Table of contributions

4.1. Introduction	*K. Ganias*
BOX 4.1	*H. Murua*
4.2. Gravimetric estimation of fish fecundity	
4.2.1. Basic principles	*P. Gonçalves*
BOX 4.2	*K. Ganias*
4.2.2. Ovary fixation and preservation	*K. Ganias*
4.2.3. Effect of preservation on oocyte size	*F. Juanes, N. Klibansky*
4.2.4. Preparation of ovarian whole mounts	*S. Lowerre-Barbieri*
4.2.5. Oocyte counting using particle analysis	*A. Thorsen*
4.2.6. Whole mount staining	*H. Murua*
4.2.7. Low cost alternatives to microscopy	*F. Juanes, N. Klibansky*
4.3. Stereological estimation of fecundity	
4.3.1. Basic principles	*A. Medina*
4.3.2. Model-based methods	
4.3.2.1. The Weibel method	*A. Medina*
4.3.2.2. Ovarian packing density	*Y. Kurita*
4.3.3. Assumption-free methods	
4.3.3.1. The physical dissector	*A. Medina*
4.3.3.2. The fractionator	*A. Medina*
4.3.4. Final remarks	*A. Medina*
4.4. Bacth fecundity	
4.4.1. Hydrated oocyte method	*P. Gonçalves*
4.4.2. Use of other stages	*K. Ganias*
4.4.3. Use of intermediate batches	*G. Plaza*
4.5. Daily fecundity and spawning frequency	
4.5.1. Estimation of daily fecundity	*S. Somarakis*
4.5.2. Estimation of spawning frequency	*K. Ganias, A. Uriarte*
4.5.3. The postovulatory follicle method	
4.5.3.1. POF staging: an interspecific approach	*G. Macchi*
4.5.3.2 POF 3-D reconstruction	*M. Korta*
4.5.3.3 POF ageing: basic principles	*A. Uriarte*
4.5.3.4 Tank experiments	*M. Matsuyama*
4.5.3.5 Using POF size in POF ageing	*K. Ganias*

4.5.4. Methods based on imminent spawners	
4.5.4.1 The hydrated females method	*K. Ganias*
4.5.4.2 The gonadosomatic index method	*G. Claramunt*
4.5.4.3 The oocyte growth method	*K. Ganias*
4.5.5. Methods for species with high S	
4.5.5.1 Relationship between Day_0 and Day_1 spawners	*A. Uriarte*
4.5.5.2 Co-occurrence of spawning stages	*A. Uriarte, M. Yoneda*
4.5.6. Assessment of spawning sites	*S. Lowerre-Barbieri*
4.6. Annual fecundity	
4.6.1. Determinate spawners	
4.6.1.1 The autodiametric method	*A. Thorsen*
4.6.1.2 Fecundity down-regulation	*J. Kennedy*
4.6.1.3 Skipped spawning	*R. Rideout*
4.6.2. Indeterminate spawners	
4.6.2.1 Annual fecundity	*C. Nunes*
4.6.2.2 Total egg production	*R. Dominguez-Petit*

4.9 AUTHORS INDEX

Kostas Ganias
Aristotle University of Thessaloniki.
Greece
kganias@bio.auth.gr

Hilario Murua
AZTI-Tecnalia
Spain
hmurua@azti.es

Gabriel Claramunt
University Arturo Prat
Chile
gclaramu@unap.cl

Rosario Dominguez-Petit
Institute of Marine Research-CSIC
Spain
rosario@iim.csic.es

Patricia Gonçalves
Instituto Português do Mar e da Atmosfera
Portugal
patricia@ipma.pt

Francis Juanes
University of Victoria
USA
juanes@uvic.ca

James Keneddy
Marine Research Institute
Iceland
jim@hafro.is

Nikolas Klibansky
University of North Carolina Wilmington
USA
nk5371@uncw.edu

Maria Korta
AZTI-Tecnalia
Spain
mkorta@azti.es

Yutaka Kurita
Tohoku National Fisheries Research Institute
Japan
kurita@affrc.go.jp

Susan Lowerre-Barbieri
Florida Fish and Wildlife Research Institute
USA
Susan.Barbieri@MyFWC.com

Gustavo J. Macchi
INIDEP-CONICET
Argentina
gmacchi@inidep.edu.ar

M Matsuyama
Kyushu University
Japan
rinya_m@agr.kyushu-u.ac.jp

Antonio Medina
University of Cadiz
Spain
antonio.medina@uca.es

Cristina Nunes
Instituto Português do Mar e da Atmosfera
Portugal
cnunes@ipma.pt

Guido Plaza
Catholic University of Valparaíso
Chile
guido.plaza@ucv.cl

Rick Rideout
Department of Fisheries and Oceans
Canada
Rick.Rideout@DFO-MPO.GC.CA

Stylianos Somarakis
Hellenic Center for Marine Research. Greece.
somarak@upatras.gr

Anders Thorsen
Institute of Marine Research
Norway
anders.thorsen@imr.no

Andrés Uriarte
AZTI-Tecnalia
Spain
aduriarte@azti.es

Michio Yoneda
National Research Institute of Fisheries and
Environment of Inland Sea
Japan
myoneda@fra.affrc.go.ip